



CMS-HIN-23-004

CERN-EP-2025-014
2025/05/23

Observation of nuclear modification of energy-energy correlators inside jets in heavy ion collisions

The CMS Collaboration^{*}

Abstract

Energy-energy correlators are constructed by averaging the number of charged particle pairs within jets, weighted by the product of their transverse momenta, as a function of the angular separation of the particles within a pair. They are sensitive to a multitude of perturbative and nonperturbative quantum chromodynamics phenomena in high-energy particle collisions. Using lead-lead data recorded with the CMS detector, energy-energy correlators inside high transverse momentum jets are measured in heavy ion collisions for the first time. The data are obtained at a nucleon-nucleon center-of-mass energy of 5.02 TeV and correspond to an integrated luminosity of 1.70 nb^{-1} . A similar analysis is done for proton-proton collisions at the same center-of-mass energy to establish a reference. The ratio of lead-lead to proton-proton energy-energy correlators reveals significant jet substructure modifications in the quark-gluon plasma. The results are compared to different models that incorporate either color coherence or medium response effects, where the two effects predict similar substructure modifications.

Published in Physics Letters B as doi:10.1016/j.physletb.2025.139556.

1 Introduction

Energy-energy correlators are important observables for studying quantum chromodynamics (QCD) [1, 2]. They can be calculated with great accuracy in asymptotically free perturbation theory and can be experimentally measured with excellent precision. The two-point energy correlator is defined as a weighted distribution of angular separation of all possible particle pairs within a jet cone, where the weights are the product of the transverse momenta (p_T) of the two particles in a pair, as illustrated in the left panel of Fig. 1. Recent theoretical work has explored energy-energy correlators at LHC energies [3–7], and theory comparisons have been made to the CMS open data from 7 TeV proton-proton (pp) collisions [8, 9]. One of the most useful properties of the energy-energy correlator in $e^+ e^-$ and pp collisions is that different time scales in jet evolution are imprinted in different angular scales of the correlator. It follows from QCD color coherence that daughter parton emissions to angles larger than the opening angle of the parent partons are strongly suppressed [10–13], which leads to angular ordering of parton showers. In jet evolution, early times correspond to large angles, while late times correspond to small angles. A schematic illustration of how this translates to a structure of an energy-energy correlator distribution in pp collisions is given in the right panel of Fig. 1, following the discussion in Ref. [8]. The energy-energy correlators at small angles are approximately proportional to the angle squared, which is expected from the propagation of uniformly distributed noninteracting hadrons. At large angles, the relevant dynamics to explain the scaling behavior are the perturbative interactions of asymptotically free quarks and gluons [14]. In between, there is a transition region that reflects the impact of hadronization.

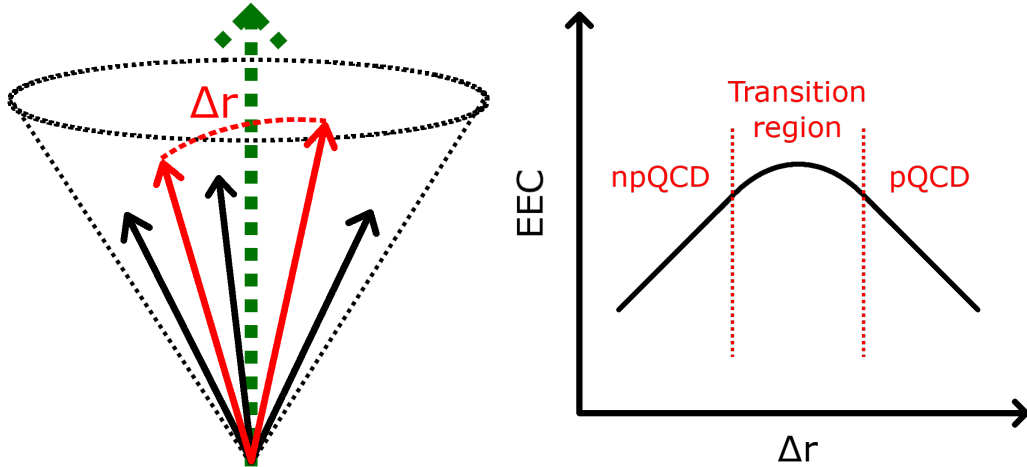


Figure 1: Left: Illustration on how energy-energy correlators are constructed. The green dashed arrow represents the jet axis and the solid arrows represent charged particles. Right: Schematic structure of an energy-energy correlator distribution in pp collisions.

While previously studied in $e^+ e^-$ collisions at LEP [15], many experimental collaborations are now undertaking measurements of these correlators in hadron collisions. These measurements include correlators within jets from pp collisions at 200 GeV by the STAR Collaboration [16], at 5.02 TeV by the ALICE Collaboration [17], and at 13 TeV by the CMS Collaboration [18]. The transition region between the perturbative and nonperturbative QCD regimes is found to scale inversely with the mean jet energy [17]. The scaling factor is proportional to Λ_{QCD} , the fundamental energy scale of QCD below which nonperturbative effects become dominant. With increasing jet momenta, the transition region moves to smaller angles. At larger angular distances, where perturbative QCD is probed, the correlators are sensitive to the strong coupling constant α_S and to the various color factors associated with parton-initiated showers [18].

In heavy ion collisions, the interaction of scattered hard partons with quark-gluon plasma leads to jet quenching [19–22]. This phenomenon has been studied for nearly two decades through measurements ranging from the suppression of high- p_T hadrons [23–25] and jets [26, 27] to more differential observables, such as jet shapes [28–30] and other substructure observables [31–37]. The CMS heavy ion program is heavily involved in these studies, with a summary description of previous results presented in Ref. [38]. Recent theoretical papers propose energy-energy correlators as complementary observables that may further enhance our understanding of the quark-gluon plasma [39–45]. In particular, energy-energy correlators in heavy ion collisions are predicted to be sensitive to color coherence effects [40], where only the gluons emitted above some critical angle can independently emit more gluons. They are also predicted to be sensitive to the “jet wake” effect [45], where a high- p_T parton traversing the plasma drags medium particles with it. While the relative contribution of these two mechanisms of energy loss in the quark-gluon plasma has yet to be experimentally established, energy-energy correlators promise to be important new observables for their study [46].

In this Letter, two-point energy correlators within high- p_T jets are measured using charged particles in lead-lead (PbPb) collisions at a nucleon-nucleon center-of-mass energy of $\sqrt{s_{\text{NN}}} = 5.02 \text{ TeV}$, recorded in 2018 by the CMS experiment. This is the first time these correlators have been measured in heavy ion collisions. The PbPb results are compared to those from pp collisions recorded in 2017 at the same center-of-mass energy to uncover possible modifications in the correlator shapes resulting from the presence of the quark-gluon plasma. The total integrated luminosities are 1.70 nb^{-1} [47] for the PbPb data set and 302 pb^{-1} for the pp data set [48]. The PbPb energy-energy correlators are extracted in four ranges of nuclear overlap and jet p_T , two charged particle p_T thresholds, and with two different choices of p_T weights that offer different sensitivities to hard- and soft-parton interactions. Tabulated results are provided in the HEPData record for this analysis [49].

2 The CMS experiment

The central feature of the CMS apparatus is a superconducting solenoid of 6 m internal diameter, providing a magnetic field of 3.8 T. Within the solenoid volume are a silicon pixel and strip tracker, a lead tungstate crystal electromagnetic calorimeter, and a brass and scintillator hadron calorimeter, each composed of a barrel and two endcap sections. The silicon tracker measures charged particles within the pseudorapidity range $|\eta| < 3.0$. During the LHC running period relevant to this Letter, the silicon tracker consisted of 1856 silicon pixel and 15 148 silicon strip detector modules. Two hadron forward steel and quartz-fiber calorimeters complement the barrel and endcap detectors, extending the calorimeter from the range $|\eta| < 3.0$ provided by the barrel and endcap out to $|\eta| < 5.2$. The hadron forward calorimeters are azimuthally subdivided into 20° modular wedges and further segmented to form $0.175 \times 0.175 (\Delta\eta \times \Delta\varphi)$ towers. The distribution of the sum of the transverse energies detected in the hadron forward detectors ($3.0 < |\eta| < 5.2$) is used to define the event centrality [50] in term of percentiles of the total distribution. Here, 0% centrality corresponds to the largest overlap of the colliding nuclei. Muons are measured in the range $|\eta| < 2.4$, with detection planes made using three technologies: drift tubes, cathode strip chambers, and resistive plate chambers. A detailed description of the CMS detector, together with a definition of the coordinate system used and the relevant kinematic variables, can be found in Refs. [51, 52].

Events of interest are selected using a two-tiered trigger system. The first tier, composed of custom hardware processors, uses information from the calorimeters and muon detectors to select events at a rate of around 100 kHz [53]. The second tier, known as the high-level trigger,

consists of a farm of processors running a version of the full event reconstruction software optimized for fast processing. It reduces the event rate to around 1 kHz before data storage [54].

3 Event selection and simulated event samples

Events are selected using high-level triggers that require at least one calorimeter-based jet with high p_T . These jets are reconstructed using the anti- k_T jet clustering algorithm with a distance parameter of $R = 0.4$ [55]. For PbPb collisions, we combine triggers with jet thresholds $p_T > 60\text{ GeV}$, $p_T > 80\text{ GeV}$, and $p_T > 100\text{ GeV}$. This combination achieves full trigger efficiency in the entire jet p_T range covered in this analysis, while minimizing the statistical uncertainty of the results. Heavy ion collisions produce many soft particles in addition to those resulting from the hard scattering processes associated with jets. This underlying event contribution is subtracted from the jets using an iterative method [56] before comparing the jet p_T to one of the threshold values. For pp collisions, a combination of triggers with thresholds $p_T > 60\text{ GeV}$ and $p_T > 80\text{ GeV}$ is used. No underlying event subtraction is applied for pp collisions.

For PbPb collisions, a minimum bias triggered sample is also used, where the aim is to select any hadronic interactions. The minimum bias trigger requires a signal on each side of the interaction point in the hadron forward calorimeters above the readout threshold of a fixed analog-to-digital converter count number that translates to $6\text{--}12\text{ GeV}$, depending on the tower.

To reduce contamination from beam-gas collisions, vertex and noise filters are applied to both the pp and PbPb data following the example of previous analyses [57]. At least two hadron forward calorimeter towers on each side of the detector are required to have an energy deposit of at least 4 GeV per tower. The primary vertex is required to have at least two tracks. In addition, it needs to be reconstructed within 15 cm of the nominal interaction point in the beam direction (z) and within 2 cm in the transverse direction. Additionally, in PbPb collisions the shapes of the clusters in the pixel detector are required to be compatible with those expected at the measured vertex location.

The average number of collisions per beam bunch crossing (pileup) is about 2 in pp and smaller than 0.01 in PbPb collisions, respectively. As the pileup is low in both of the data samples, no pileup corrections are necessary.

Simulated event samples are used in the analysis to unfold the measurements to particle level, thus accounting for detector resolution effects. The hard jet events are generated with the PYTHIA 8.230 event generator [58] with tune CP5 [59] and parton distribution function set NNPDF3.1 at next-to-next-to-leading order [60]. As an alternative event generator for systematic uncertainty studies, the HERWIG 7.2.2 generator [61, 62] with tune CH3 [63] and NNPDF3.1 is also used. The CMS detector response is simulated using the GEANT4 toolkit [64]. The soft underlying event for the PbPb collisions is simulated with the HYDJET 1.9 event generator [65], which is tuned to reproduce global event properties, such as the charged-hadron p_T spectrum. The energy density in the HYDJET simulation is tuned to match the data by shifting the centrality binning in the standard HYDJET simulation by 4 percentage points upwards. This tuning is based on a random-cone study, where cones with a radius of 0.4 are placed in random directions in events, and the energy densities in the cones are determined by summing the particle transverse momenta within the cone. The above tuning provides the best agreement in random-cone energy density distribution shapes between data and HYDJET. To simulate jet events in PbPb collisions, PYTHIA generated hard events are embedded into HYDJET events. This sample is denoted as PYTHIA+HYDJET.

In PbPb collisions, jets are produced more frequently in central events than in noncentral events because of a larger number of binary nucleon-nucleon collisions. A centrality-based weighting is applied to the PYTHIA+HYDJET sample to match the centrality distribution of the jet-triggered PbPb data after event selection. An additional weighting procedure is performed to match the simulated vertex distributions with data for both the pp and PbPb samples.

4 Jet and track reconstruction

The track reconstruction used for pp and PbPb collisions is described in Ref. [66]. The charged particle tracks in PbPb collisions are required to have at least eleven hits in the tracker layers and satisfy a stringent fit quality requirement $\chi^2/\text{dof}/N_{\text{layers}} < 0.18$, where the χ^2 and the number of degrees of freedom are related to the fit, and N_{layers} is the number of tracker layers hit. To reduce the likelihood of counting nonprompt charged particles originating from secondary decay products in both pp and PbPb collisions, it is required that the distance of closest approach of a charged particle track to the primary vertex, divided by its uncertainty, is less than three. Furthermore, the relative p_{T} uncertainty $\delta p_{\text{T}}/p_{\text{T}}$ for the tracks must be less than 10%. Finally, for PbPb collisions, in order to reduce the contribution of misreconstructed tracks with very high p_{T} values, it is required that tracks with $p_{\text{T}} > 20 \text{ GeV}$ have an associated energy deposit in the calorimeters corresponding to at least half of the track momentum. Corrections for tracking efficiency, detector acceptance, and misreconstructed tracks are obtained and applied following the procedures discussed in Ref. [57].

A particle-flow algorithm using an optimized combination of information from various elements of the CMS detector is used to reconstruct leptons, photons, and charged and neutral hadrons [67]. Jets in both pp and PbPb collisions are reconstructed using the anti- k_{T} algorithm with a distance parameter $R = 0.4$, as implemented in the FASTJET framework [68], with particle-flow candidates as an input. The jets are first clustered using E-scheme clustering [68] and then, using the same constituents, the jet axis is recalculated using the winner-take-all algorithm [69, 70]. In the E-scheme clustering, particle pairs are iteratively combined to form pseudo-jets (an object that is a combination of particles or other pseudo-jets), with the direction of the new pseudo-jet given by the sum of the four-momenta of the particles. In the winner-take-all scheme, the direction of the new pseudo-jet in each iteration is aligned with the direction of the particle or pseudo-jet with the highest p_{T} value. It follows that the E-scheme axis for the final jet is given by the sum of pseudo-jet four-momenta, while the winner-take-all axis is determined by the direction of the hardest pseudo-jet. The axis recalculation is done to avoid an artificial dip in the particle density distributions close to the jet radius, which is a feature for an E-scheme jet axis.

In order to subtract the soft underlying event contribution from the jet energy in PbPb collisions, a constituent subtraction method [71] is employed. This involves a particle-by-particle approach that corrects the jet constituents based on the local average underlying event density. The energy density is estimated using an event-by-event, iterative algorithm [56] that finds the mean value and dispersion of the energies from the particle-flow candidates in η -strips [19, 50]. To take into account the global hydrodynamic flow [72], the azimuthal angle (φ) distribution of the particle-flow candidates is fitted with second- and third-order Fourier components on an event-by-event basis. The background energy density is modulated by the results of this fit. In pp collisions, where the underlying event level is negligible, jets are reconstructed without any underlying event subtraction.

5 Energy-energy correlators

Energy-energy correlators are constructed for charged particles in the vicinity of high- p_{T} jets. The analysis is done for jet p_{T} ($p_{\text{T,jet}}$) ranges $120 < p_{\text{T,jet}} < 140 \text{ GeV}$, $140 < p_{\text{T,jet}} < 160 \text{ GeV}$, $160 < p_{\text{T,jet}} < 180 \text{ GeV}$, and $180 < p_{\text{T,jet}} < 200 \text{ GeV}$. Two different charged particle p_{T} (p_{T}^{ch}) thresholds are used, with $p_{\text{T}}^{\text{ch}} > 1 \text{ GeV}$ and $p_{\text{T}}^{\text{ch}} > 2 \text{ GeV}$, respectively. While limiting the selection to higher- p_{T} particles reduces background, this also reduces part of the expected signal related to medium-induced radiation and soft-particle emissions within the jet. In PbPb collisions, the measurement is done in four centrality ranges of 0–10%, 10–30%, 30–50%, and 50–90%. The jets are selected with $|\eta| < 1.6$ to ensure stable detector performance within the jet cone. During the PbPb run, there was a region in the tracker with a low track reconstruction efficiency. Since the analysis is not statistics limited, jets with $-0.1 < \varphi < 1.2$ in PbPb collisions are not included in the analysis to avoid potential bias from the poor detector performance.

The energy-energy correlators are defined as

$$\text{EEC}(\Delta r) = \frac{1}{W_{\text{pairs}}} \frac{1}{\delta r} \sum_{\text{jets} \in [p_{\text{T},1}, p_{\text{T},2}]} \sum_{\text{pairs} \in [\Delta r_a, \Delta r_b]} (p_{\text{T},i} p_{\text{T},j})^n, \quad (1)$$

where (i, j) refer to paired particles, $\Delta r \equiv \Delta r_{ij} = \sqrt{(\eta_i - \eta_j)^2 + (\varphi_i - \varphi_j)^2}$, Δr_a and Δr_b are Δr bin boundaries, $\delta r = \Delta r_b - \Delta r_a$ is the bin width, and $p_{\text{T},1}$ and $p_{\text{T},2}$ are $p_{\text{T,jet}}$ bin borders. The particle pairs are constructed using all possible pairs of charged particles corresponding to the selected p_{T}^{ch} threshold that are within $\Delta r_{\text{ch}}^{\text{jet}} = 0.4$ from a selected jet axis. One-dimensional histograms of $\text{EEC}(\Delta r)$ are produced by weighting each entry with the product of the particle transverse momenta $(p_{\text{T},i} p_{\text{T},j})^n$, with either $n = 1$ or 2 . Similar to higher charged particle p_{T} thresholds, employing higher powers for the momentum weight exponent helps to reduce the underlying event background in heavy ion collisions. We note that in this analysis the $(p_{\text{T},i} p_{\text{T},j})^n$ weight for the particle pairs does not include the normalization factor $1/p_{\text{T,jet}}^2$ that is present in many theoretical publications because the single-particle p_{T} resolution is much better than that of $p_{\text{T,jet}}$. Instead, the hard scale enters in Eq. (1) through the choice of narrow $p_{\text{T,jet}}$ ranges. We have checked in simulation that the resolution effects for the weights are negligible if the $p_{\text{T,jet}}$ term is not included. Finally, the distribution is normalized by the weighted number of pairs W_{pairs} such that the integral of the distribution in the analysis region is unity.

There are two kinds of particles within the jet cone. The fragmentation products of the hard-scattered parton, together with particles related to jet-medium interactions, are considered signal particles. All other particles, which mainly come from the underlying event and are not correlated with the signal particles, are considered background particles. When constructing the energy-energy correlators, we pair all selected charged particles with all other charged particles, resulting in three different types of pairings in our signal event:

- Signal+Signal (S + S);
- Signal+Background (S + B); and
- Background+Background (B + B).

In pp collisions, the p_{T}^{ch} thresholds are sufficiently high to keep background components at negligible levels. For PbPb collisions, we estimate the background distribution using the mixed cone method. For each signal event, we find two minimum bias events with similar underlying event distributions as the signal event. This is achieved by requiring that the primary vertex z position is within 0.5 cm and the centrality within the same 0.5% wide bin in the minimum bias events compared to those in the signal event. We then place a jet cone at the same (η, φ)

position as in the signal event to ensure the same detector performance. We call this cone in the minimum bias event a mixed cone. After this, three different pairings are constructed:

- Signal Event + Minimum Bias Event 1 (SE + M1);
- Minimum Bias Event 1 + Minimum Bias Event 1 (M1 + M1); and
- Minimum Bias Event 1 + Minimum Bias Event 2 (M1 + M2).

For each of these pairings, each particle within the jet cone in the first event is paired with each particle within the jet cone in the second event. From these components, the background estimation is constructed as follows. The SE + M1 pairing provides a good description of the S + B component, since the underlying event is uncorrelated from the signal. However, it does not describe the B + B component properly. This occurs for two reasons. First, correlations in the underlying event are lost when pairing underlying event particles between two cones. Second, the B + B component is overestimated when pairing all underlying event particles from the signal cone with those from the mixed cone. This overestimation is illustrated in a simple example. Assume you have ten underlying event particles in the signal cone. The number of unique particle pairs in the true B + B background is $\binom{10}{2} = 45$. However, if also the mixed cone has ten underlying event particles, pairing all underlying event particles from the signal cone with all underlying event particles in the mixed cone gives $10 \times 10 = 100$ unique pairings. Thus, we need to subtract this mismodeled B + B component from the background estimator, and add a properly modeled B + B component into it. This is done by using pairings from only minimum bias events. The probability that a random cone in a minimum bias event contains jet signal is negligible; hence, M1 + M1 pairings provide an accurate description of the B + B component as they retain correlations within the underlying event and avoid overcounting pairs. Conversely, M1 + M2 pairings give the B + B component that suffers from issues of losing correlations in the underlying events and overestimating background pairs. Using these pairings, we can construct the mixed cone background estimation with:

$$\text{BG}_{\text{mixed}} = (\text{SE} + \text{M1}) + (\text{M1} + \text{M1}) - (\text{M1} + \text{M2}). \quad (2)$$

This method accurately reproduces the generator-level background in the PYTHIA+HYDJET simulation for the entire kinematic region used in the analysis.

To correct for detector and background fluctuation effects that can affect the p_T range to which a given jet is associated, we apply an iterative D'Agostini unfolding method [73] with early stopping, as implemented in the ROOUNFOLD software package [74]. The response matrices are constructed using PYTHIA simulation for pp and PYTHIA+HYDJET simulation for PbPb collisions. To take into account possible bin-by-bin statistical correlations in Δr , a covariance matrix determined from data is provided to the unfolding procedure to properly treat the statistical uncertainties. The number of iterations is chosen by calculating the χ^2 value between consecutive unfolded distributions and determining the iteration number where the corresponding p -value [75] describing if the two distributions match becomes larger than 0.05. This method gives four as the best number of iterations for this analysis.

In addition to single-track efficiency corrections mentioned in Section 4, track pair efficiency corrections were derived from PYTHIA simulation for pp and PYTHIA+HYDJET simulation for PbPb collisions. These corrections account for remaining reconstruction effects for charged particles. The efficiency to reconstruct a pair of tracks drops sharply for opening angles $\Delta r \lesssim 0.015$. After applying the pair efficiency correction, the simulation shows good closure. Bin-to-bin resolution effects in Δr are not significant above $\Delta r \gtrsim 0.008$, negating the need to unfold Δr when restricting the analysis to this region. This choice does not impact the results, as the substructure modifications are expected to manifest themselves for $\Delta r \gtrsim 0.08$.

The analysis flow is as follows: first, construct the energy-energy correlators with tracking efficiency corrections; next, unfold the detector and background fluctuation effects that can lead to the migration of a $p_{T,jet}$ value across a range boundary; and finally, subtract the background from the unfolded distribution. The unfolding is done before background subtraction to correct for the higher average underlying event level within a jet cone compared to a random cone. In the background subtraction step, an additional scaling factor for BG_{mixed} is needed. Because of detector resolution effects, a true $p_{T,jet}$ value is likely to be slightly smaller than the corresponding reconstructed $p_{T,jet}$ value. Thus, the unfolding procedure applies a slight upward shift to the ranges of reconstructed $p_{T,jet}$ values considered, such that the defined $p_{T,jet}$ range boundaries correspond to true $p_{T,jet}$ values after unfolding. Having higher mean $p_{T,jet}$ corresponds to having either more signal particles or signal particles having a higher mean p_T . Because the underlying event level does not strongly depend on $p_{T,jet}$, this leads to a better signal-to-background ratio for energy-energy correlators within higher p_T jets. Thus, we scale the BG_{mixed} distribution using a data-driven method to avoid over subtracting the unfolded distributions. This is done by noting that the peak position in the energy-energy correlator distribution depends on $p_{T,jet}$, as previously measured in pp collisions [17, 18]. Before unfolding, the mean $p_{T,jet}$ value in each $p_{T,jet}$ range is determined from the measured $p_{T,jet}$ distributions, and the $(S + B)/B$ ratio is estimated taking the ratio of integrals of the unsubtracted energy-energy correlator distribution and BG_{mixed} . We then relate the Δr positions of the energy-energy correlator peaks to the mean $p_{T,jet}$ values. Locating the peak positions after unfolding gives us the mean $p_{T,jet}$ values of the unfolded distributions. By interpolating between the $(S + B)/B$ and mean $p_{T,jet}$ values determined from the data before unfolding, the expected $(S + B)/B$ ratio at the unfolded mean $p_{T,jet}$ is found. Unfolding improves the $(S + B)/B$ ratio by 2–8%, depending on the kinematic selection. We then scale the BG_{mixed} such that this ratio is met. Denoting the scaled background as BG_{mixed}^{scaled} , the unfolded and fully corrected signal is extracted as

$$EEC_{signal} = EEC_{unfolded} - BG_{mixed}^{scaled}. \quad (3)$$

We have verified that the final closure of this method in PYTHIA+HYDJET simulation is consistent with unity within statistical uncertainties.

6 Systematic uncertainties

The systematic uncertainties of the energy-energy correlator distributions are categorized into two types: point-by-point uncertainties and shape uncertainties. To illustrate the sizes of uncertainties, we provide representative relative uncertainty values for low, intermediate, and high Δr ranges from the 0–10% central energy-energy correlator distributions with $n = 1$ and $p_T^{ch} > 1\text{ GeV}$ selection. The quoted relative uncertainty ranges reflect the span for different selections of $p_{T,jet}$. The point-by-point uncertainty sources are:

- *Tracking efficiency.* Following the method in Ref. [57], it is estimated that tracking efficiency differences between data and simulation are as much as 5% for PbPb collisions and 2.2% for pp collisions. To estimate uncertainties arising from this, the tracking efficiency corrections are varied by these amounts up and down. The resulting differences to nominal values are found to be negligible, since they do not induce a shape change and the distributions are normalized to unity in the analysis region.
- *Track selection.* For this uncertainty, we vary the track selections to be looser or tighter than the nominal ones. The looser selections are $\delta p_T/p_T < 0.15$ for PbPb only, and the distance of closest approach to a vertex divided by its uncertainty smaller than

five for both pp and PbPb. The tighter selections are $\chi^2/\text{dof}/N_{\text{layers}} < 0.15$ for PbPb only, $\delta p_T/p_T < 0.05$, and the distance of closest approach to a vertex divided by its uncertainty smaller than two for both pp and PbPb. The bigger difference to the nominal result is taken as a systematic uncertainty. Representative relative uncertainties are <5% in the low Δr region, <1% in the intermediate Δr region, and <3% in the high Δr region.

- *Track pair efficiency.* For the track pair efficiency, we vary the pair efficiency corrections to twice the amount of the single-track corrections. This is because the Δr dependent efficiency might be different between data and simulation compared to the general tracking efficiency. Doubling the variation covers possible extra differences. The track pair correction is thus varied up and down by 10% for PbPb collisions and 4.4% for pp collisions. The larger variation in the resulting distributions with respect to the nominal one is taken to be the systematic uncertainty. Representative relative uncertainties are <1% in the low and intermediate Δr regions, and 1–8% in the high Δr region.
- *Response matrix statistics.* To estimate the uncertainty coming from limited statistics in the simulations used to construct the unfolding response, we create 50 randomized response matrices. Each point in the original response matrix is randomized with a Gaussian distribution where the mean is the original value and σ is the uncertainty of this value. We then calculate the standard deviation of the unfolded results for each Δr value and assign this as the systematic uncertainty. Representative relative uncertainties are 1–2% in the low Δr region, and <1% in the intermediate and high Δr regions.

The shape uncertainty sources are:

- *Background subtraction.* The background subtraction uncertainty has two components.

First, there is an uncertainty for the background scaling factor that we use to obtain agreement with the expected signal-to-background ratio after unfolding. The nominal value is determined using an average of the scaling factors for the different jet p_T ranges, with the uncertainty taken as the largest difference of the individual values from the average. Representative relative uncertainties are <1% in the low and intermediate Δr regions, and 15–21% in the high Δr region.

Second, to estimate the uncertainty of the mixed cone background subtraction, we compare the results from this method to those from a reflected-cone method. In the reflected-cone method, we place a new jet cone in the same signal event, but reflect the η value of the jet axis (or shift it by $2R = 0.8$ if we are close to midrapidity to avoid the cones overlapping). We then pair each particle from the signal cone with each particle from the reflected cone to estimate the background. To overcome the background pair overcounting issues discussed earlier, we apply a scaling factor determined from the ratio of generator-level background to the reflected-cone background in the Monte Carlo simulation. This gives a reliable background estimate in the region where the B + B component of the background is small. For $n = 1$ and $p_T^{\text{ch}} > 1 \text{ GeV}$, where the B + B component is significant, we double the uncertainty found for the $n = 1$, $p_T^{\text{ch}} > 2 \text{ GeV}$ selection, as the reflected cone fails to provide a reasonable background estimate in this lower- p_T threshold case. Representative relative uncertainties are <1% in the low and intermediate Δr regions, and 11–17% in the high Δr region.

For pp collisions, where no background subtraction is done for the nominal results, we compare the nominal results to reflected-cone subtracted results. Here the scaling factors for the reflected cone are derived from the peripheral 85–95% centrality bin using the PYTHIA+HYDJET simulation, where differentiating signal and background is easier compared to pure PYTHIA. The reflected-cone background scaled using these factors is then subtracted from the unfolded distribution, and these results are compared to the nonsubtracted results to evaluate the uncertainty. Representative relative uncertainties are <1% in the low and intermediate Δr regions, and 1–2% in the high Δr region.

- *Jet energy resolution.* The uncertainties in the jet energy resolution are divided into centrality independent and centrality dependent parts. The centrality-independent part is applied for both pp and PbPb collisions. In the nominal result, the jet p_T response matrices for unfolding are constructed by increasing the jet p_T resolution by the estimated data-to-simulation difference. Different amounts of broadening are applied to account for uncertainties in data-to-simulation differences, and new response matrices are constructed for the different resolution values. The difference to nominal is taken as the uncertainty. Representative relative uncertainties are 1–3% in the low Δr region, <2% in the intermediate Δr region, and 4–7% in the high Δr region.

For the centrality-dependent uncertainty in PbPb collisions, we construct response matrices using 2% and 6% centrality shifts and compare the results to the nominal 4% shifted result. This degree of shift covers the possible difference in background energy density between data and simulation. Representative relative uncertainties are 1–4% in the low Δr region, <3% in the intermediate Δr region, and 6–10% in the high Δr region.

- *Jet energy scale.* To evaluate the uncertainties from the jet energy scale, we shift the jet p_T in the PYTHIA or PYTHIA+HYDJET simulations up and down by the uncertainty of the jet energy corrections. The procedure to estimate the uncertainty of the corrections is explained in detail in Ref. [76]. The jet energy correction uncertainties vary between 3–7% of the jet p_T , and are 3.6% on average. After shifting the jet p_T , we construct new response matrices using the shifted p_T values, and compare the final unfolded results to the nominal ones. Representative relative uncertainties are 6–10% in the low Δr region, 3–5% in the intermediate Δr region, and 30–45% in the high Δr region.
- *Unfolding prior.* The nominal response matrices for the analysis are constructed using the nominal PYTHIA and PYTHIA+HYDJET simulations. To estimate the uncertainty related to the shape of the prior, we find a function that scales the reconstructed jet p_T spectrum in PYTHIA to match the one in pp data. Then both generator- and reconstructed-level jet p_T spectra in PYTHIA and PYTHIA+HYDJET simulations are weighted with this function. The difference between the data unfolded with the nominal response matrices to the data unfolded with the weighted response matrices is taken as the systematic uncertainty of the prior distribution. Representative relative uncertainties are <4% in the low Δr region, <2% in the intermediate Δr region, and 3–6% in the high Δr region.
- *Monte Carlo model.* To evaluate the dependence of the unfolding performance on the used Monte Carlo model, the full analysis procedure with corrections and unfolding matrices derived from PYTHIA simulation was performed for HERWIG simulation and a second, statistically independent PYTHIA simulation. Both cases close

within the relevant systematics and are compatible with each other, so no additional uncertainty from the Monte Carlo model is needed.

- *Unfolding iterations.* The optimal number of iterations for the D’Agostini method is found to be four, as explained in Section 5. As an uncertainty for this number, we use three or five iterations and compare the resulting distributions to those unfolded with the nominal number of iterations. Representative relative uncertainties are <2% in the low and intermediate Δr regions, and 3–8% in the high Δr region.

To obtain the total point-by-point and shape systematic uncertainties, the uncertainties within each of these categories are added together in quadrature. These are then reported as two distinct sources of uncertainty. For PbPb to pp ratio plots, both categories of uncertainties are propagated as uncorrelated. Since the data-taking periods occurred in different years, uncertainties in the ratios do not cancel out. For double ratios of the PbPb to pp ratios with different p_T^{ch} thresholds, the jet related uncertainties fully cancel, and the track related uncertainties cancel for the overlapping part. The uncertainties are the highest in central collisions for low- p_T jets. They strongly depend on Δr , with the largest relative uncertainties occurring at high Δr , with somewhat smaller uncertainties at low Δr , and significantly smaller uncertainties at intermediate Δr . This happens as multiple sources of uncertainty “tilt” the distribution around a fixed central point, leading to an increase on one side and a decrease on the other. The relative uncertainties at high Δr are much higher because the energy-energy correlator distributions are steeply falling towards larger Δr values. The dominant source of systematic uncertainty is the jet energy scale, which is much larger than any other source. This results from the relatively narrow jet p_T ranges that are used in this analysis and from the dependence of the energy-energy correlator distribution shape on jet p_T .

7 Results

The energy-energy correlators for $p_T^{\text{ch}} > 1 \text{ GeV}$ are presented in Fig. 2 and for $p_T^{\text{ch}} > 2 \text{ GeV}$ in Fig. 3. First, comparing the shapes of the distributions in PbPb collisions to those from pp collisions, we observe the same general structure. An ascending slope marking the free-hadron region at small Δr , a peak related to a transition region at moderate Δr , and a descending slope interpreted as a free quark/gluon region at large Δr , as illustrated in Ref. [8] for pp collisions, are all also clearly visible in the PbPb data. Medium-induced emissions can break the angular ordering of emissions in vacuum QCD parton showers [77]. However, the similarity in the energy-energy correlator shapes between the collision systems suggests that at small Δr , the shower in PbPb collisions effectively follows angular ordering. The peak in the transition region consistently appears at lower Δr values in PbPb than in pp data, with a larger difference in more central collisions. This experimental result could be explained by virtuality evolution [78]. If the jets in PbPb collisions start with higher virtuality, they will have a longer shower duration to reach the scale of Λ_{QCD} and begin the hadronization process. Higher initial virtuality corresponds to higher initial jet p_T . Because jets in heavy ion collisions have, on average, experienced some amount of energy loss [27], the measured final-state jet p_T corresponds to higher initial jet p_T in PbPb collisions compared to pp collisions. Thus, the shift of the peak can be interpreted as an independent sign of jet quenching in PbPb collisions. It also provides an additional handle of the initial virtuality of the jet without requiring a photon or a Z boson tag. The shifting of the peak position towards lower Δr is also observed as a function of jet p_T . This follows naturally from the fact that higher p_T jets have higher initial virtuality.

To investigate predicted modifications to the jet substructure from interactions with quark-gluon plasma, we examine the ratios of the PbPb distributions to pp distributions from Figs. 2

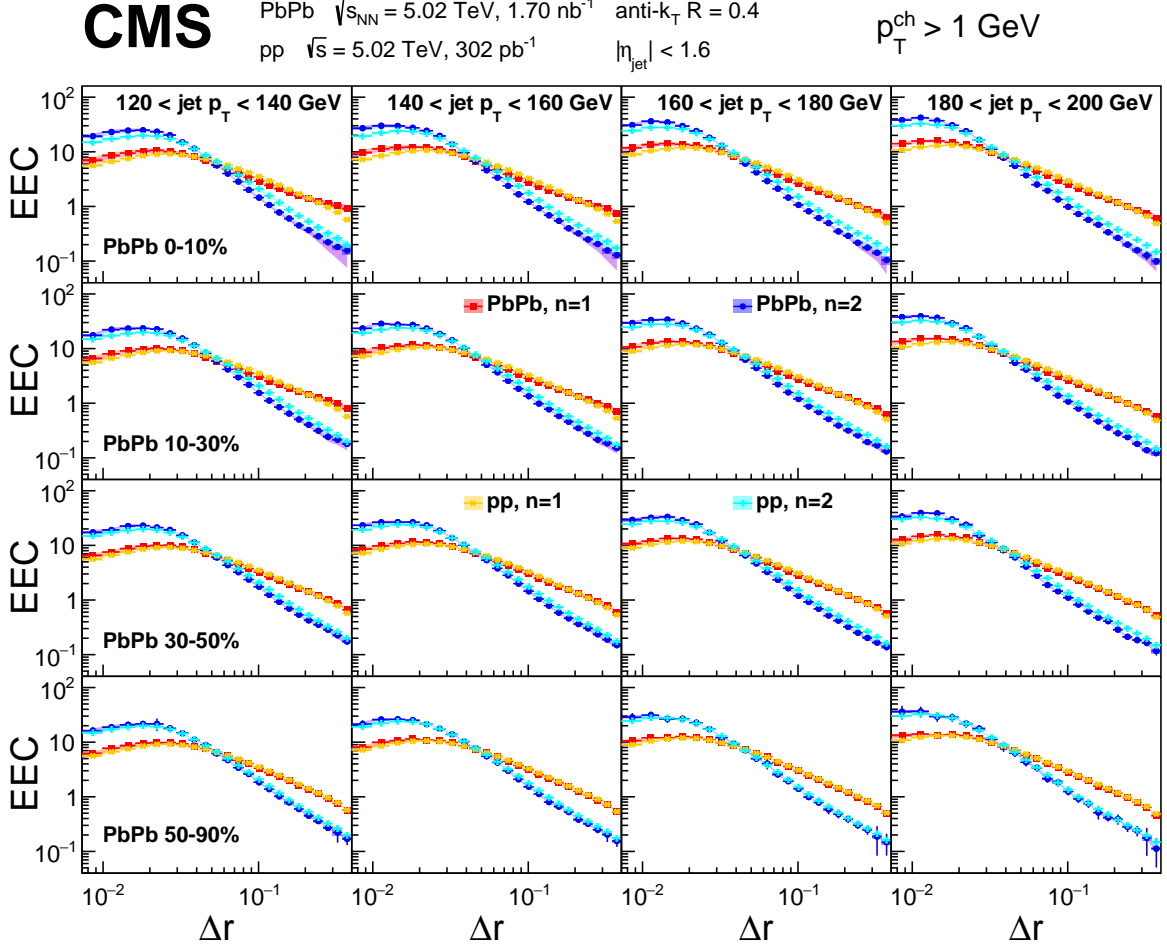


Figure 2: Centrality and $p_{\text{T,jet}}$ dependent energy-energy correlators for $p_{\text{T}}^{\text{ch}} > 1 \text{ GeV}$. The red squares show the $n = 1$ and the blue circles the $n = 2$ distributions for PbPb collisions. The pp results for different centralities are identical, with orange crosses showing the $n = 1$ and cyan triangle crosses the $n = 2$ distributions. The error bars show statistical uncertainties, the point-by-point systematic uncertainties are shown in boxes, while the error bands show systematic uncertainties related to the shape of the distribution. The two colors illustrate that the shape uncertainties tend to tilt the distribution one way or another. All correlators have been normalized to unity in the plotted range.

and 3 in Figs. 4 and 5, respectively. The shift in the peak position observed in the distributions appears as an enhancement in the ratios at small Δr . The effects of selecting different initial populations of jets between collision systems have been previously observed as inclusive jet substructure distributions getting narrower by ALICE [36, 79] and ATLAS [37]. A recent CMS γ -jet measurement shows that this narrowing occurs when selecting jets with minimal energy loss and vanishes when more quenched jets are included [80]. All of these results highlight the importance of understanding the biases in jet selection when comparing jets between different systems.

A key observation from the ratios is the enhancement of the PbPb to pp ratio for central collisions at large Δr with $n = 1$ and $p_{\text{T}}^{\text{ch}} > 1 \text{ GeV}$. This is the kinematic region of the highest sensitivity to medium modifications. Interestingly, if either the charged particle p_{T} threshold is increased to $p_{\text{T}}^{\text{ch}} > 2 \text{ GeV}$ or the momentum weight is increased to $n = 2$, this enhancement largely disappears. Both of these selections reduce the sensitivity to medium modifications by

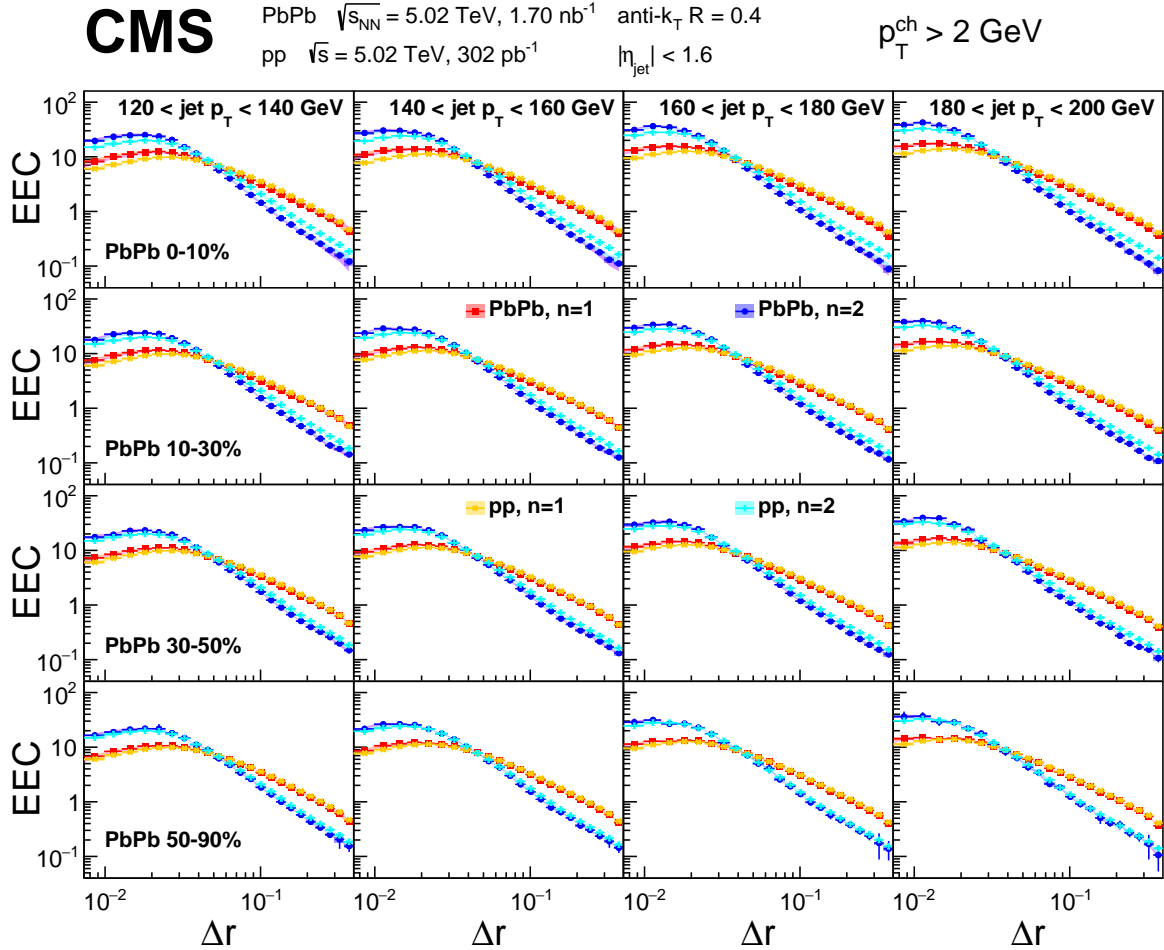


Figure 3: Centrality and $p_{\text{jet}}^{\text{ch}}$ dependent energy-energy correlators for $p_{\text{T}}^{\text{ch}} > 2 \text{ GeV}$. The red squares show the $n = 1$ and the blue circles the $n = 2$ distributions for PbPb collisions. The pp results for different centralities are identical, with orange crosses showing the $n = 1$ and cyan triangle crosses the $n = 2$ distributions. The error bars show statistical uncertainties, the point-by-point systematic uncertainties are shown in boxes, while the error bands show systematic uncertainties related to the shape of the distribution. The two colors illustrate that the shape uncertainties tend to tilt the distribution one way or another. All correlators have been normalized to unity in the plotted range.

reducing the impact of soft particles at the periphery of the jet cone [29, 30]. For $n = 1$ with $p_{\text{T}}^{\text{ch}} > 1 \text{ GeV}$, where the enhancement is visible, the change of shape from descending slope at low Δr to ascending slope at large Δr happens around $\Delta r \approx 0.07\text{--}0.09$. Similar values have been recently suggested to be the relevant angular scales for the coherence length [81]. The size of the enhancement at large Δr gradually decreases when going from central to more peripheral collisions, and is no longer visible in the 50–90% centrality class. The enhancement is also stronger for lower jet p_{T} values compared to higher jet p_{T} selections.

We also focus on the low- Δr region in the ratios. In particular, in the lower jet p_{T} ranges, the first few Δr bins in the ratios correspond to the free-hadron regime. It can be observed that regardless of the p_{T}^{ch} threshold or the value of the momentum weight n , the results are similar. Additionally, the PbPb to pp ratio in the low- Δr region is relatively flat, before transitioning to a descending slope around the transition and free quark/gluon regimes. The flat ratio suggests a universal scaling behavior for free hadrons, even for jets that have propagated through quark-

gluon plasma.

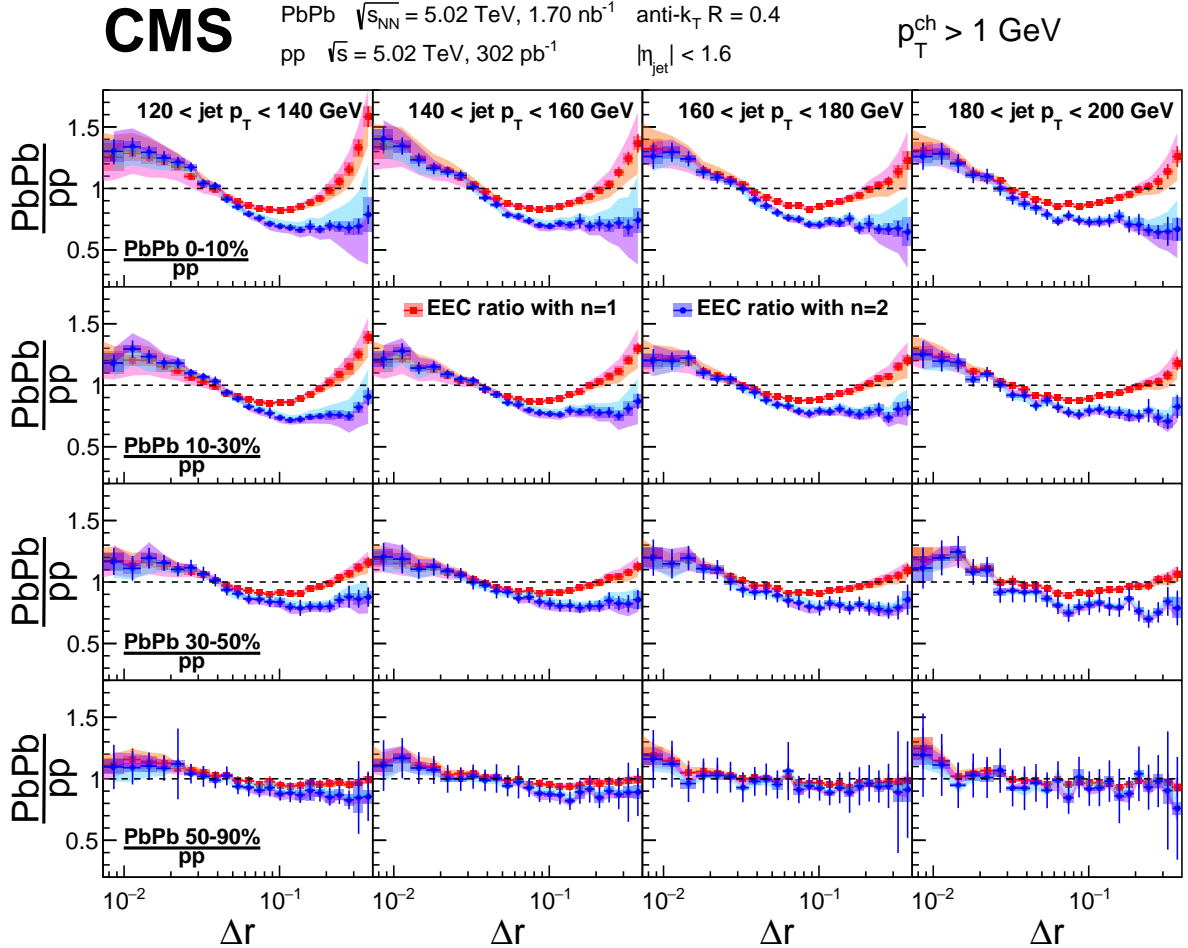


Figure 4: Centrality- and $p_{T,\text{jet}}$ -dependent ratios of PbPb to pp energy-energy correlators with $p_{T}^{\text{ch}} > 1 \text{ GeV}$ and for both $n = 1$ (red squares) and $n = 2$ (blue circles). The error bars show statistical uncertainties, the point-by-point systematic uncertainties are shown in boxes, while the error bands show systematic uncertainties related to the shape of the ratio. The two colors illustrate that the shape uncertainties tend to tilt the ratio one way or another.

Predictions from PYTHIA8 [58] tune CP5 [59], HERWIG7 [61, 62] tune CH3 [63], and a hybrid strong/weak coupling model [82–84] are compared to the pp results in Fig. 6. The vacuum in the hybrid strong/weak coupling model is described by a specific tune of PYTHIA8. The comparison is shown for $p_{T}^{\text{ch}} > 1 \text{ GeV}$, $120 < p_{T,\text{jet}} < 140 \text{ GeV}$, and for both momentum weights $n = 1$ and $n = 2$. Concentrating first on the comparison with $n = 1$, all models are found within 5–10% of the measurement, with HERWIG and the hybrid model slightly outperforming PYTHIA. Interestingly, the agreement with data gets worse for all of the models when the momentum weight is increased with $n = 2$. In this case, the models predict an energy-energy correlator distribution that is too narrow.

To better understand the observed medium modifications to energy-energy correlators, we compare the results to different model predictions, focusing on the high- Δr region. First, specifically to study the jet wake effects, we compare the PbPb to pp ratios with the hybrid model predictions in Fig. 7. The hybrid model predictions are shown with three different wake settings: no wake, only positive wake, and full wake. The “only positive” configuration disre-

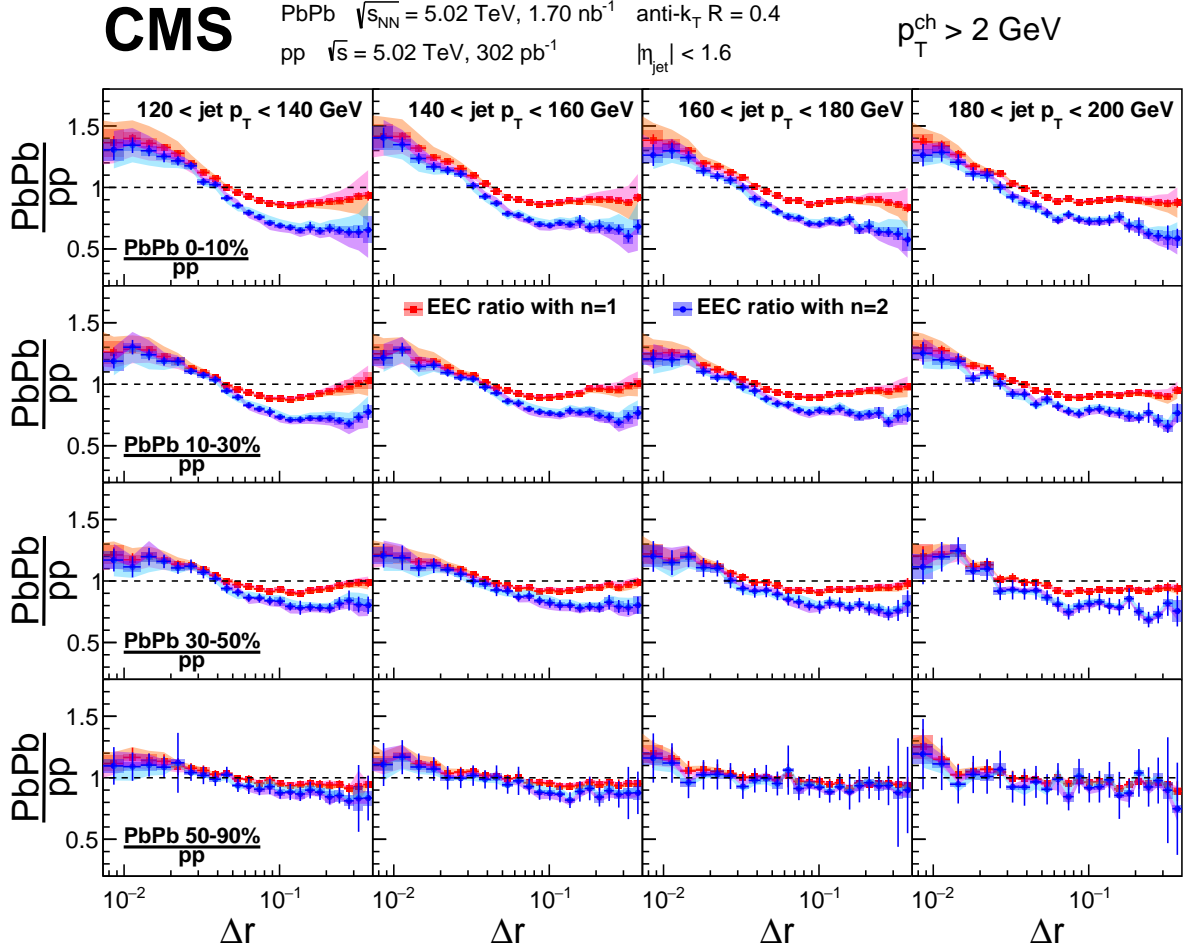


Figure 5: Centrality- and $p_{\text{T,jet}}$ -dependent ratios of PbPb to pp energy-energy correlators with $p_{\text{T}}^{\text{ch}} > 2 \text{ GeV}$ and for both $n = 1$ (red squares) and $n = 2$ (blue circles). The error bars show statistical uncertainties, the point-by-point systematic uncertainties are shown in boxes, while the error bands show systematic uncertainties related to the shape of the ratio. The two colors illustrate that the shape uncertainties tend to tilt the ratio one way or another.

gards the contribution from energy-momentum depletion the wake leaves to the quark-gluon plasma, while this is included in the “full wake” contribution. It can be seen that in both of the shown $p_{\text{T,jet}}$ selections, the change of slope from descending to ascending in the ratio only happens if the wake contributions are included. However, the location of the turning point and the magnitude of enhancement are different in the hybrid model prediction compared to data. While the wake likely influences the modifications at large angles, it cannot fully explain the observed effects.

We isolate the effects of the jet wake by taking a double ratio of PbPb to pp ratios between $p_{\text{T}}^{\text{ch}} > 2 \text{ GeV}$ and $p_{\text{T}}^{\text{ch}} > 1 \text{ GeV}$ thresholds, as shown in Fig. 8. The jet wake is created by jet particles, which generally have high- p_{T} values, interacting with mostly low- p_{T} underlying event particles. Contributions from these low-high p_{T} pairs are highlighted in the double ratio. By isolating the wake behavior, the hybrid model predictions that include a wake show significantly better agreement with the experimental results.

The measured PbPb to pp ratios are compared with a perturbative calculation by Holguin and collaborators [85] and with the JEWEL 2.4.0 simulation [86, 87] in Fig. 9. The perturbative

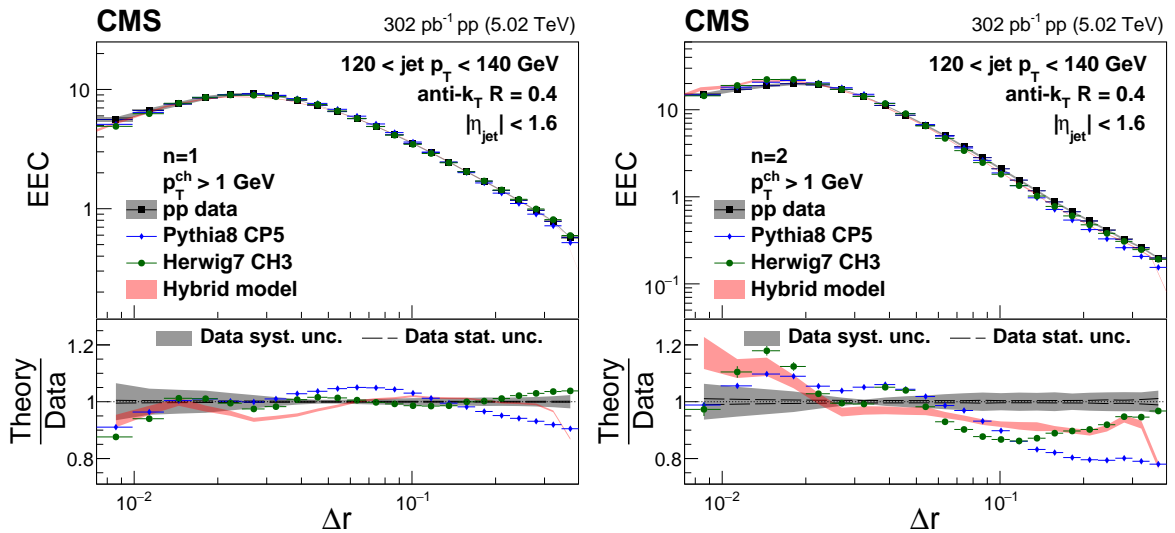


Figure 6: Comparison of PYTHIA [58], HERWIG [61, 62], and the hybrid model [82–84] calculations to the observed energy-energy correlators for $p_T^{\text{ch}} > 1 \text{ GeV}$, $120 < p_{T,\text{jet}} < 140 \text{ GeV}$ and $n = 1$ (left) and $n = 2$ (right) in pp collisions. In the lower panels, the experimental uncertainties are indicated by the bands around unity.

calculation includes physics from color coherence effects. It has two free parameters that have been fitted to the measured data. First, there is an overall normalization that is determined by matching the integral to the data in the region $0.042 < \Delta r < 0.126$. The second parameter is k , the constant of proportionality between the linear density of the medium and the temperature. In practice, k controls the amount of enhancement seen at large Δr . The small- Δr region is described by a simple nonperturbative model, so the predicted values below $\Delta r < 0.042$ are not expected to be reliable. The most robust prediction of this calculation is the turn-on angle, when the descending slope in the ratio turns into an ascending one, since neither of the free parameters affects this value. It can be seen that this calculation predicts the turn-on angle well for both $p_{T,\text{jet}}$ ranges shown in Fig. 9. This is a strong hint that this turn-on angle is indeed related to color coherence effects.

The medium response in JEWEL is implemented by thermal partons that undergo an elastic scattering with the jet parton. The thermal parton will receive a four-momentum kick from the jet parton, which makes it recoil from its original trajectory. After this recoil, these partons do not further interact before hadronization. Comparison with data is shown with and without these recoils. It can be seen that the JEWEL simulation with recoils and the associated thermal background subtraction has a descending slope with Δr , turning into an ascending slope around the same turn-on angle as in the data, although with poor agreement with the magnitude of the ratio. Without recoils, we see a falling trend in the ratio without a turn-on angle.

The PbPb to pp ratio is compared to CoLBT model [88–90] predictions in Fig. 10 for two different q values. The q parameter in the CoLBT model describes the minimum virtuality scale for the vacuum splittings, with $q = 0.5$ in the case of the pp reference data. The CoLBT model does not describe the data qualitatively when q is set to 0.5 for PbPb collisions. In data, we see a clear shift in initial virtuality for PbPb collisions compared to pp collisions. This shift in virtuality in the CoLBT model is reproduced by increasing the value of the q parameter, and we do indeed see much better qualitative agreement with $q = 1$. However, the turn-on angle is smaller than what is seen in the data, and not enough enhancement is predicted at large

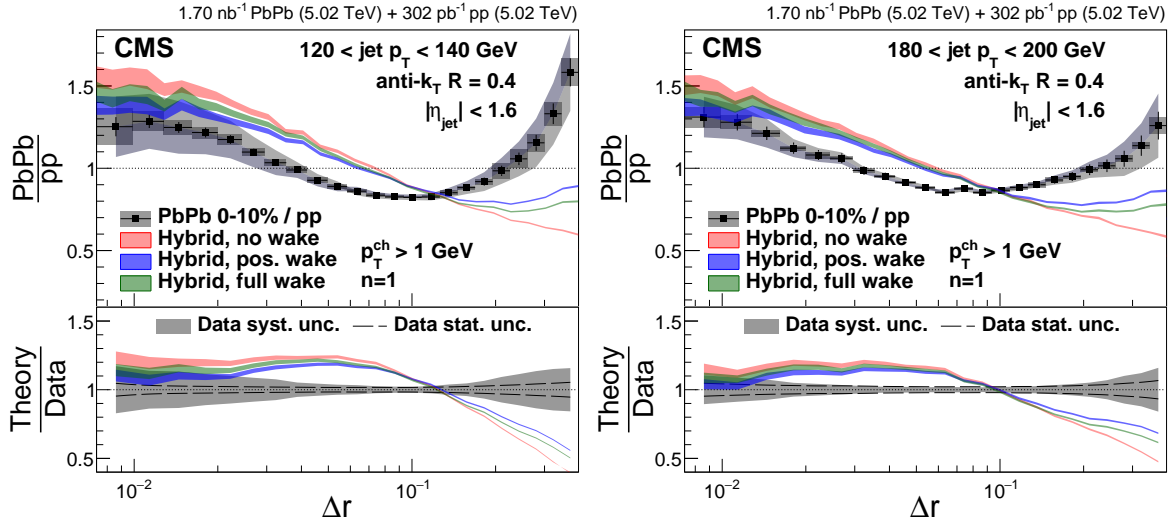


Figure 7: The PbPb to pp ratios of energy-energy correlators with $p_T^{\text{ch}} > 1 \text{ GeV}$ and $n = 1$ are shown for $120 < p_{T,\text{jet}} < 140 \text{ GeV}$ (left) and $180 < p_{T,\text{jet}} < 200 \text{ GeV}$ (right) together with the hybrid model [82–84] predictions with three different wake settings. In the lower panels, the experimental uncertainties are indicated by the bands around unity.

angles. The enhancement at large angles in the CoLBT model is coming from the medium response and medium-induced gluon radiation contributions, with the medium response being more important. This response includes recoil partons from interactions with the jet and the underlying event. The energy-momentum depletion in the quark-gluon plasma due to recoils is modeled as negative back reaction partons.

Model comparisons for more kinematic selections are available in Appendix A.

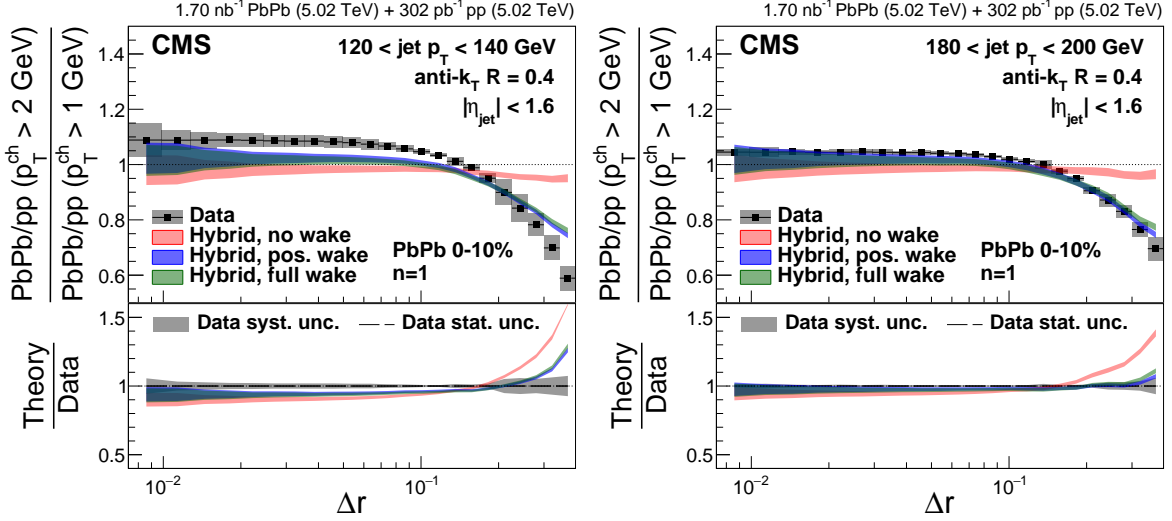


Figure 8: The double ratios of $n = 1$ PbPb to pp single ratios with $p_T^{\text{ch}} > 2 \text{ GeV}$ to $p_T^{\text{ch}} > 1 \text{ GeV}$ are shown for $120 < p_{T,\text{jet}} < 140 \text{ GeV}$ (left) and $180 < p_{T,\text{jet}} < 200 \text{ GeV}$ (right) together with the hybrid model [82–84] predictions with three different wake settings. In the lower panels, the experimental uncertainties are indicated by the bands around unity.

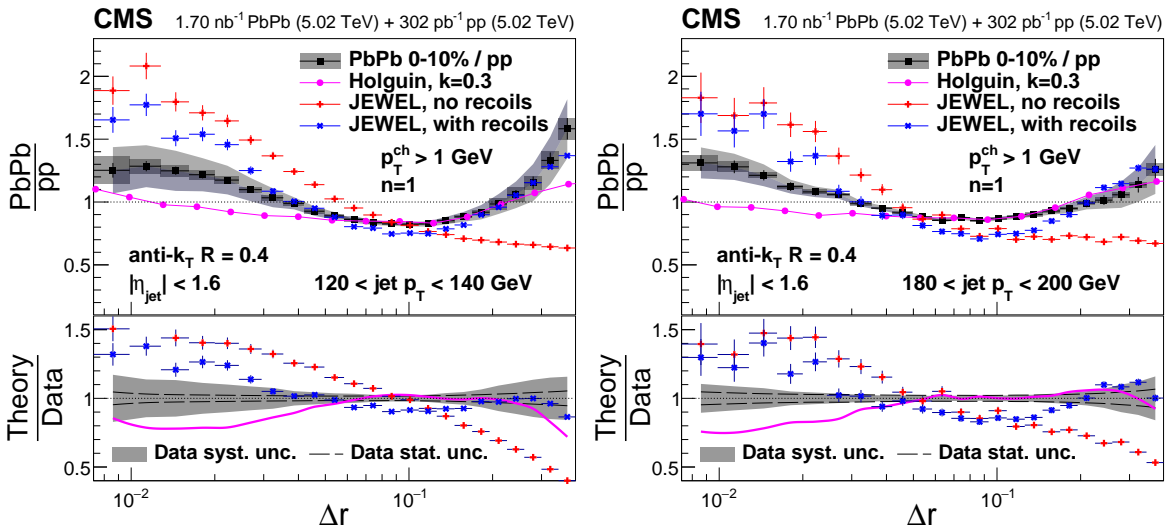


Figure 9: The PbPb to pp ratios of energy-energy correlators with $p_T^{\text{ch}} > 1 \text{ GeV}$ and $n = 1$ are shown for $120 < p_{T,\text{jet}} < 140 \text{ GeV}$ (left) and $180 < p_{T,\text{jet}} < 200 \text{ GeV}$ (right) together with predictions from perturbative calculation by Holguin and collaborators [85] and from JEWEL simulation [86, 87]. In the lower panels, the experimental uncertainties are indicated by the bands around unity.

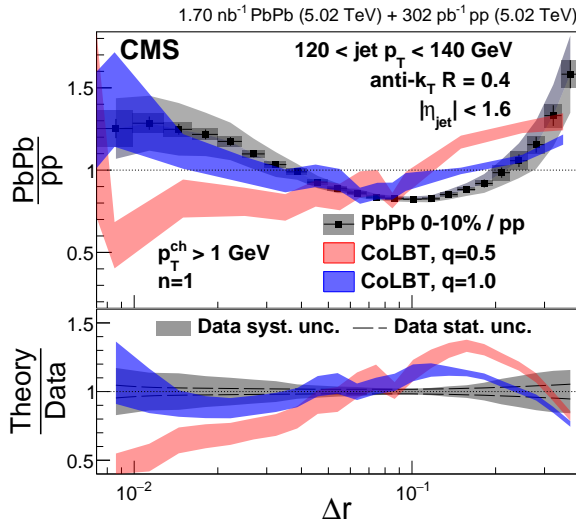


Figure 10: The PbPb to pp ratios of energy-energy correlators with $p_T^{\text{ch}} > 1 \text{ GeV}$ and $n = 1$ are shown for $120 < p_{T,\text{jet}} < 140 \text{ GeV}$ together with predictions from CoLBT model [88–90]. The q -values are shown for PbPb collisions, the value is fixed to 0.5 for pp. In the lower panel, the experimental uncertainties are indicated by the bands around unity.

8 Summary

For the first time, energy-energy correlators inside high transverse momentum (p_T) jets are measured in heavy ion collisions. The correlators from lead-lead (PbPb) data are compared to those from proton-proton (pp) collisions at the same nucleon-nucleon center-of-mass energy of 5.02 TeV obtained using the CMS detector. A highly differential measurement of the two-point energy correlators is presented as a function of separation in azimuth and pseudorapidity of two charged particles within a jet cone, Δr .

The time evolution of the jet fragmentation is imprinted in the shapes of the energy-energy correlator distributions. For both PbPb and pp collisions, we see similar large scale trends. There is a negative slope at large Δr in the data, which is interpreted to correspond to the dynamics of the parton shower phase. The positive slope at low Δr is expected to reflect the propagation of noninteracting hadrons. The transition region between these two limits is conjectured to be sensitive to information regarding the hadronization process. Within the same kinematic selections, the transition region in PbPb collisions is shifted to lower Δr values compared to pp collisions, consistent with parton energy loss. A pronounced enhancement at large Δr is observed in the ratio of the PbPb to pp distributions when using a low charged particle p_T threshold of $p_T^{\text{ch}} > 1 \text{ GeV}$ and taking the product of the p_T^{ch} of the two particles as the momentum weight. This enhancement disappears if the sensitivity to low- p_T particles is decreased by increasing the p_T^{ch} threshold to 2 GeV or by taking the square of the product as the momentum weight. A comparison of our data to several models suggests that medium response is partially accountable for the observed enhancement for large Δr values. A perturbative calculation with color coherence effects also appears to favor enhancement in this ratio at large Δr values. This measurement establishes a powerful new tool for studying the influence of medium response and color coherence on jet substructure and helps to elucidate how jets are affected by interactions with the quark-gluon plasma.

Acknowledgments

We congratulate our colleagues in the CERN accelerator departments for the excellent performance of the LHC and thank the technical and administrative staffs at CERN and at other CMS institutes for their contributions to the success of the CMS effort. In addition, we gratefully acknowledge the computing centers and personnel of the Worldwide LHC Computing Grid and other centers for delivering so effectively the computing infrastructure essential to our analyses. Finally, we acknowledge the enduring support for the construction and operation of the LHC, the CMS detector, and the supporting computing infrastructure provided by the following funding agencies: SC (Armenia), BMBWF and FWF (Austria); FNRS and FWO (Belgium); CNPq, CAPES, FAPERJ, FAPERGS, and FAPESP (Brazil); MES and BNSF (Bulgaria); CERN; CAS, MoST, and NSFC (China); MINCIENCIAS (Colombia); MSES and CSF (Croatia); RIF (Cyprus); SENESCYT (Ecuador); ERC PRG, RVTT3 and MoER TK202 (Estonia); Academy of Finland, MEC, and HIP (Finland); CEA and CNRS/IN2P3 (France); SRNSF (Georgia); BMBF, DFG, and HGF (Germany); GSRI (Greece); NKFIH (Hungary); DAE and DST (India); IPM (Iran); SFI (Ireland); INFN (Italy); MSIP and NRF (Republic of Korea); MES (Latvia); LMELT (Lithuania); MOE and UM (Malaysia); BUAP, CINVESTAV, CONACYT, LNS, SEP, and UASLP-FAI (Mexico); MOS (Montenegro); MBIE (New Zealand); PAEC (Pakistan); MES and NSC (Poland); FCT (Portugal); MESTD (Serbia); MICIU/AEI and PCTI (Spain); MOSTR (Sri Lanka); Swiss Funding Agencies (Switzerland); MST (Taipei); MHESI and NSTDA (Thailand); TUBITAK and TENMAK (Turkey); NASU (Ukraine); STFC (United Kingdom); DOE and NSF (USA).

Individuals have received support from the Marie-Curie program and the European Research Council and Horizon 2020 Grant, contract Nos. 675440, 724704, 752730, 758316, 765710, 824093, 101115353, 101002207, and COST Action CA16108 (European Union); the Leventis Foundation; the Alfred P. Sloan Foundation; the Alexander von Humboldt Foundation; the Science Committee, project no. 22rl-037 (Armenia); the Fonds pour la Formation à la Recherche dans l'Industrie et dans l'Agriculture (FRIA-Belgium); the Beijing Municipal Science & Technology Commission, No. Z191100007219010 and Fundamental Research Funds for the Central Universities (China); the Ministry of Education, Youth and Sports (MEYS) of the Czech Republic; the Shota Rustaveli National Science Foundation, grant FR-22-985 (Georgia); the Deutsche Forschungsgemeinschaft (DFG), among others, under Germany's Excellence Strategy – EXC 2121 "Quantum Universe" – 390833306, and under project number 400140256 - GRK2497; the Hellenic Foundation for Research and Innovation (HFRI), Project Number 2288 (Greece); the Hungarian Academy of Sciences, the New National Excellence Program - ÚNKP, the NKFIH research grants K 131991, K 133046, K 138136, K 143460, K 143477, K 146913, K 146914, K 147048, 2020-2.2.1-ED-2021-00181, TKP2021-NKTA-64, and 2021-4.1.2-NEMZ-KI-2024-00036 (Hungary); the Council of Science and Industrial Research, India; ICSC – National Research Center for High Performance Computing, Big Data and Quantum Computing and FAIR – Future Artificial Intelligence Research, funded by the NextGenerationEU program (Italy); the Latvian Council of Science; the Ministry of Education and Science, project no. 2022/WK/14, and the National Science Center, contracts Opus 2021/41/B/ST2/01369 and 2021/43/B/ST2/01552 (Poland); the Fundação para a Ciência e a Tecnologia, grant CEECIND/01334/2018 (Portugal); the National Priorities Research Program by Qatar National Research Fund; MICIU/AEI/10.13039/501100011033, ERDF/EU, "European Union NextGenerationEU/PRTR", and Programa Severo Ochoa del Principado de Asturias (Spain); the Chulalongkorn Academic into Its 2nd Century Project Advancement Project, and the National Science, Research and Innovation Fund via the Program Management Unit for Human Resources & Institutional Development, Research and Innovation, grant B39G670016 (Thailand); the Kavli Foundation; the Nvidia Corporation; the SuperMicro Corporation; the Welch Foundation, contract C-1845; and the Weston Havens Foundation (USA).

References

- [1] C. L. Basham, L. S. Brown, S. D. Ellis, and S. T. Love, "Energy correlations in electron-positron annihilation: Testing quantum chromodynamics", *Phys. Rev. Lett.* **41** (1978) 1585, doi:[10.1103/PhysRevLett.41.1585](https://doi.org/10.1103/PhysRevLett.41.1585).
- [2] C. L. Basham, L. S. Brown, S. D. Ellis, and S. T. Love, "Energy correlations in electron-positron annihilation in quantum chromodynamics: Asymptotically free perturbation theory", *Phys. Rev. D* **19** (1979) 2018, doi:[10.1103/PhysRevD.19.2018](https://doi.org/10.1103/PhysRevD.19.2018).
- [3] H. Chen et al., "Three point energy correlators in the collinear limit: symmetries, dualities and analytic results", *JHEP* **08** (2020) 028, doi:[10.1007/JHEP08\(2020\)028](https://doi.org/10.1007/JHEP08(2020)028), arXiv:[1912.11050](https://arxiv.org/abs/1912.11050).
- [4] H. Chen, I. Moult, X. Zhang, and H. X. Zhu, "Rethinking jets with energy correlators: Tracks, resummation, and analytic continuation", *Phys. Rev. D* **102** (2020) 054012, doi:[10.1103/PhysRevD.102.054012](https://doi.org/10.1103/PhysRevD.102.054012), arXiv:[2004.11381](https://arxiv.org/abs/2004.11381).
- [5] Y. Li et al., "Extending precision perturbative QCD with track functions", *Phys. Rev. Lett.* **128** (2022) 182001, doi:[10.1103/PhysRevLett.128.182001](https://doi.org/10.1103/PhysRevLett.128.182001), arXiv:[2108.01674](https://arxiv.org/abs/2108.01674).

- [6] E. Craft, K. Lee, B. Meçaj, and I. Moult, “Beautiful and charming energy correlators”, 2022. arXiv:2210.09311.
- [7] H. Chen et al., “Collinear parton dynamics beyond Dokshitzer-Gribov-Lipatov-Altarelli-Parisi framework”, *Phys. Rev. D* **111** (2025) 076021, doi:10.1103/PhysRevD.111.076021, arXiv:2210.10061.
- [8] P. T. Komiske, I. Moult, J. Thaler, and H. X. Zhu, “Analyzing n-point energy correlators inside jets with CMS open data”, *Phys. Rev. Lett.* **130** (2023) 051901, doi:10.1103/PhysRevLett.130.051901, arXiv:2201.07800.
- [9] K. Lee, B. Meçaj, and I. Moult, “Conformal collider physics meets LHC data”, *Phys. Rev. D* **111** (2025) L011502, doi:10.1103/PhysRevD.111.L011502, arXiv:2205.03414.
- [10] A. H. Mueller, “On the multiplicity of hadrons in QCD jets”, *Phys. Lett. B* **104** (1981) 161, doi:10.1016/0370-2693(81)90581-5.
- [11] B. I. Ermolaev and V. S. Fadin, “Log - log asymptotic form of exclusive cross-sections in quantum chromodynamics”, *JETP Lett.* **33** (1981) 269.
- [12] A. Bassutto, M. Ciafaloni, G. Marchesini, and A. H. Mueller, “Jet multiplicity and soft gluon factorization”, *Nucl. Phys. B* **207** (1982) 189, doi:10.1016/0550-3213(82)90161-4.
- [13] Y. L. Dokshitzer, V. A. Khoze, S. I. Troian, and A. H. Mueller, “QCD coherence in high-energy reactions”, *Rev. Mod. Phys.* **60** (1988) 373, doi:10.1103/RevModPhys.60.373.
- [14] C. Andrés et al., “Simple scaling laws for energy correlators in nuclear matter”, 2024. arXiv:2411.15298.
- [15] ALEPH Collaboration, “Measurement of α_s from the structure of particle clusters produced in hadronic Z decays”, *Phys. Lett. B* **257** (1991) 479, doi:10.1016/0370-2693(91)91926-M.
- [16] STAR Collaboration, “Measurement of two-point energy correlators within jets in $p+p$ collisions at $\sqrt{s} = 200 \text{ GeV}$ ”, 2025. arXiv:2502.15925.
- [17] ALICE Collaboration, “Exposing the parton-hadron transition within jets with energy-energy correlators in pp collisions at $\sqrt{s} = 5.02 \text{ TeV}$ ”, 2024. arXiv:2409.12687.
- [18] CMS Collaboration, “Measurement of energy correlators inside jets and determination of the strong coupling $\alpha_S(m_Z)$ ”, *Phys. Rev. Lett.* **133** (2024) 071903, doi:10.1103/PhysRevLett.133.071903, arXiv:2402.13864.
- [19] CMS Collaboration, “Observation and studies of jet quenching in PbPb collisions at $\sqrt{s_{\text{NN}}} = 2.76 \text{ TeV}$ ”, *Phys. Rev. C* **84** (2011) 024906, doi:10.1103/PhysRevC.84.024906, arXiv:1102.1957.
- [20] M. Arslanbek et al., “Hot QCD white paper”, 2023. arXiv:2303.17254.
- [21] S. Cao and X.-N. Wang, “Jet quenching and medium response in high-energy heavy-ion collisions: a review”, *Rept. Prog. Phys.* **84** (2021) 024301, doi:10.1088/1361-6633/abc22b, arXiv:2002.04028.

- [22] L. Apolinário, Y.-J. Lee, and M. Winn, “Heavy quarks and jets as probes of the QGP”, *Prog. Part. Nucl. Phys.* **127** (2022) 103990, doi:[10.1016/j.ppnp.2022.103990](https://doi.org/10.1016/j.ppnp.2022.103990), arXiv:[2203.16352](https://arxiv.org/abs/2203.16352).
- [23] PHENIX Collaboration, “Suppression of hadrons with large transverse momentum in central Au+Au collisions at $\sqrt{s_{\text{NN}}} = 130 \text{ GeV}$ ”, *Phys. Rev. Lett.* **88** (2002) 022301, doi:[10.1103/PhysRevLett.88.022301](https://doi.org/10.1103/PhysRevLett.88.022301), arXiv:[nucl-ex/0109003](https://arxiv.org/abs/nucl-ex/0109003).
- [24] STAR Collaboration, “Centrality dependence of high p_{T} hadron suppression in Au+Au collisions at $\sqrt{s_{\text{NN}}} = 130 \text{ GeV}$ ”, *Phys. Rev. Lett.* **89** (2002) 202301, doi:[10.1103/PhysRevLett.89.202301](https://doi.org/10.1103/PhysRevLett.89.202301), arXiv:[nucl-ex/0206011](https://arxiv.org/abs/nucl-ex/0206011).
- [25] CMS Collaboration, “Study of high- p_{T} charged particle suppression in PbPb compared to pp collisions at $\sqrt{s_{\text{NN}}} = 2.76 \text{ TeV}$ ”, *Eur. Phys. J. C* **72** (2012) 1945, doi:[10.1140/epjc/s10052-012-1945-x](https://doi.org/10.1140/epjc/s10052-012-1945-x), arXiv:[1202.2554](https://arxiv.org/abs/1202.2554).
- [26] ATLAS Collaboration, “Measurements of the nuclear modification factor for jets in Pb+Pb collisions at $\sqrt{s_{\text{NN}}} = 2.76 \text{ TeV}$ with the ATLAS detector”, *Phys. Rev. Lett.* **114** (2015) 072302, doi:[10.1103/PhysRevLett.114.072302](https://doi.org/10.1103/PhysRevLett.114.072302), arXiv:[1411.2357](https://arxiv.org/abs/1411.2357).
- [27] CMS Collaboration, “First measurement of large area jet transverse momentum spectra in heavy-ion collisions”, *JHEP* **05** (2021) 284, doi:[10.1007/JHEP05\(2021\)284](https://doi.org/10.1007/JHEP05(2021)284), arXiv:[2102.13080](https://arxiv.org/abs/2102.13080).
- [28] CMS Collaboration, “Modification of jet shapes in PbPb collisions at $\sqrt{s_{\text{NN}}} = 2.76 \text{ TeV}$ ”, *Phys. Lett. B* **730** (2014) 243, doi:[10.1016/j.physletb.2014.01.042](https://doi.org/10.1016/j.physletb.2014.01.042), arXiv:[1310.0878](https://arxiv.org/abs/1310.0878).
- [29] CMS Collaboration, “Jet properties in PbPb and pp collisions at $\sqrt{s_{\text{NN}}} = 5.02 \text{ TeV}$ ”, *JHEP* **05** (2018) 006, doi:[10.1007/JHEP05\(2018\)006](https://doi.org/10.1007/JHEP05(2018)006), arXiv:[1803.00042](https://arxiv.org/abs/1803.00042).
- [30] CMS Collaboration, “In-medium modification of dijets in PbPb collisions at $\sqrt{s_{\text{NN}}} = 5.02 \text{ TeV}$ ”, *JHEP* **05** (2021) 116, doi:[10.1007/JHEP05\(2021\)116](https://doi.org/10.1007/JHEP05(2021)116), arXiv:[2101.04720](https://arxiv.org/abs/2101.04720).
- [31] CMS Collaboration, “Measurement of jet fragmentation into charged particles in pp and PbPb collisions at $\sqrt{s_{\text{NN}}} = 2.76 \text{ TeV}$ ”, *JHEP* **10** (2012) 087, doi:[10.1007/JHEP10\(2012\)087](https://doi.org/10.1007/JHEP10(2012)087), arXiv:[1205.5872](https://arxiv.org/abs/1205.5872).
- [32] CMS Collaboration, “Measurement of the splitting function in pp and PbPb collisions at $\sqrt{s_{\text{NN}}} = 5.02 \text{ TeV}$ ”, *Phys. Rev. Lett.* **120** (2018) 142302, doi:[10.1103/PhysRevLett.120.142302](https://doi.org/10.1103/PhysRevLett.120.142302), arXiv:[1708.09429](https://arxiv.org/abs/1708.09429).
- [33] CMS Collaboration, “Measurement of the groomed jet mass in PbPb and pp collisions at $\sqrt{s_{\text{NN}}} = 5.02 \text{ TeV}$ ”, *JHEP* **10** (2018) 161, doi:[10.1007/JHEP10\(2018\)161](https://doi.org/10.1007/JHEP10(2018)161), arXiv:[1805.05145](https://arxiv.org/abs/1805.05145).
- [34] CMS Collaboration, “Measurement of quark- and gluon-like jet fractions using jet charge in PbPb and pp collisions at 5.02 TeV”, *JHEP* **07** (2020) 115, doi:[10.1007/JHEP07\(2020\)115](https://doi.org/10.1007/JHEP07(2020)115), arXiv:[2004.00602](https://arxiv.org/abs/2004.00602).
- [35] ALICE Collaboration, “Measurements of the groomed and ungroomed jet angularities in pp collisions at $\sqrt{s_{\text{NN}}} = 5.02 \text{ TeV}$ ”, *JHEP* **05** (2022) 061, doi:[10.1007/JHEP05\(2022\)061](https://doi.org/10.1007/JHEP05(2022)061), arXiv:[2107.11303](https://arxiv.org/abs/2107.11303).

- [36] ALICE Collaboration, “Measurement of the angle between jet axes in Pb–Pb collisions at $\sqrt{s_{\text{NN}}} = 5.02 \text{ TeV}$ ”, 2023. arXiv:2303.13347.
- [37] ATLAS Collaboration, “Measurement of substructure-dependent jet suppression in Pb+Pb collisions at 5.02 TeV with the ATLAS detector”, *Phys. Rev. C* **107** (2023) 054909, doi:10.1103/PhysRevC.107.054909, arXiv:2211.11470.
- [38] CMS Collaboration, “Overview of high-density QCD studies with the CMS experiment at the LHC”, *Phys. Rept.* **1115** (2025) 219, doi:10.1016/j.physrep.2024.11.007, arXiv:2405.10785.
- [39] C. Andrés, F. Dominguez, A. V. Sadofyev, and C. A. Salgado, “Jet broadening in flowing matter: Resummation”, *Phys. Rev. D* **106** (2022) 074023, doi:10.1103/PhysRevD.106.074023, arXiv:2207.07141.
- [40] C. Andrés et al., “Resolving the scales of the quark-gluon plasma with energy correlators”, *Phys. Rev. Lett.* **130** (2023) 262301, doi:10.1103/PhysRevLett.130.262301, arXiv:2209.11236.
- [41] C. Andrés et al., “A coherent view of the quark-gluon plasma from energy correlators”, *JHEP* **09** (2023) 088, doi:10.1007/JHEP09(2023)088, arXiv:2303.03413.
- [42] J. Barata, X. Mayo López, A. V. Sadofyev, and C. A. Salgado, “Medium induced gluon spectrum in dense inhomogeneous matter”, *Phys. Rev. D* **108** (2023) 034018, doi:10.1103/PhysRevD.108.034018, arXiv:2304.03712.
- [43] J. Barata, J.-P. Blaizot, and Y. Mehtar-Tani, “Quantum to classical parton dynamics in QCD media”, *Phys. Rev. D* **108** (2023) 014039, doi:10.1103/PhysRevD.108.014039, arXiv:2305.10476.
- [44] J. Barata, P. Caucal, A. Soto-Ontoso, and R. Szafron, “Advancing the understanding of energy-energy correlators in heavy-ion collisions”, *JHEP* **11** (2024) 060, doi:10.1007/JHEP11(2024)060, arXiv:2312.12527.
- [45] Z. Yang, Y. He, I. Moult, and X.-N. Wang, “Probing the short-distance structure of the quark-gluon plasma with energy correlators”, *Phys. Rev. Lett.* **132** (2024) 011901, doi:10.1103/PhysRevLett.132.011901, arXiv:2310.01500.
- [46] H. Bossi et al., “Imaging the wakes of jets with energy-energy-energy correlators”, *JHEP* **12** (2024) 073, doi:10.1007/JHEP12(2024)073, arXiv:2407.13818.
- [47] CMS Collaboration, “CMS luminosity measurement using nucleus-nucleus collisions at $\sqrt{s_{\text{NN}}} = 5.02 \text{ TeV}$ in 2018”, CMS Physics Analysis Summary CMS-PAS-LUM-18-001, 2022.
- [48] CMS Collaboration, “Precision luminosity measurement in proton-proton collisions at $\sqrt{s} = 13 \text{ TeV}$ in 2015 and 2016 at CMS”, *Eur. Phys. J. C* **81** (2021) 800, doi:10.1140/epjc/s10052-021-09538-2, arXiv:2104.01927.
- [49] HEPData record for this analysis, 2025. doi:10.17182/hepdata.156187.
- [50] CMS Collaboration, “Jet momentum dependence of jet quenching in PbPb collisions at $\sqrt{s_{\text{NN}}} = 2.76 \text{ TeV}$ ”, *Phys. Lett. B* **712** (2012) 176, doi:10.1016/j.physletb.2012.04.058, arXiv:1202.5022.

- [51] CMS Collaboration, “The CMS experiment at the CERN LHC”, *JINST* **3** (2008) S08004, doi:[10.1088/1748-0221/3/08/S08004](https://doi.org/10.1088/1748-0221/3/08/S08004).
- [52] CMS Collaboration, “Development of the CMS detector for the CERN LHC Run 3”, *JINST* **19** (2024) P05064, doi:[10.1088/1748-0221/19/05/P05064](https://doi.org/10.1088/1748-0221/19/05/P05064), arXiv:[2309.05466](https://arxiv.org/abs/2309.05466).
- [53] CMS Collaboration, “Performance of the CMS level-1 trigger in proton-proton collisions at $\sqrt{s} = 13\text{ TeV}$ ”, *JINST* **15** (2020) P10017, doi:[10.1088/1748-0221/15/10/P10017](https://doi.org/10.1088/1748-0221/15/10/P10017), arXiv:[2006.10165](https://arxiv.org/abs/2006.10165).
- [54] CMS Collaboration, “The CMS trigger system”, *JINST* **12** (2017) P01020, doi:[10.1088/1748-0221/12/01/P01020](https://doi.org/10.1088/1748-0221/12/01/P01020), arXiv:[1609.02366](https://arxiv.org/abs/1609.02366).
- [55] M. Cacciari, G. P. Salam, and G. Soyez, “The anti- k_T jet clustering algorithm”, *JHEP* **04** (2008) 063, doi:[10.1088/1126-6708/2008/04/063](https://doi.org/10.1088/1126-6708/2008/04/063), arXiv:[0802.1189](https://arxiv.org/abs/0802.1189).
- [56] O. Kodolova, I. Vardanyan, A. Nikitenko, and A. Oulianov, “The performance of the jet identification and reconstruction in heavy ions collisions with CMS detector”, *Eur. Phys. J. C* **50** (2007) 117, doi:[10.1140/epjc/s10052-007-0223-9](https://doi.org/10.1140/epjc/s10052-007-0223-9).
- [57] CMS Collaboration, “Charged-particle nuclear modification factors in PbPb and pPb collisions at $\sqrt{s_{\text{NN}}} = 5.02\text{ TeV}$ ”, *JHEP* **04** (2017) 039, doi:[10.1007/JHEP04\(2017\)039](https://doi.org/10.1007/JHEP04(2017)039), arXiv:[1611.01664](https://arxiv.org/abs/1611.01664).
- [58] T. Sjöstrand et al., “An introduction to PYTHIA 8.2”, *Comput. Phys. Commun.* **191** (2015) 159, doi:[10.1016/j.cpc.2015.01.024](https://doi.org/10.1016/j.cpc.2015.01.024), arXiv:[1410.3012](https://arxiv.org/abs/1410.3012).
- [59] CMS Collaboration, “Extraction and validation of a new set of CMS PYTHIA8 tunes from underlying-event measurements”, *Eur. Phys. J. C* **80** (2020) 4, doi:[10.1140/epjc/s10052-019-7499-4](https://doi.org/10.1140/epjc/s10052-019-7499-4), arXiv:[1903.12179](https://arxiv.org/abs/1903.12179).
- [60] NNPDF Collaboration, “Parton distributions from high-precision collider data”, *Eur. Phys. J. C* **77** (2017) 663, doi:[10.1140/epjc/s10052-017-5199-5](https://doi.org/10.1140/epjc/s10052-017-5199-5), arXiv:[1706.00428](https://arxiv.org/abs/1706.00428).
- [61] M. Bähr et al., “Herwig++ physics and manual”, *Eur. Phys. J. C* **58** (2008) 639, doi:[10.1140/epjc/s10052-008-0798-9](https://doi.org/10.1140/epjc/s10052-008-0798-9), arXiv:[0803.0883](https://arxiv.org/abs/0803.0883).
- [62] J. Bellm et al., “Herwig 7.0/Herwig++ 3.0 release note”, *Eur. Phys. J. C* **76** (2016) 196, doi:[10.1140/epjc/s10052-016-4018-8](https://doi.org/10.1140/epjc/s10052-016-4018-8), arXiv:[1512.01178](https://arxiv.org/abs/1512.01178).
- [63] CMS Collaboration, “Development and validation of HERWIG 7 tunes from CMS underlying-event measurements”, *Eur. Phys. J. C* **81** (2021) 312, doi:[10.1140/epjc/s10052-021-08949-5](https://doi.org/10.1140/epjc/s10052-021-08949-5), arXiv:[2011.03422](https://arxiv.org/abs/2011.03422).
- [64] GEANT4 Collaboration, “GEANT4—a simulation toolkit”, *Nucl. Instrum. Meth. A* **506** (2003) 250, doi:[10.1016/S0168-9002\(03\)01368-8](https://doi.org/10.1016/S0168-9002(03)01368-8).
- [65] I. P. Lokhtin et al., “Heavy ion event generator HYDJET++ (HYDrodynamics plus JETs)”, *Comput. Phys. Commun.* **180** (2009) 779, doi:[10.1016/j.cpc.2008.11.015](https://doi.org/10.1016/j.cpc.2008.11.015), arXiv:[0809.2708](https://arxiv.org/abs/0809.2708).
- [66] CMS Collaboration, “Description and performance of track and primary-vertex reconstruction with the CMS tracker”, *JINST* **9** (2014) P10009, doi:[10.1088/1748-0221/9/10/P10009](https://doi.org/10.1088/1748-0221/9/10/P10009), arXiv:[1405.6569](https://arxiv.org/abs/1405.6569).

- [67] CMS Collaboration, “Particle-flow reconstruction and global event description with the CMS detector”, *JINST* **12** (2017) P10003, doi:10.1088/1748-0221/12/10/P10003, arXiv:1706.04965.
- [68] M. Cacciari, G. P. Salam, and G. Soyez, “FastJet user manual”, *Eur. Phys. J. C* **72** (2012) 1896, doi:10.1140/epjc/s10052-012-1896-2, arXiv:1111.6097.
- [69] D. Bertolini, T. Chan, and J. Thaler, “Jet observables without jet algorithms”, *JHEP* **04** (2014) 013, doi:10.1007/JHEP04(2014)013, arXiv:1310.7584.
- [70] A. J. Larkoski, D. Neill, and J. Thaler, “Jet shapes with the broadening axis”, *JHEP* **04** (2014) 017, doi:10.1007/JHEP04(2014)017, arXiv:1401.2158.
- [71] P. Berta, M. Spousta, D. W. Miller, and R. Leitner, “Particle-level pileup subtraction for jets and jet shapes”, *JHEP* **06** (2014) 092, doi:10.1007/JHEP06(2014)092, arXiv:1403.3108.
- [72] ALICE Collaboration, “Higher harmonic anisotropic flow measurements of charged particles in Pb–Pb collisions at $\sqrt{s_{\text{NN}}} = 2.76 \text{ TeV}$ ”, *Phys. Rev. Lett.* **107** (2011) 032301, doi:10.1103/PhysRevLett.107.032301, arXiv:1105.3865.
- [73] G. D’Agostini, “A multidimensional unfolding method based on Bayes’ theorem”, *Nucl. Instrum. Meth. A* **362** (1995) 487, doi:10.1016/0168-9002(95)00274-X.
- [74] L. Brenner et al., “Comparison of unfolding methods using RooFitUnfold”, *Int. J. Mod. Phys. A* **35** (2020) 2050145, doi:10.1142/S0217751X20501456, arXiv:1910.14654.
- [75] E. Gross and O. Vitells, “Trial factors for the look elsewhere effect in high energy physics”, *Eur. Phys. J. C* **70** (2010) 525, doi:10.1140/epjc/s10052-010-1470-8, arXiv:1005.1891.
- [76] CMS Collaboration, “Jet energy scale and resolution in the CMS experiment in pp collisions at 8 TeV”, *JINST* **12** (2017) P02014, doi:10.1088/1748-0221/12/02/P02014, arXiv:1607.03663.
- [77] Y. Mehtar-Tani, C. A. Salgado, and K. Tywoniuk, “Anti-angular ordering of gluon radiation in QCD media”, *Phys. Rev. Lett.* **106** (2011) 122002, doi:10.1103/PhysRevLett.106.122002, arXiv:1009.2965.
- [78] S. Domdey et al., “QCD evolution of jets in the quark-gluon plasma”, *Nucl. Phys. A* **808** (2008) 178, doi:10.1016/j.nuclphysa.2008.04.010, arXiv:0802.3282.
- [79] ALICE Collaboration, “Measurement of the groomed jet radius and momentum splitting fraction in pp and Pb–Pb collisions at $\sqrt{s_{\text{NN}}} = 5.02 \text{ TeV}$ ”, *Phys. Rev. Lett.* **128** (2022) 102001, doi:10.1103/PhysRevLett.128.102001, arXiv:2107.12984.
- [80] CMS Collaboration, “Girth and groomed radius of jets recoiling against isolated photons in lead-lead and proton-proton collisions at $\sqrt{s_{\text{NN}}} = 5.02 \text{ TeV}$ ”, *Phys. Lett. B* **861** (2025) 139088, doi:10.1016/j.physletb.2024.139088, arXiv:2405.02737.
- [81] Y. Mehtar-Tani, D. Pablos, and K. Tywoniuk, “Jet suppression and azimuthal anisotropy from RHIC to LHC”, *Phys. Rev. D* **110** (2024) 014009, doi:10.1103/PhysRevD.110.014009, arXiv:2402.07869.

- [82] J. Casalderrey-Solana et al., “A hybrid strong/weak coupling approach to jet quenching”, *JHEP* **10** (2014) 019, doi:10.1007/JHEP10(2014)019, arXiv:1405.3864. [Erratum: doi:10.1007/JHEP09(2015)175].
- [83] J. Casalderrey-Solana et al., “Angular structure of jet quenching within a hybrid strong/weak coupling model”, *JHEP* **03** (2017) 135, doi:10.1007/JHEP03(2017)135, arXiv:1609.05842.
- [84] J. Casalderrey-Solana et al., “Simultaneous description of hadron and jet suppression in heavy-ion collisions”, *Phys. Rev. C* **99** (2019) 051901, doi:10.1103/PhysRevC.99.051901, arXiv:1808.07386.
- [85] C. Andrés et al., “Towards an interpretation of the first measurements of energy correlators in the quark-gluon plasma”, *JHEP* **03** (2025) 166, doi:10.1007/JHEP03(2025)166, arXiv:2407.07936.
- [86] K. Zapp et al., “A Monte Carlo model for ‘jet quenching’”, *Eur. Phys. J. C* **60** (2009) 617, doi:10.1140/epjc/s10052-009-0941-2, arXiv:0804.3568.
- [87] R. Kunawalkam Elayavalli and K. C. Zapp, “Medium response in JEWEL and its impact on jet shape observables in heavy ion collisions”, *JHEP* **07** (2017) 141, doi:10.1007/JHEP07(2017)141, arXiv:1707.01539.
- [88] W. Chen et al., “Effects of jet-induced medium excitation in γ -hadron correlation in A+A collisions”, *Phys. Lett. B* **777** (2018) 86, doi:10.1016/j.physletb.2017.12.015, arXiv:1704.03648.
- [89] W. Chen et al., “Medium modification of γ -jet fragmentation functions in Pb+Pb collisions at LHC”, *Phys. Lett. B* **810** (2020) 135783, doi:10.1016/j.physletb.2020.135783, arXiv:2005.09678.
- [90] W. Zhao et al., “From hydrodynamics to jet quenching, coalescence, and hadron cascade: A coupled approach to solving the $R_{AA} \otimes v_2$ puzzle”, *Phys. Rev. Lett.* **128** (2022) 022302, doi:10.1103/PhysRevLett.128.022302, arXiv:2103.14657.

A Supplemental material: model comparisons

Comparison between theoretical predictions and measured data in all kinematic ranges where predictions have been provided are presented in this supplemental material. The comparison between different models and pp distributions are presented in Figs. A.1–A.4. The comparisons between different models and PbPb distributions are in Figs. A.5–A.15, while the PbPb over pp ratios are presented in Figs. A.16–A.26. The comparison between measured double ratios and hybrid calculations are in Figs. A.27–A.30, while the same comparison with the JEWEL simulation is in Fig. A.31.

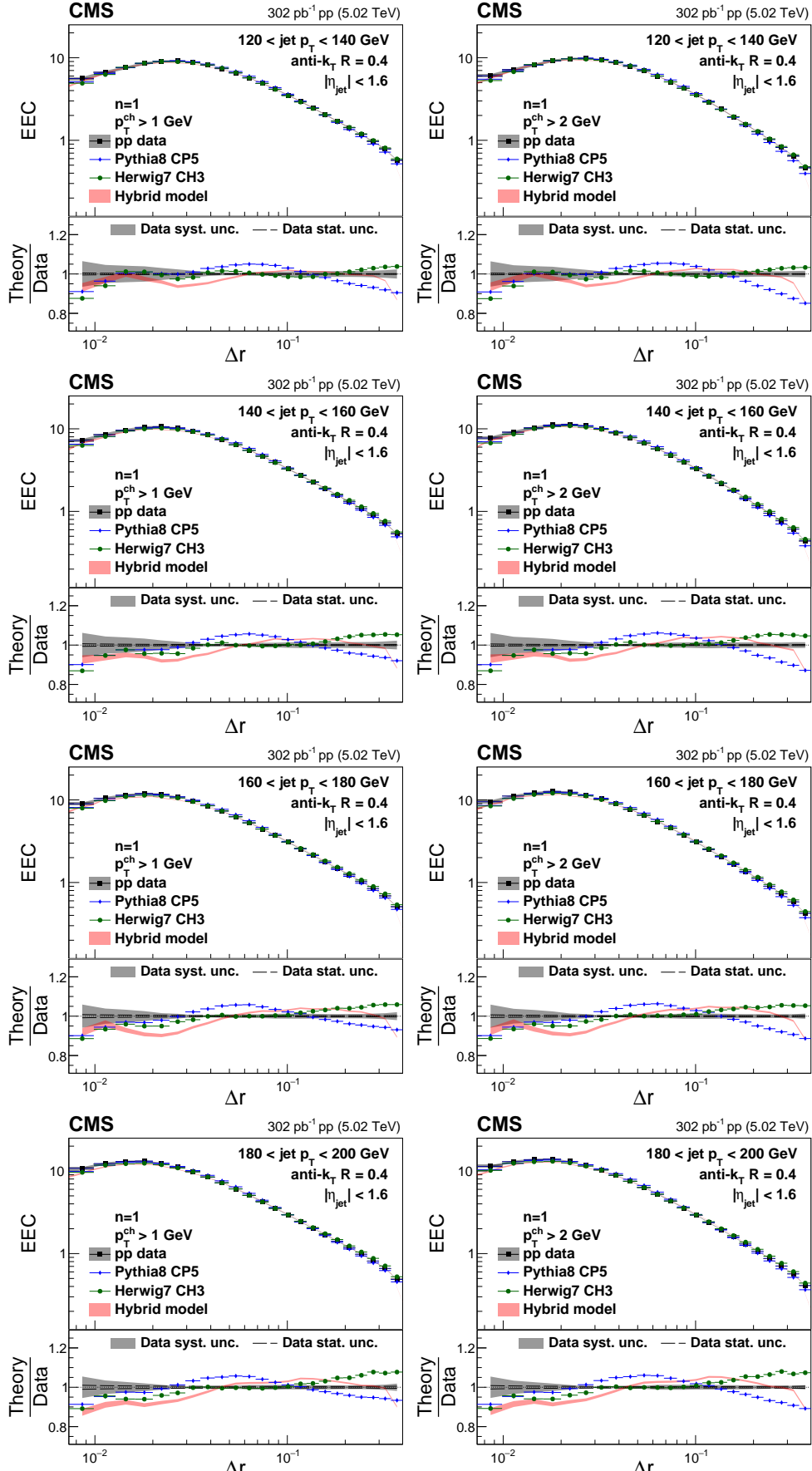


Figure A.1: Energy-energy correlator distributions from pp collisions with $n = 1$ in different p_T^{ch} and $p_{T,\text{jet}}$ bins compared to predictions from PYTHIA, HERWIG, and the hybrid model.

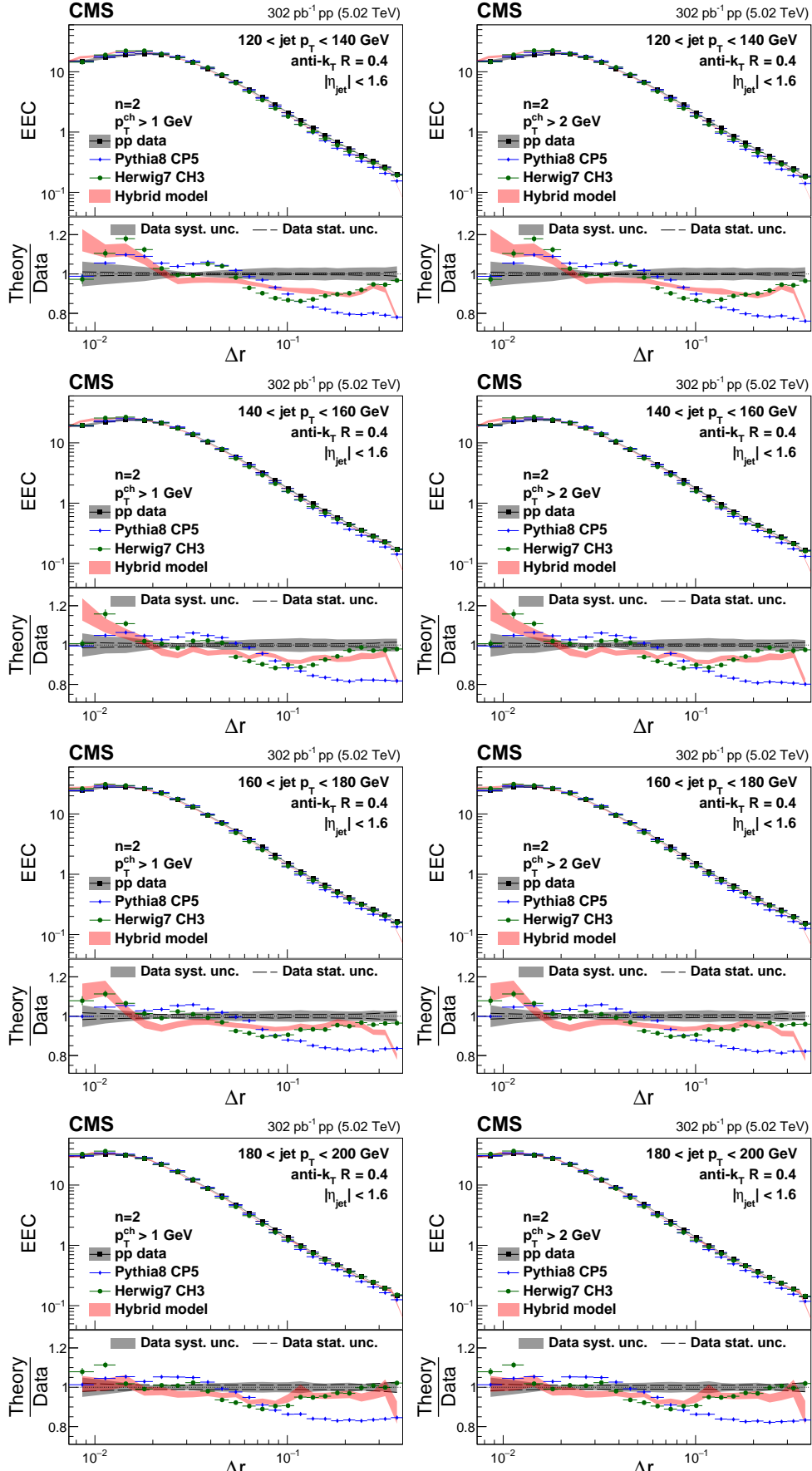


Figure A.2: Energy-energy correlator distributions from pp collisions with $n = 2$ in different p_T^{ch} and $p_{T,\text{jet}}$ bins compared to predictions from PYTHIA, HERWIG, and the hybrid model.

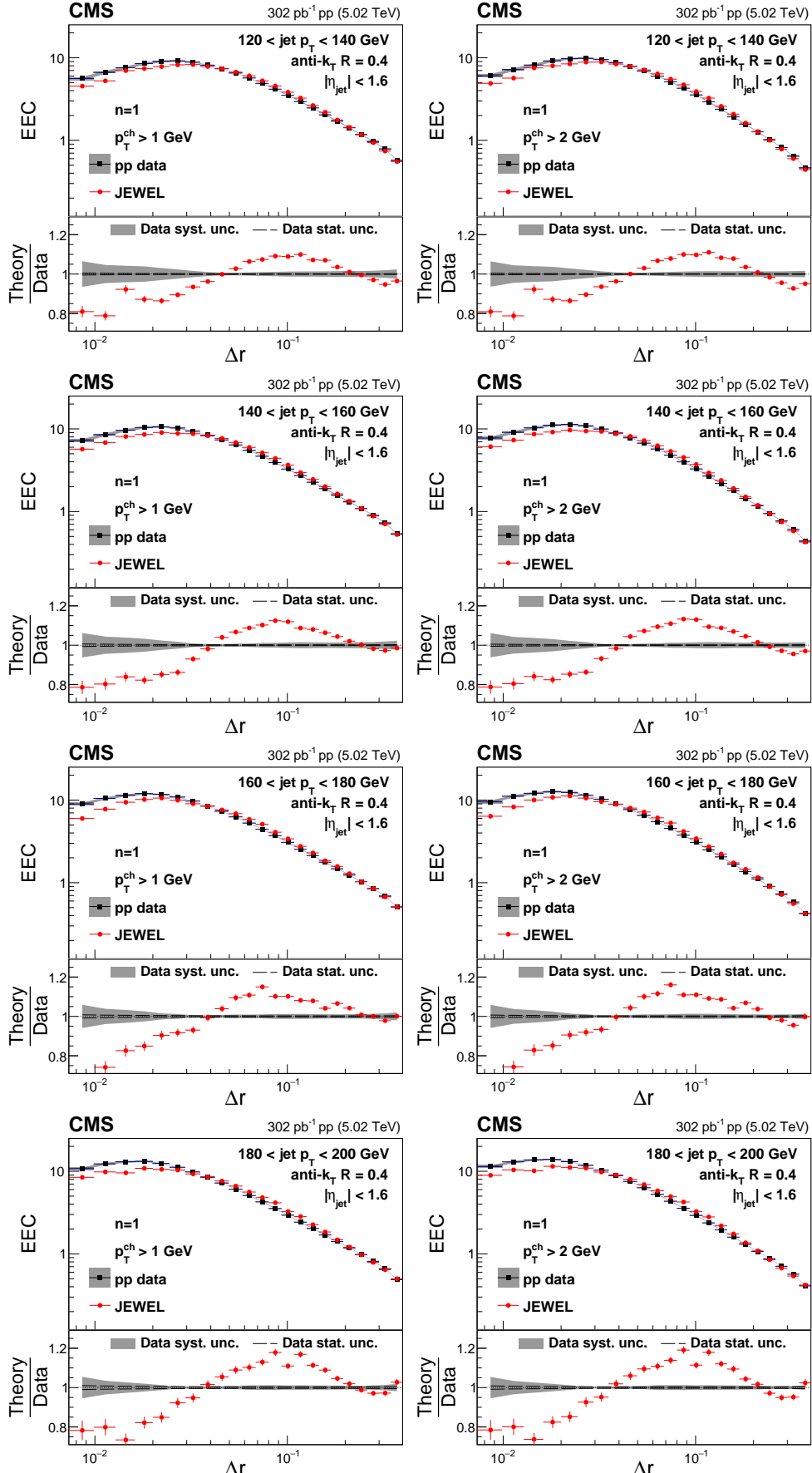


Figure A.3: Energy-energy correlator distributions from pp collisions with $n = 1$ in different p_T^{ch} and $p_{T,\text{jet}}$ bins compared to prediction from JEWEL.

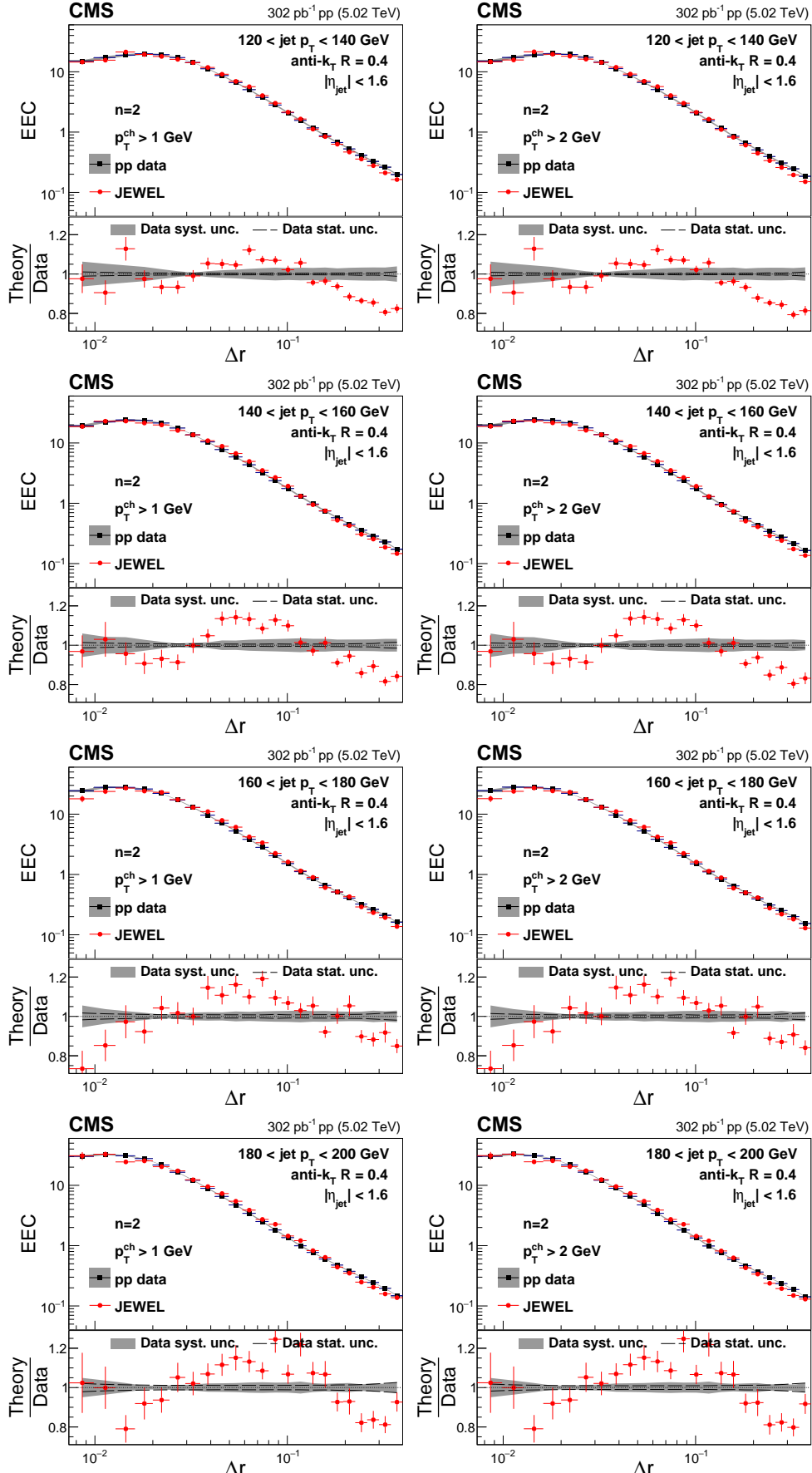


Figure A.4: Energy-energy correlator distributions from pp collisions with $n = 2$ in different p_T^{ch} and $p_{T,\text{jet}}$ bins compared to predictions from JEWEL.

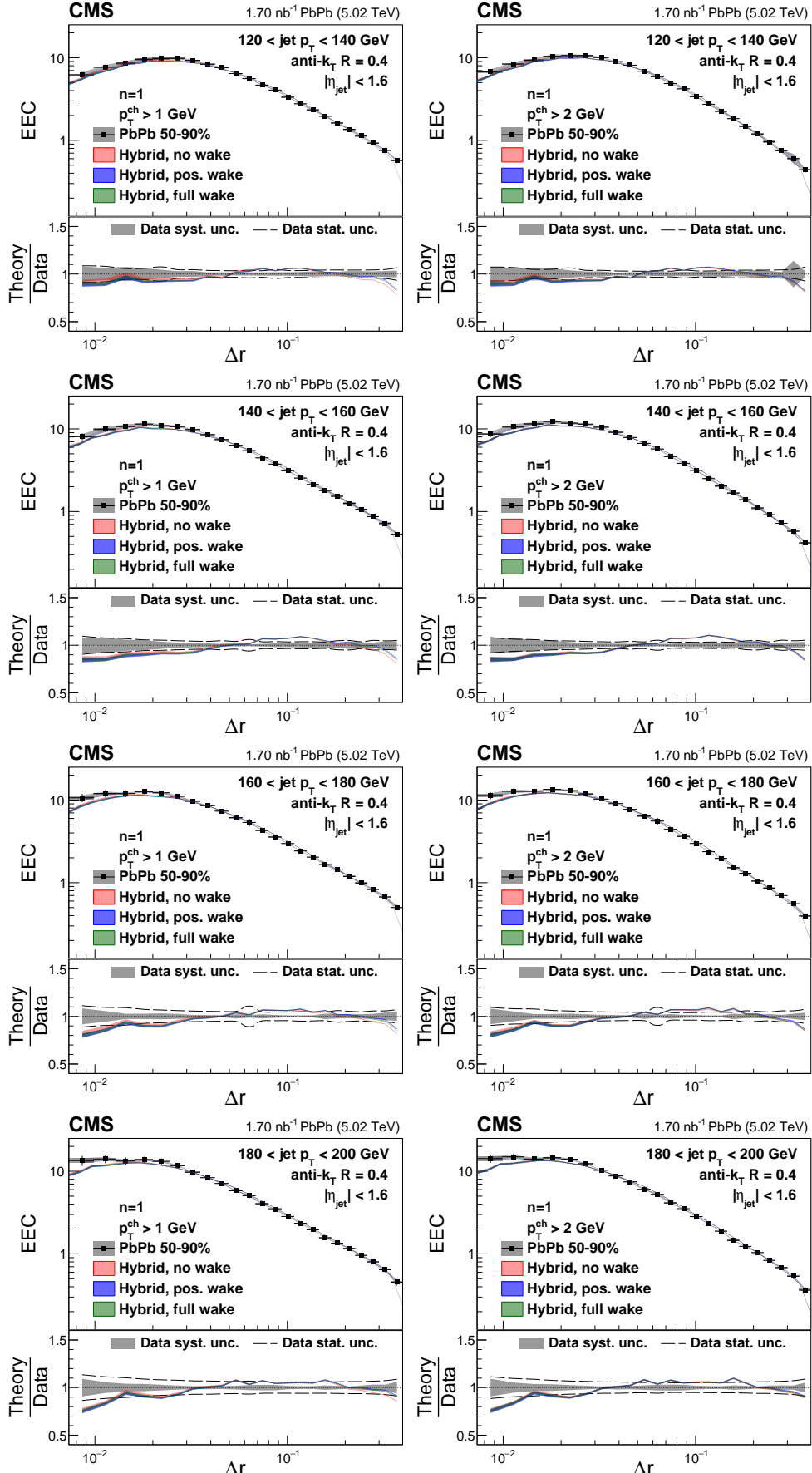


Figure A.5: Energy-energy correlator distributions from 50–90% central PbPb collisions with $n = 1$ in different p_T^{ch} and $p_{T,\text{jet}}$ bins compared to the hybrid model predictions with different jet wake settings.

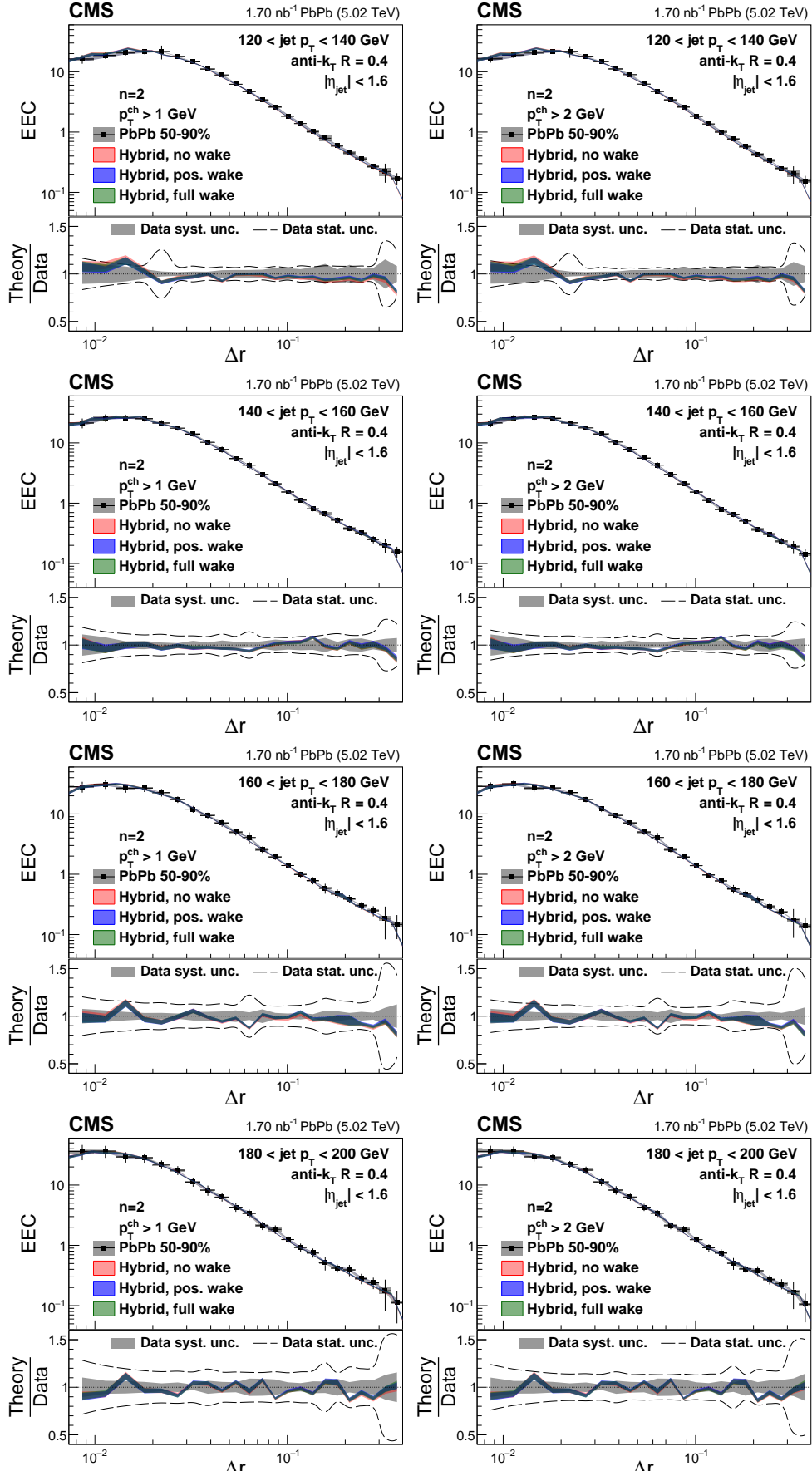


Figure A.6: Energy-energy correlator distributions from 50–90% central PbPb collisions with $n = 2$ in different p_T^{ch} and $p_{T,\text{jet}}$ bins compared to the hybrid model predictions with different jet wake settings.

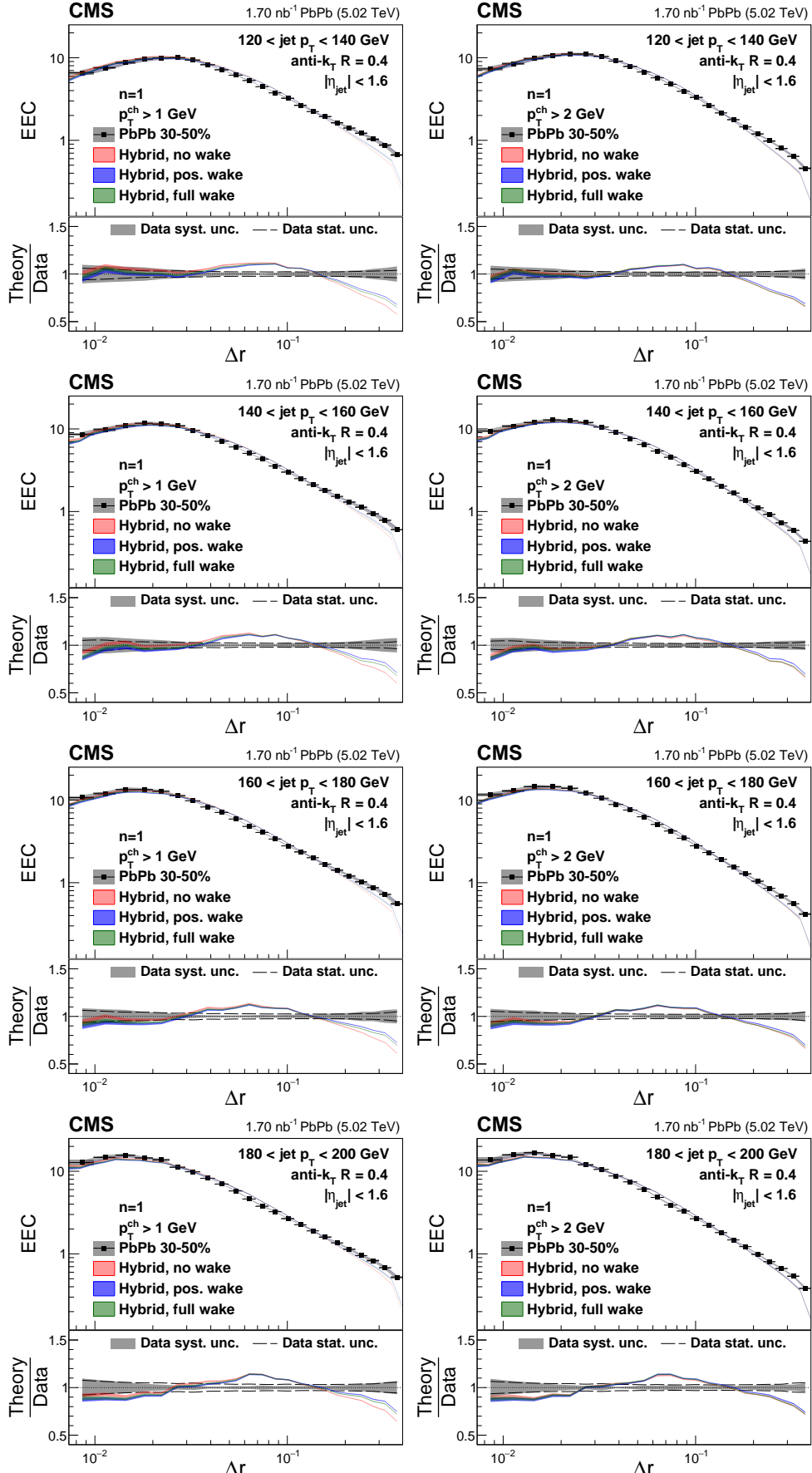


Figure A.7: Energy-energy correlator distributions from 30–50% central PbPb collisions with $n = 1$ in different p_T^{ch} and $p_{T,\text{jet}}$ bins compared to the hybrid model predictions with different jet wake settings.

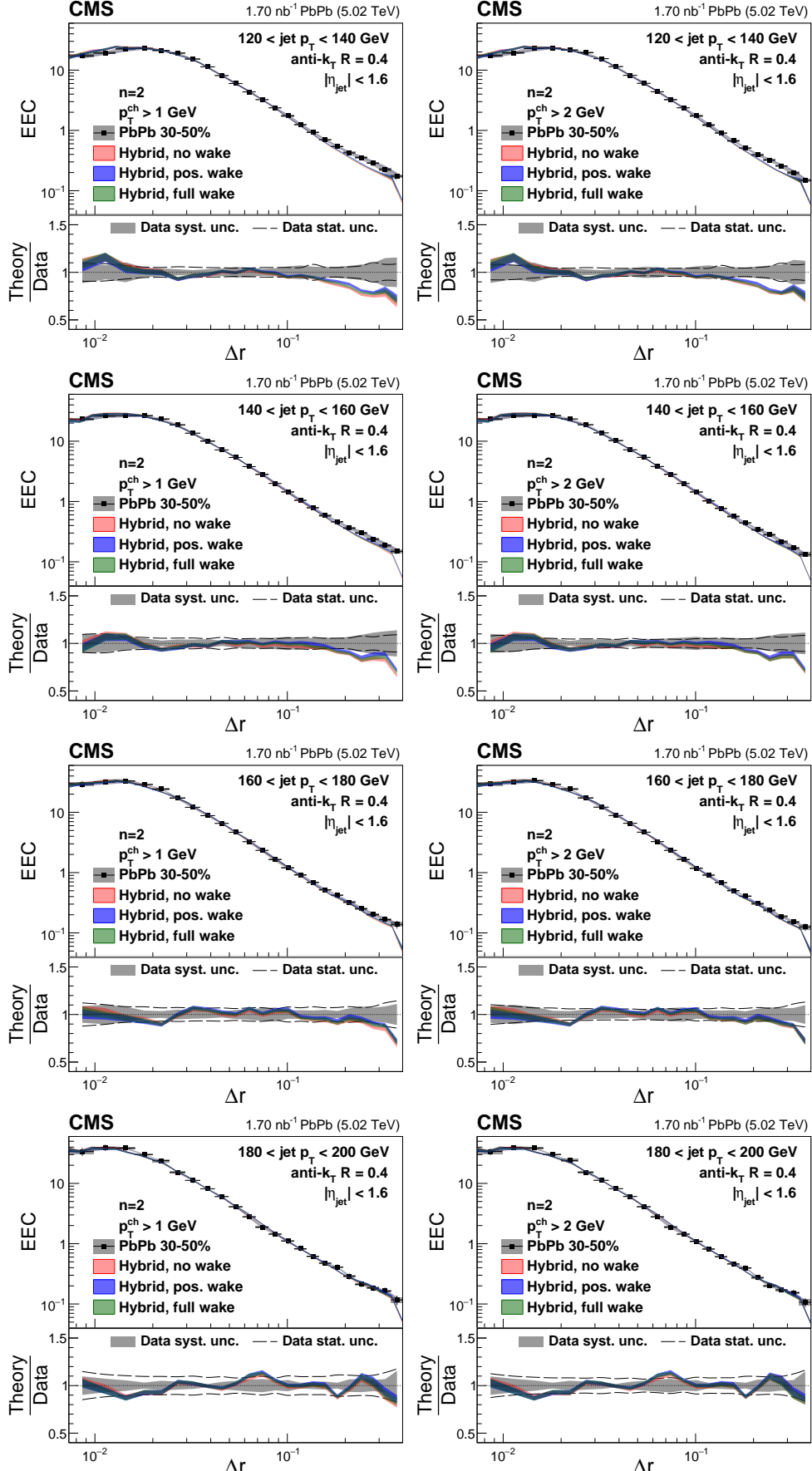


Figure A.8: Energy-energy correlator distributions from 30–50% central PbPb collisions with $n = 2$ in different $p_{T,\text{ch}}^{\text{ch}}$ and $p_{T,\text{jet}}$ bins compared to the hybrid model predictions with different jet wake settings.

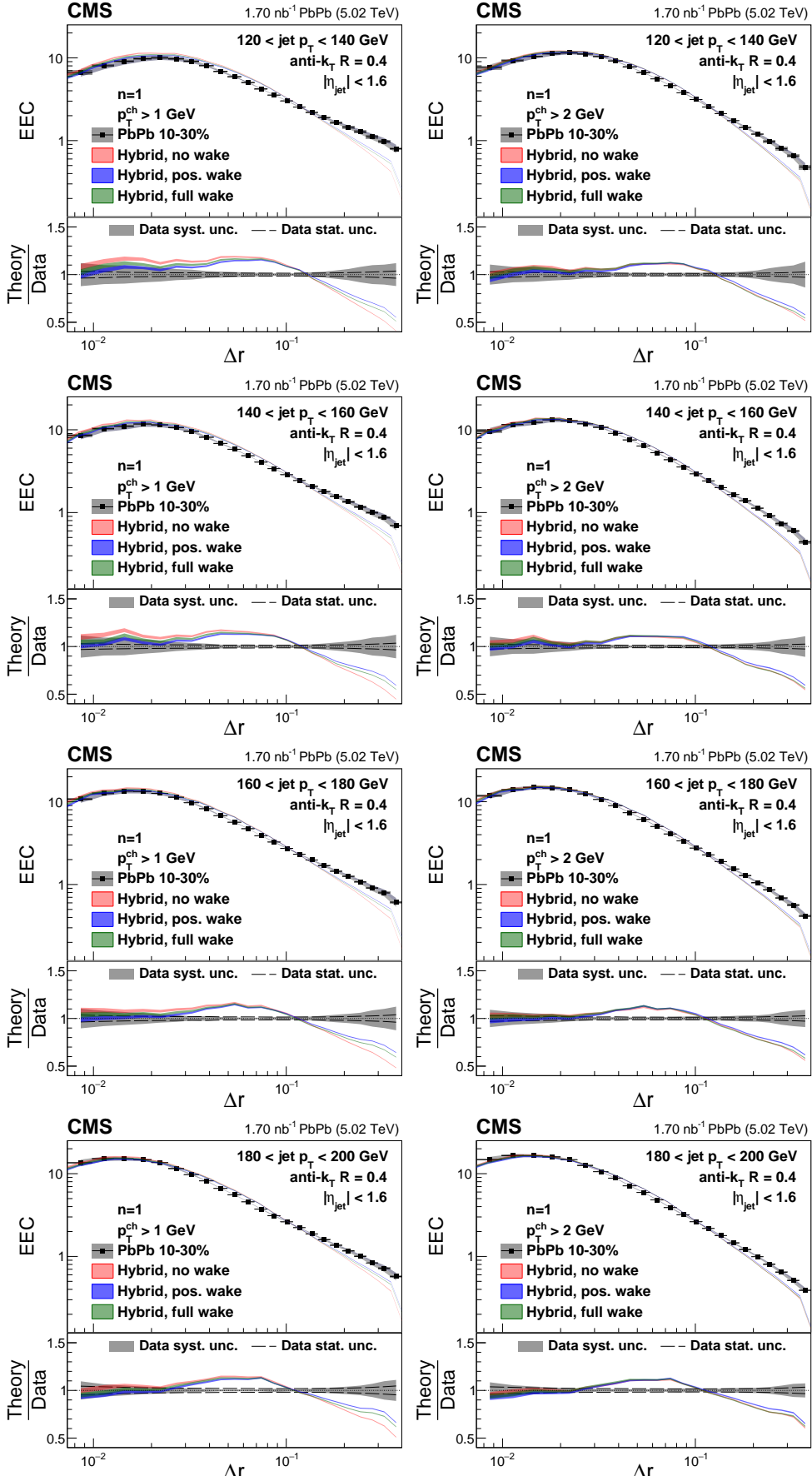


Figure A.9: Energy-energy correlator distributions from 10–30% central PbPb collisions with $n = 1$ in different p_T^{ch} and $p_{T,\text{jet}}$ bins compared to the hybrid model predictions with different jet wake settings.

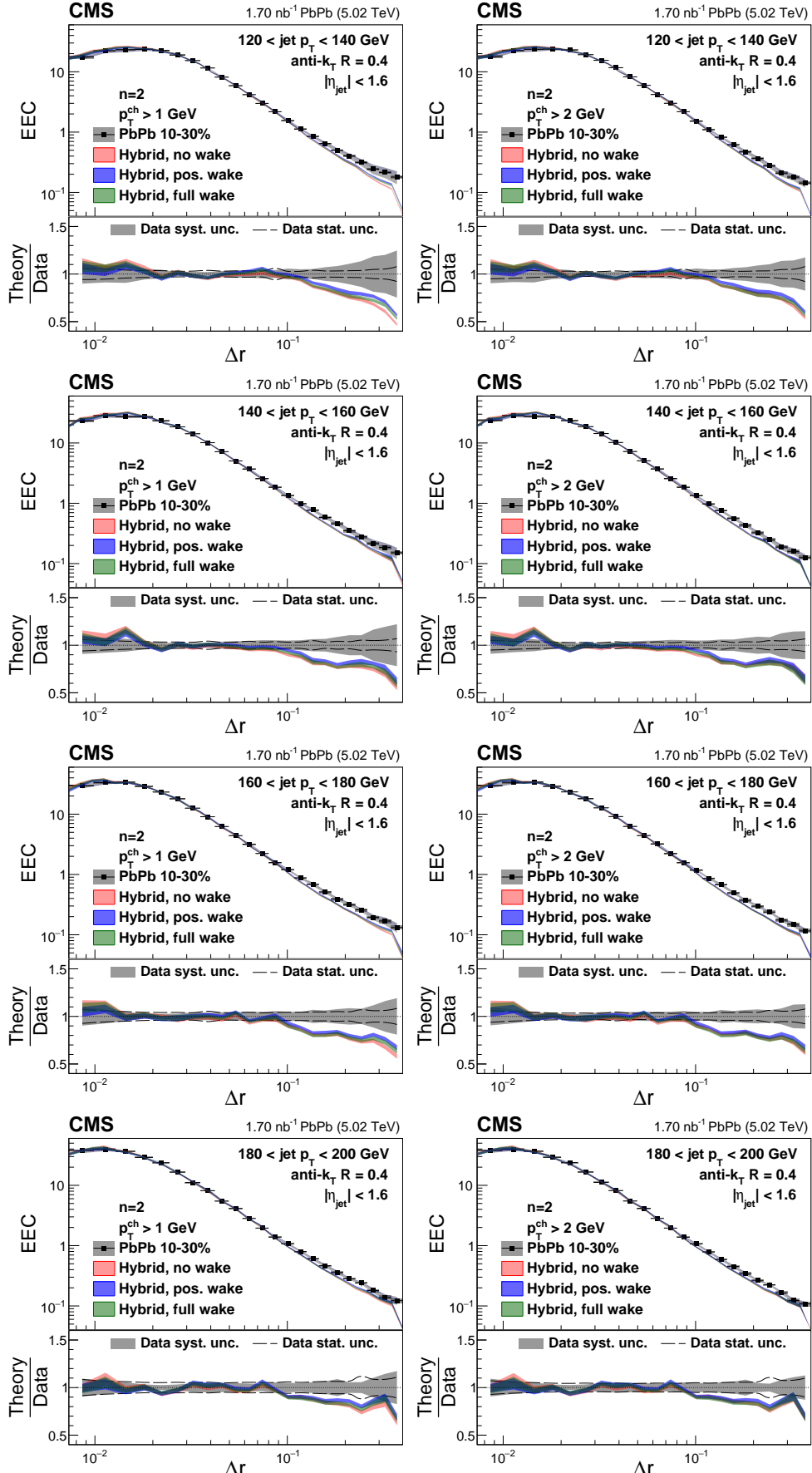


Figure A.10: Energy-energy correlator distributions from 10–30% central PbPb collisions with $n = 2$ in different p_T^{ch} and $p_{T,\text{jet}}$ bins compared to the hybrid model predictions with different jet wake settings.

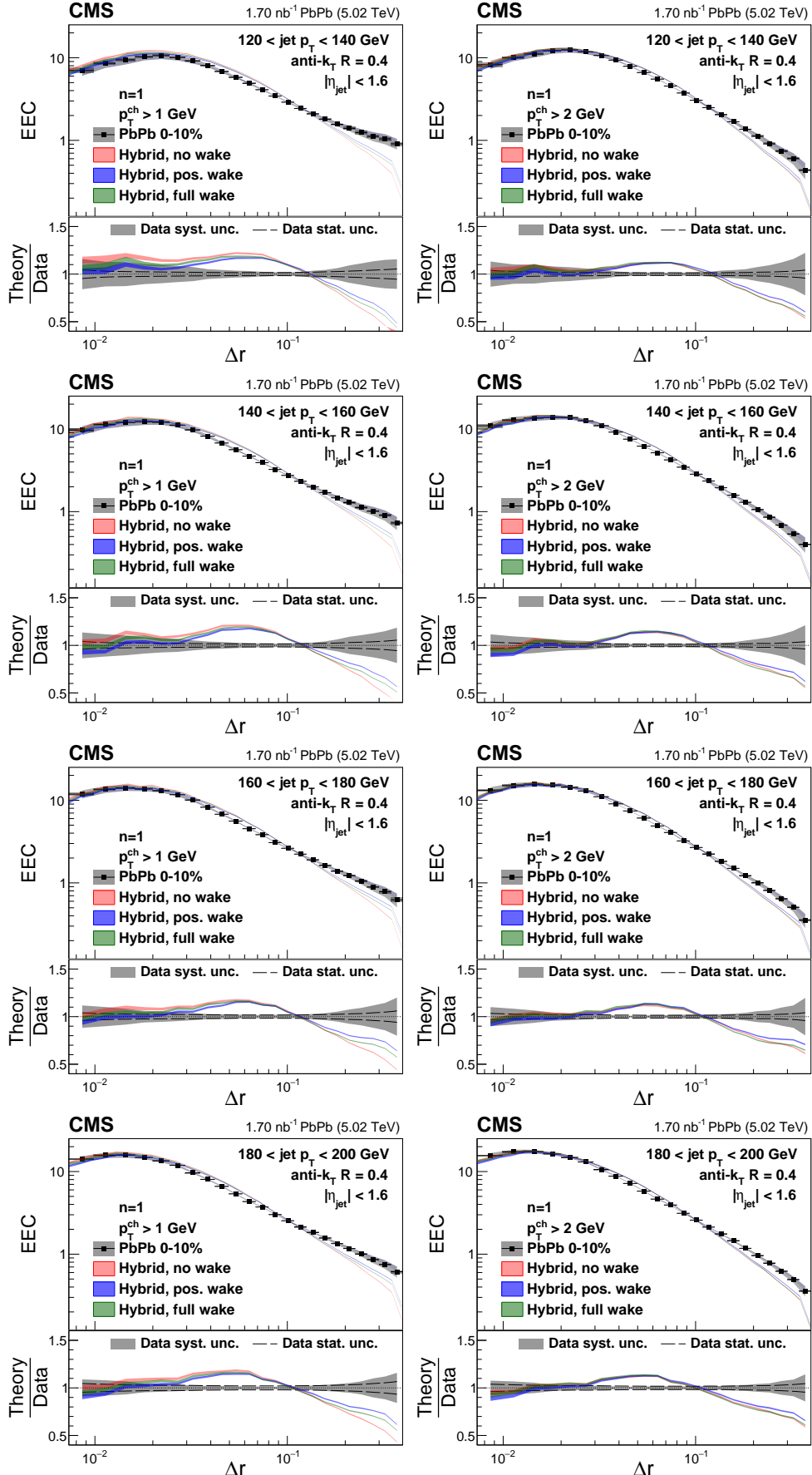


Figure A.11: Energy-energy correlator distributions from 0–10% central PbPb collisions with $n = 1$ in different p_T^{ch} and $p_{T,\text{jet}}$ bins compared to the hybrid model predictions with different jet wake settings.

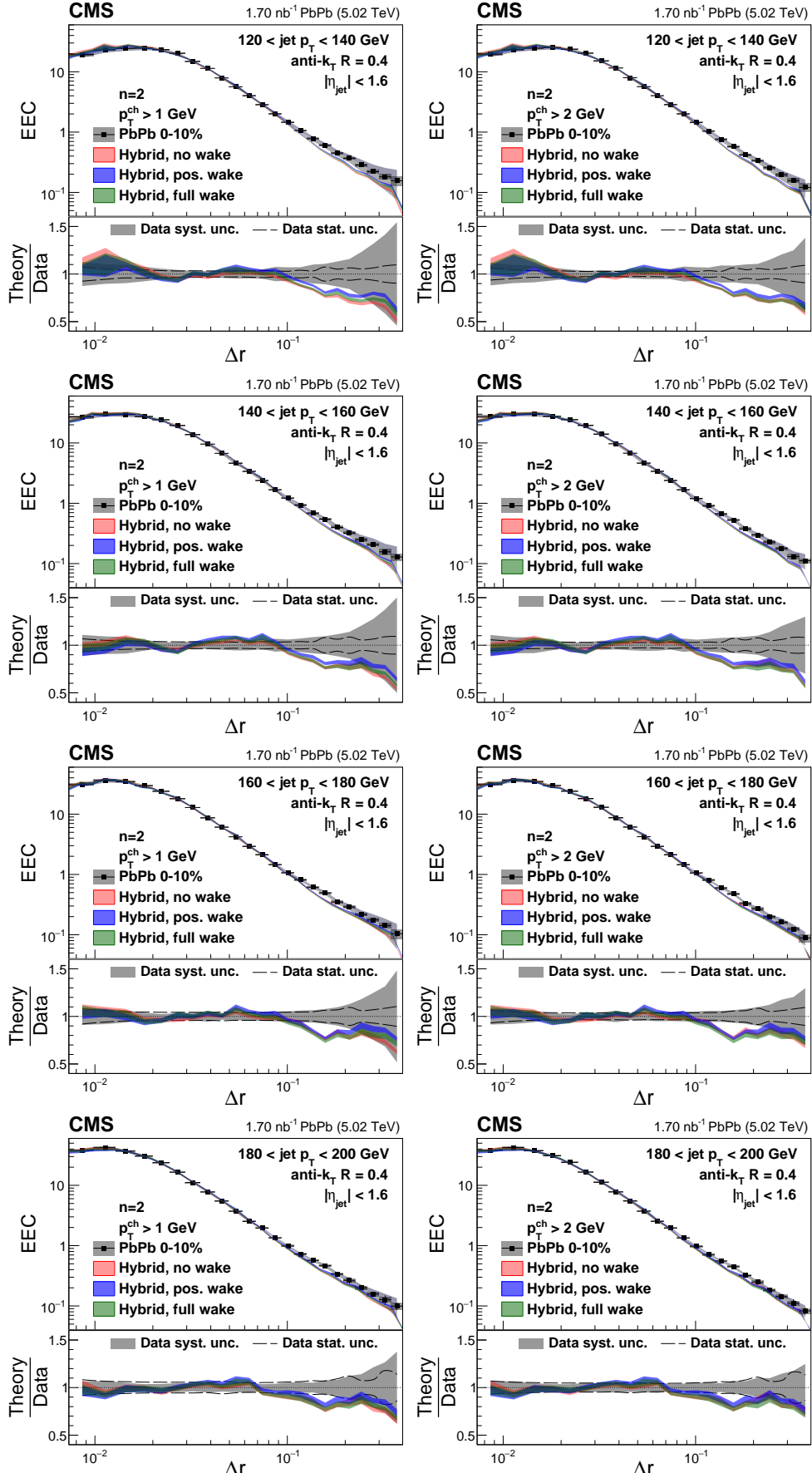


Figure A.12: Energy-energy correlator distributions from 0–10% central PbPb collisions with $n = 2$ in different p_T^{ch} and $p_{T,\text{jet}}$ bins compared to the hybrid model predictions with different jet wake settings.

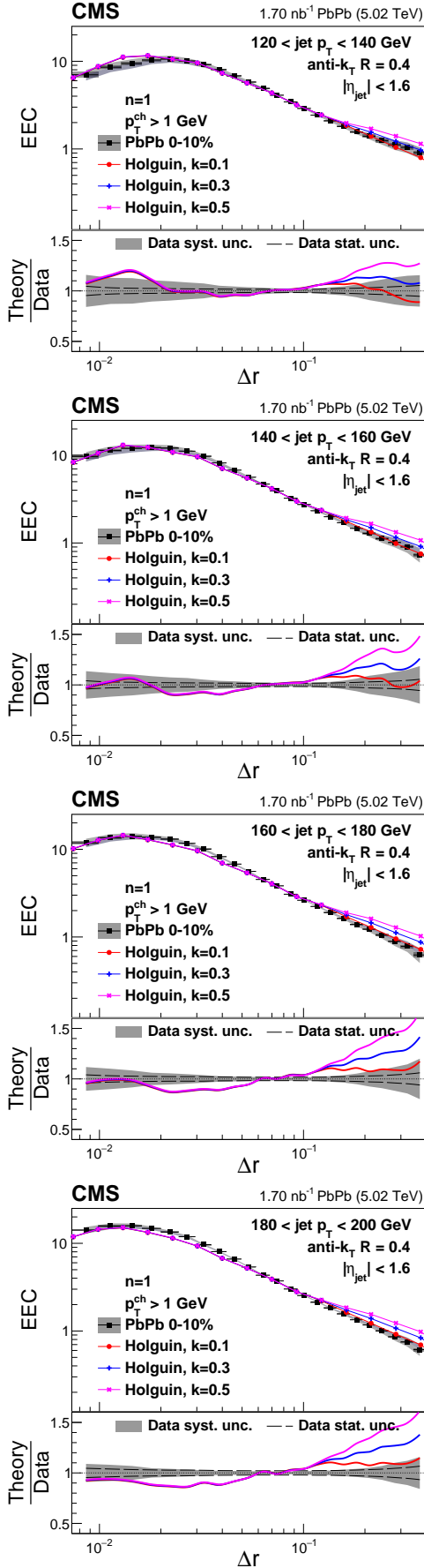


Figure A.13: Energy-energy correlator distributions from 0–10% central PbPb collisions with $n = 1$ and $p_{\text{T}}^{\text{ch}} > 1 \text{ GeV}$ in different $p_{\text{T,jet}}$ bins compared to predictions from perturbative calculation from Holguin and collaborators with different values of the k -parameter.

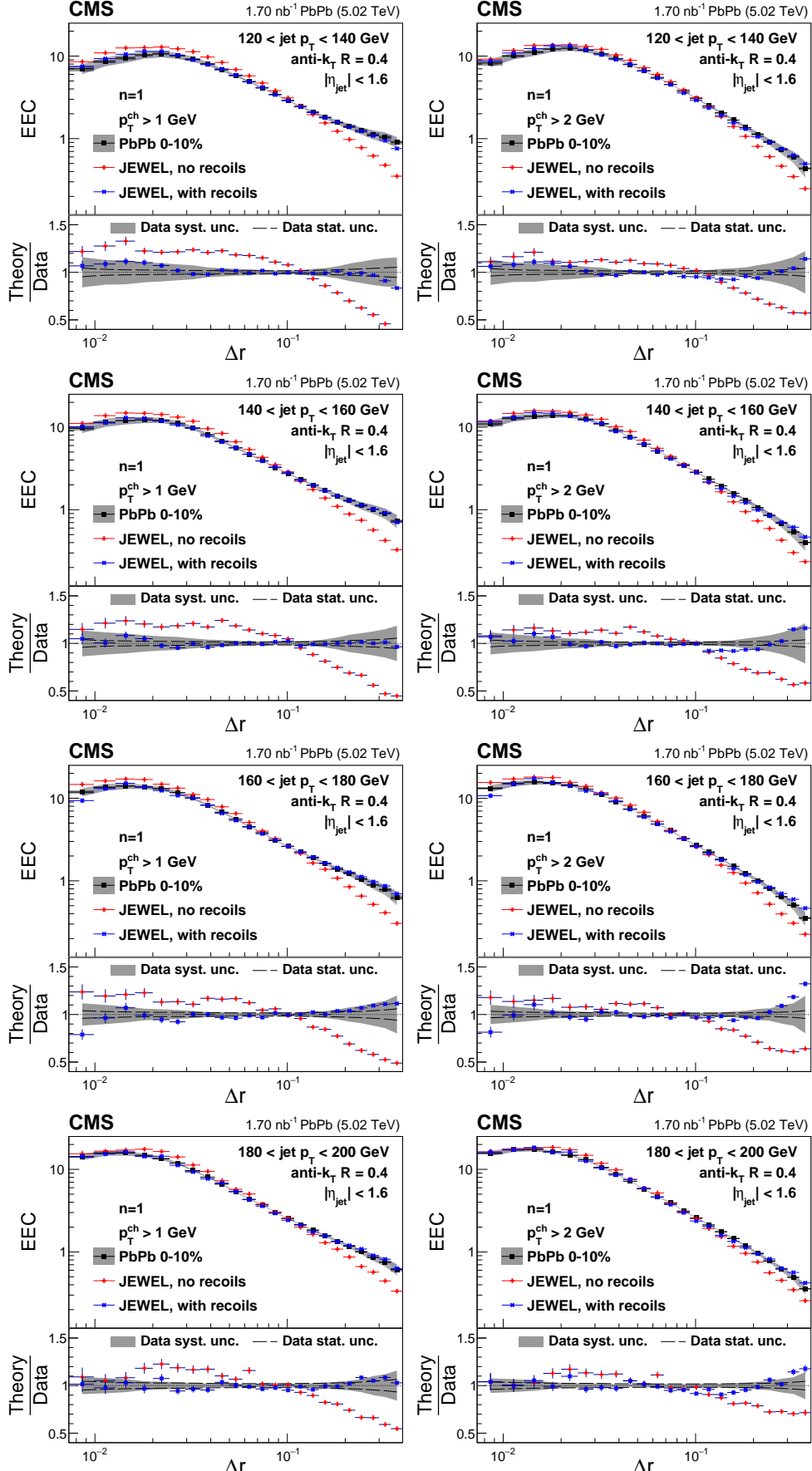


Figure A.14: Energy-energy correlator distributions from 0–10% central PbPb collisions with $n = 1$ in different p_T^{ch} and $p_{T,\text{jet}}$ bins compared to predictions from JEWEL simulation with and without recoils.

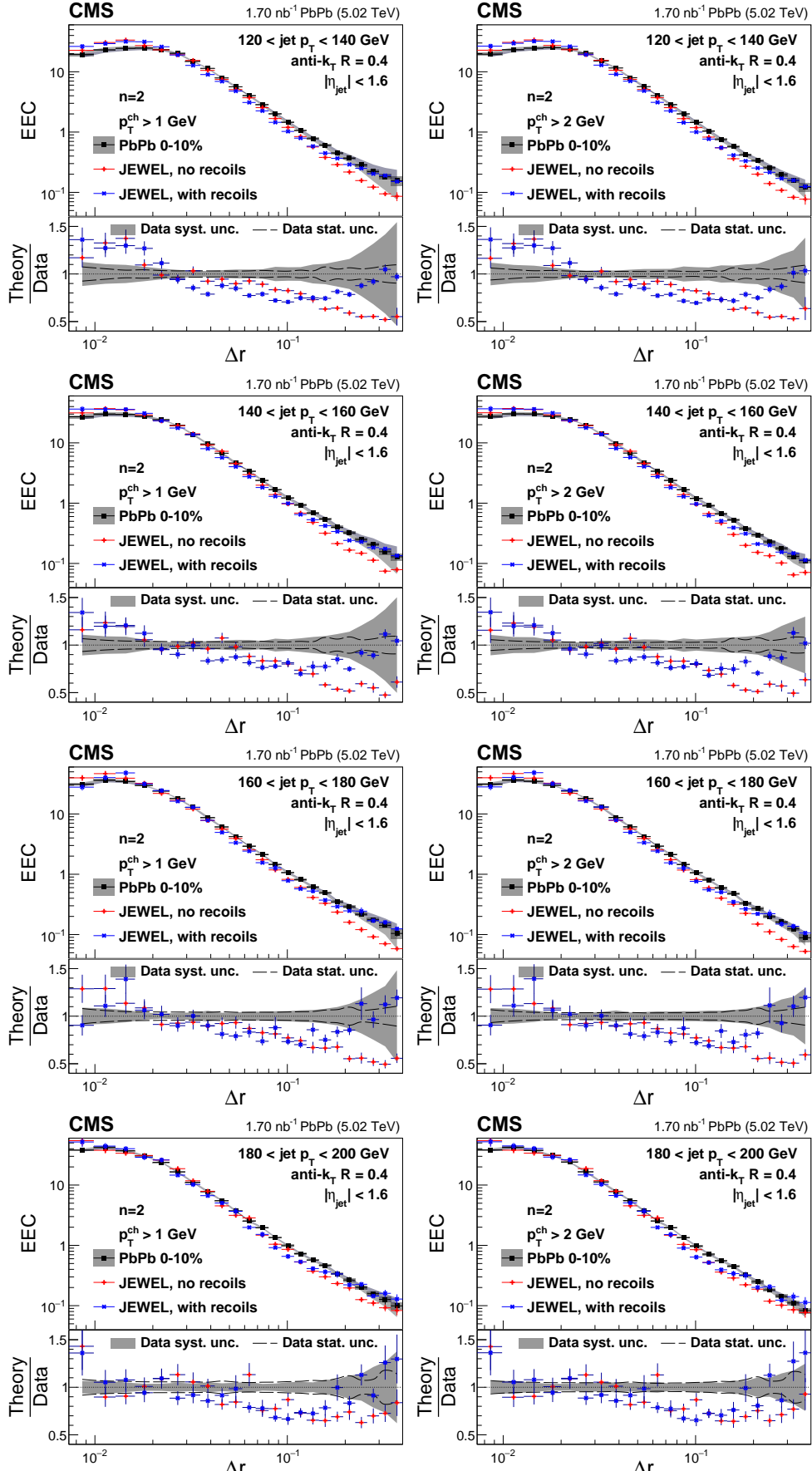


Figure A.15: Energy-energy correlator distributions from 0–10% central PbPb collisions with $n = 2$ in different p_T^{ch} and $p_{T,\text{jet}}$ bins compared to predictions from JEWEL simulation with and without recoils.

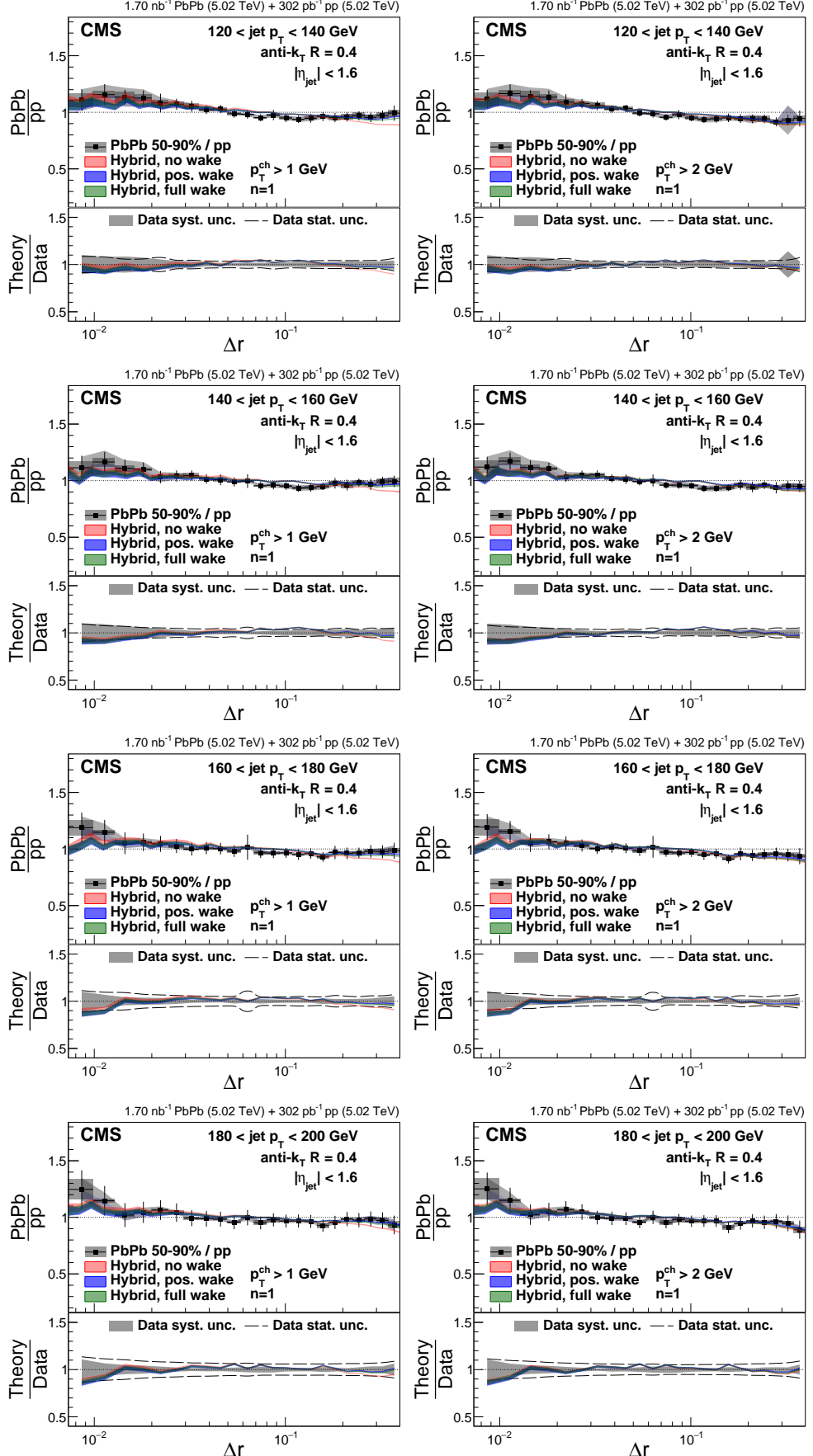


Figure A.16: Ratios of 50–90% central PbPb to pp energy-energy correlators with $n = 1$ in different $p_{T,\text{ch}}$ and $p_{T,\text{jet}}$ bins compared to the hybrid model predictions with different jet wake settings.

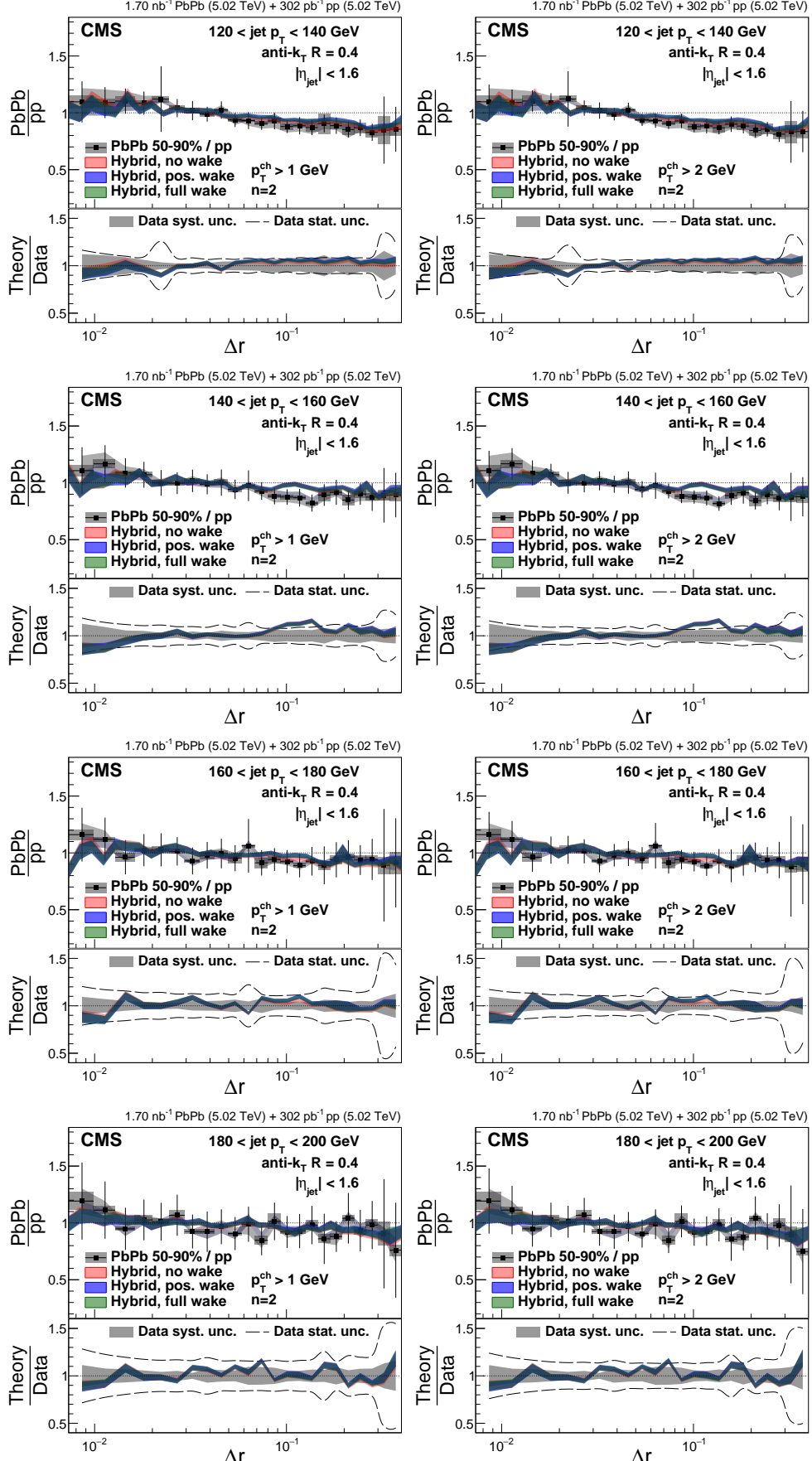


Figure A.17: Ratios of 50–90% central PbPb to pp energy-energy correlators with $n = 2$ in different $p_{T,\text{ch}}$ and $p_{T,\text{jet}}$ bins compared to the hybrid model predictions with different jet wake settings.

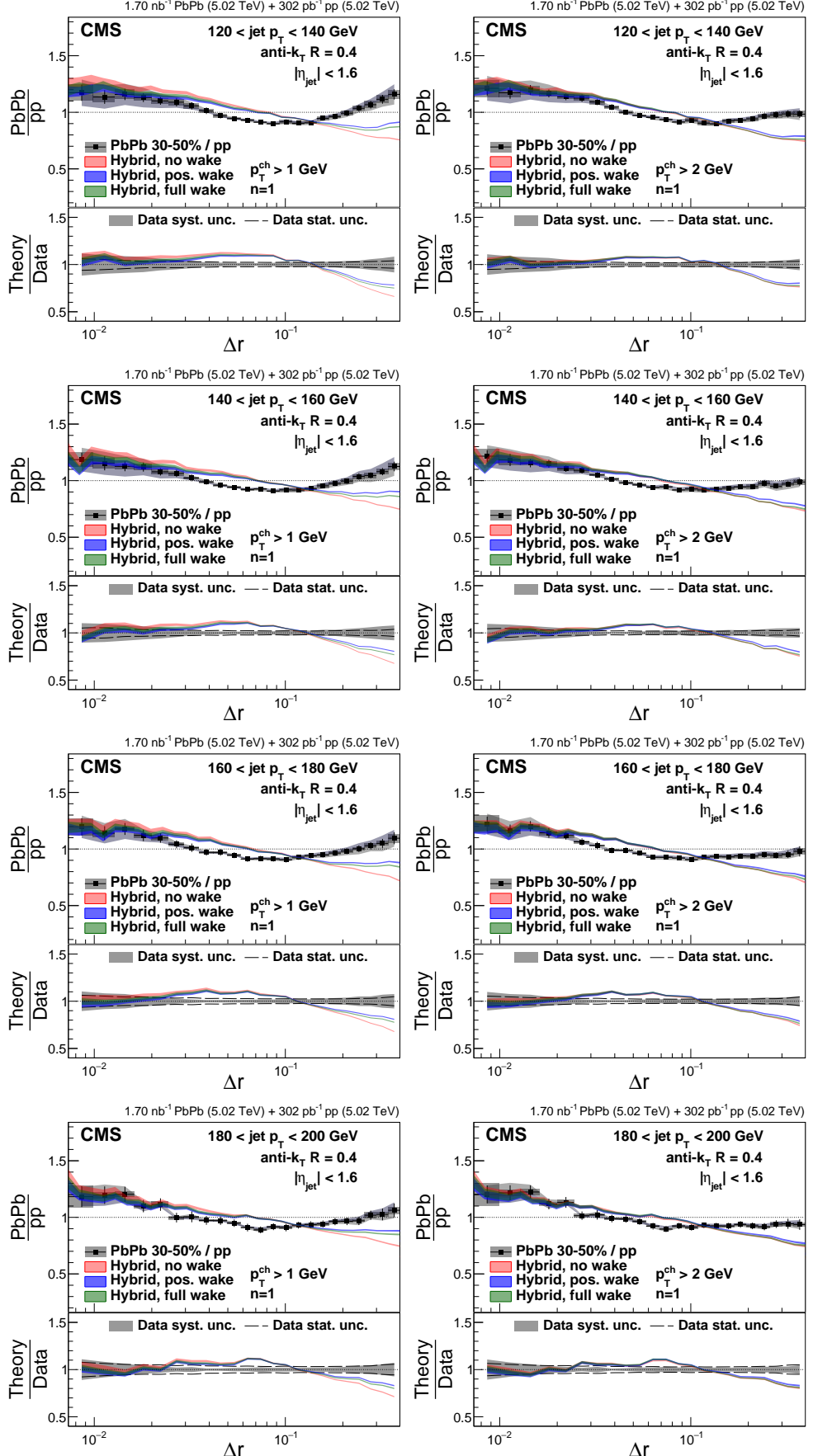


Figure A.18: Ratios of 30–50% central PbPb to pp energy-energy correlators with $n = 1$ in different p_T^{ch} and $p_{T,\text{jet}}$ bins compared to the hybrid model predictions with different jet wake settings.

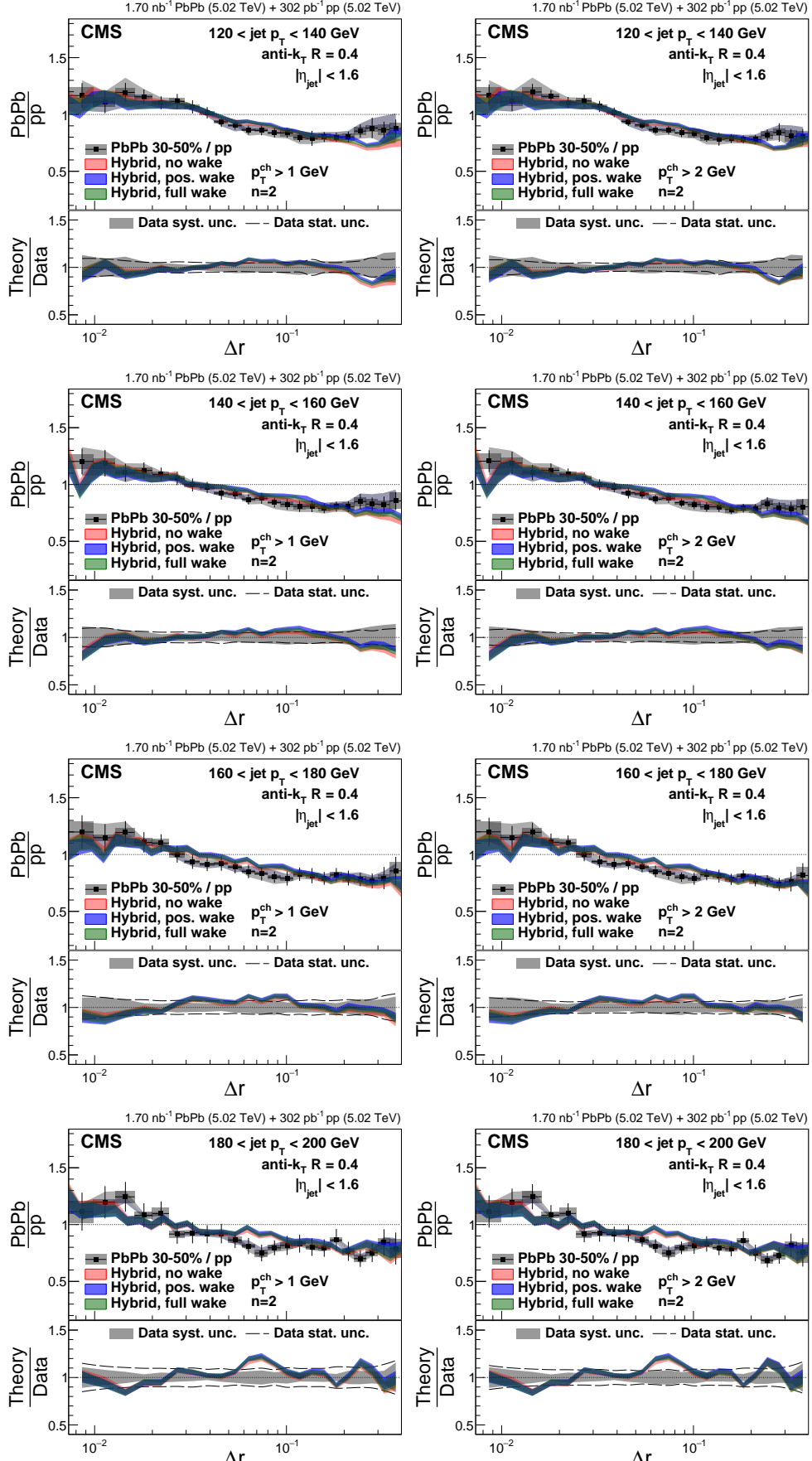


Figure A.19: Ratios of 30–50% central PbPb to pp energy-energy correlators with $n = 2$ in different p_T^{ch} and $p_{\text{T,jet}}$ bins compared to the hybrid model predictions with different jet wake settings.

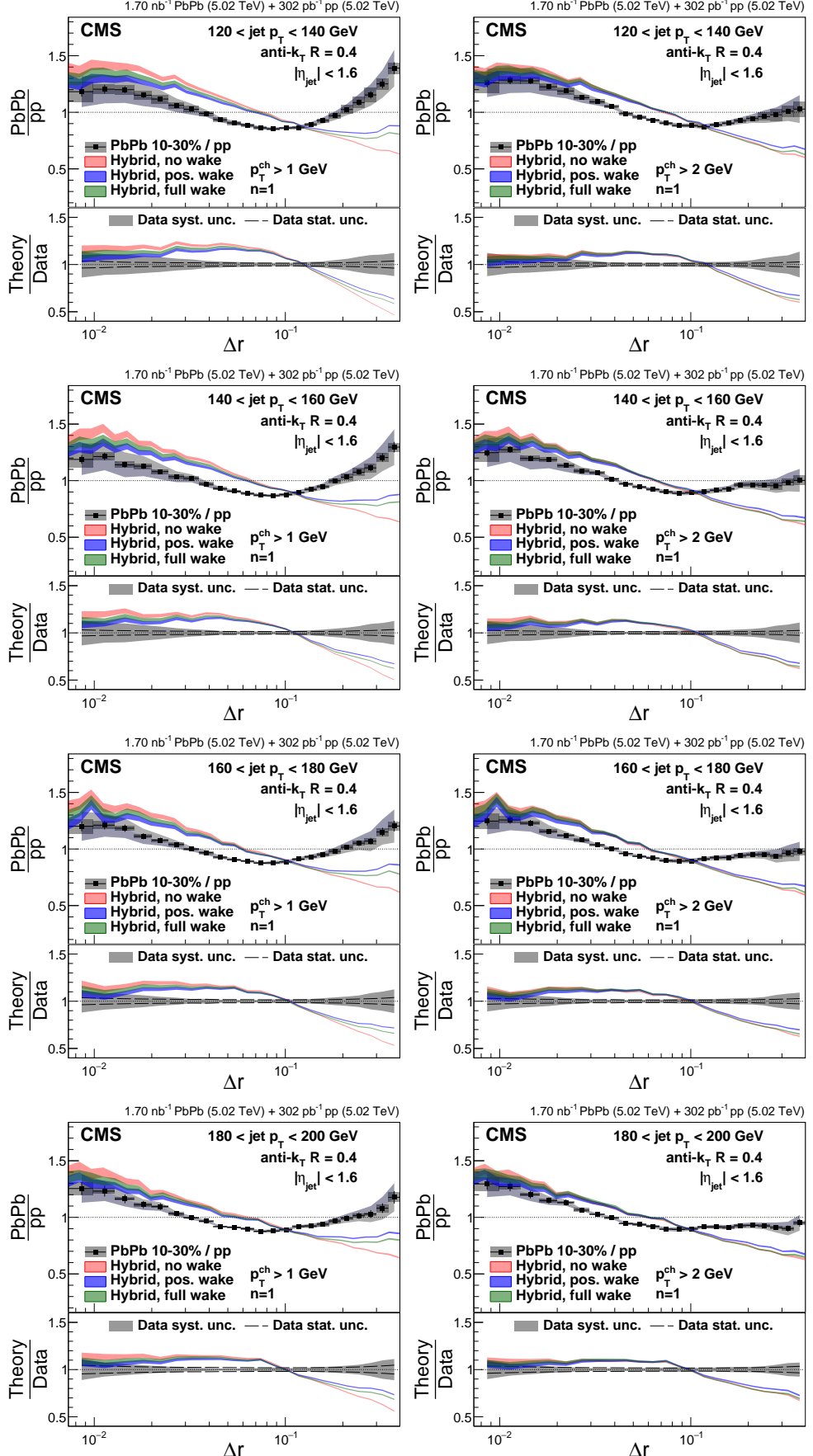


Figure A.20: Ratios of 10–30% central PbPb to pp energy-energy correlators with $n = 1$ in different p_{T}^{ch} and $p_{\text{T},\text{jet}}$ bins compared to the hybrid model predictions with different jet wake settings.

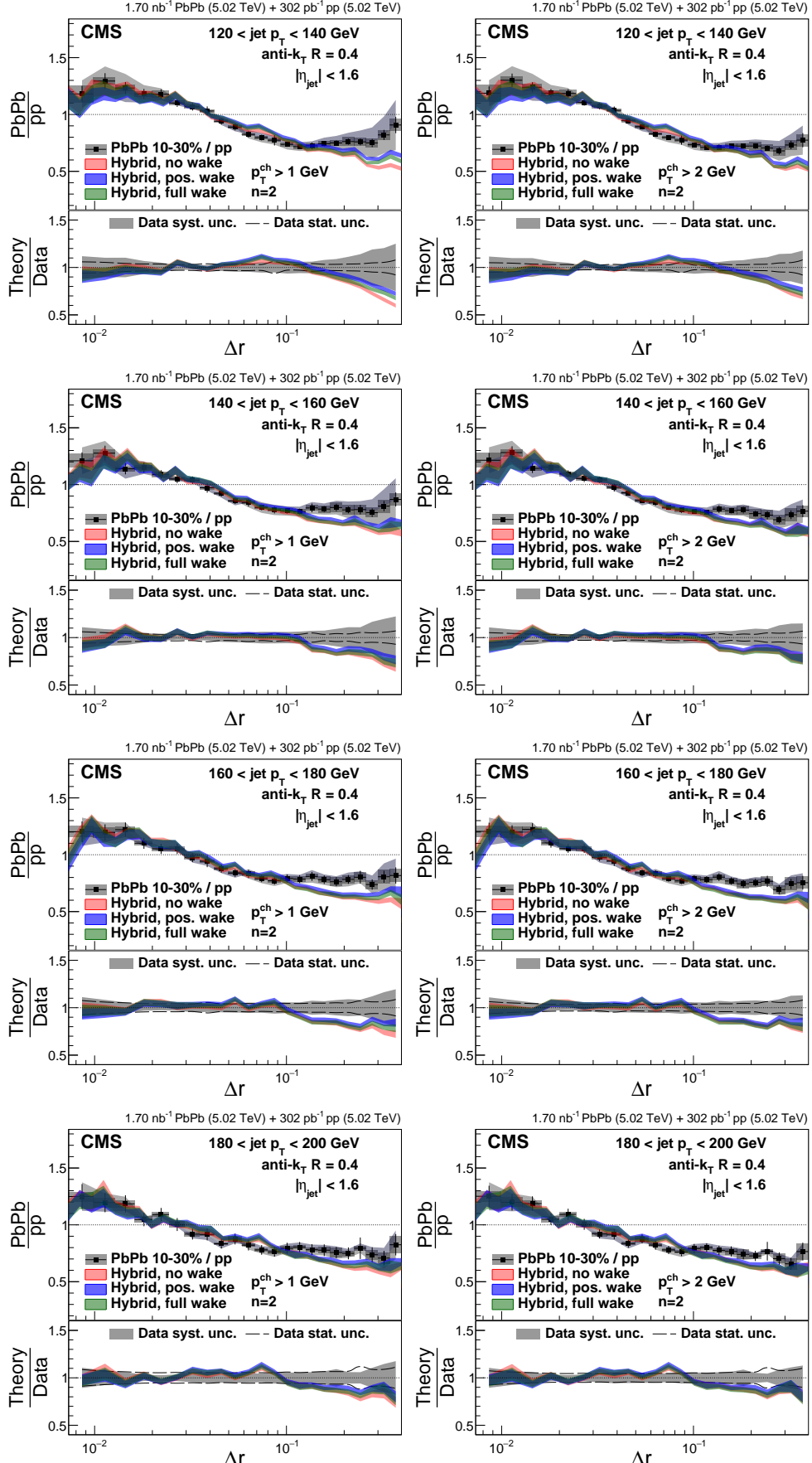


Figure A.21: Ratios of 10–30% central PbPb to pp energy-energy correlators with $n = 2$ in different p_T^{ch} and $p_{\text{T,jet}}$ bins compared to the hybrid model predictions with different jet wake settings.

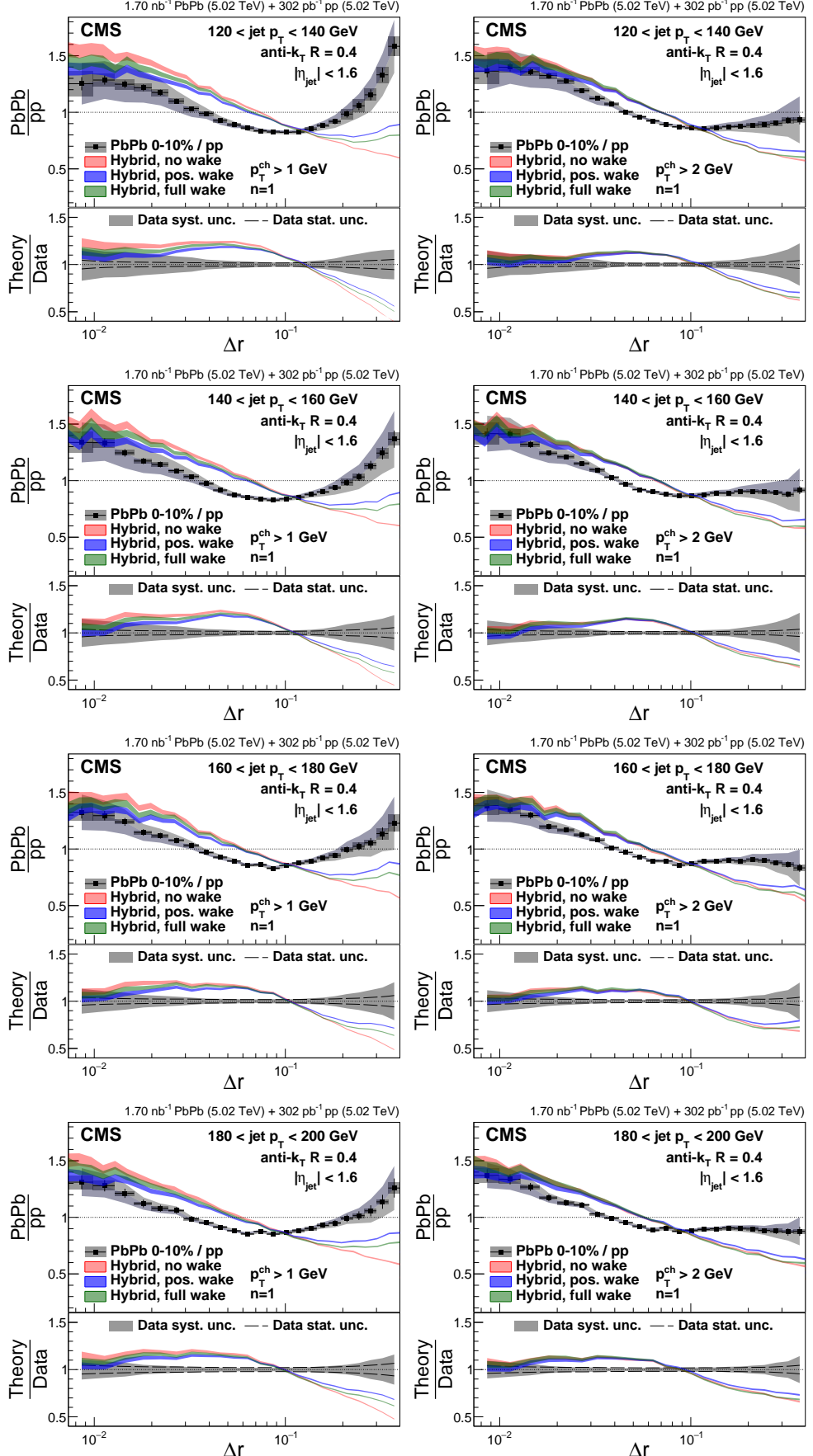


Figure A.22: Ratios of 0-10% central PbPb to pp energy-energy correlators with $n = 1$ in different $p_{T,\text{ch}}^{\text{ch}}$ and $p_{T,\text{jet}}$ bins compared to the hybrid model predictions with different jet wake settings.

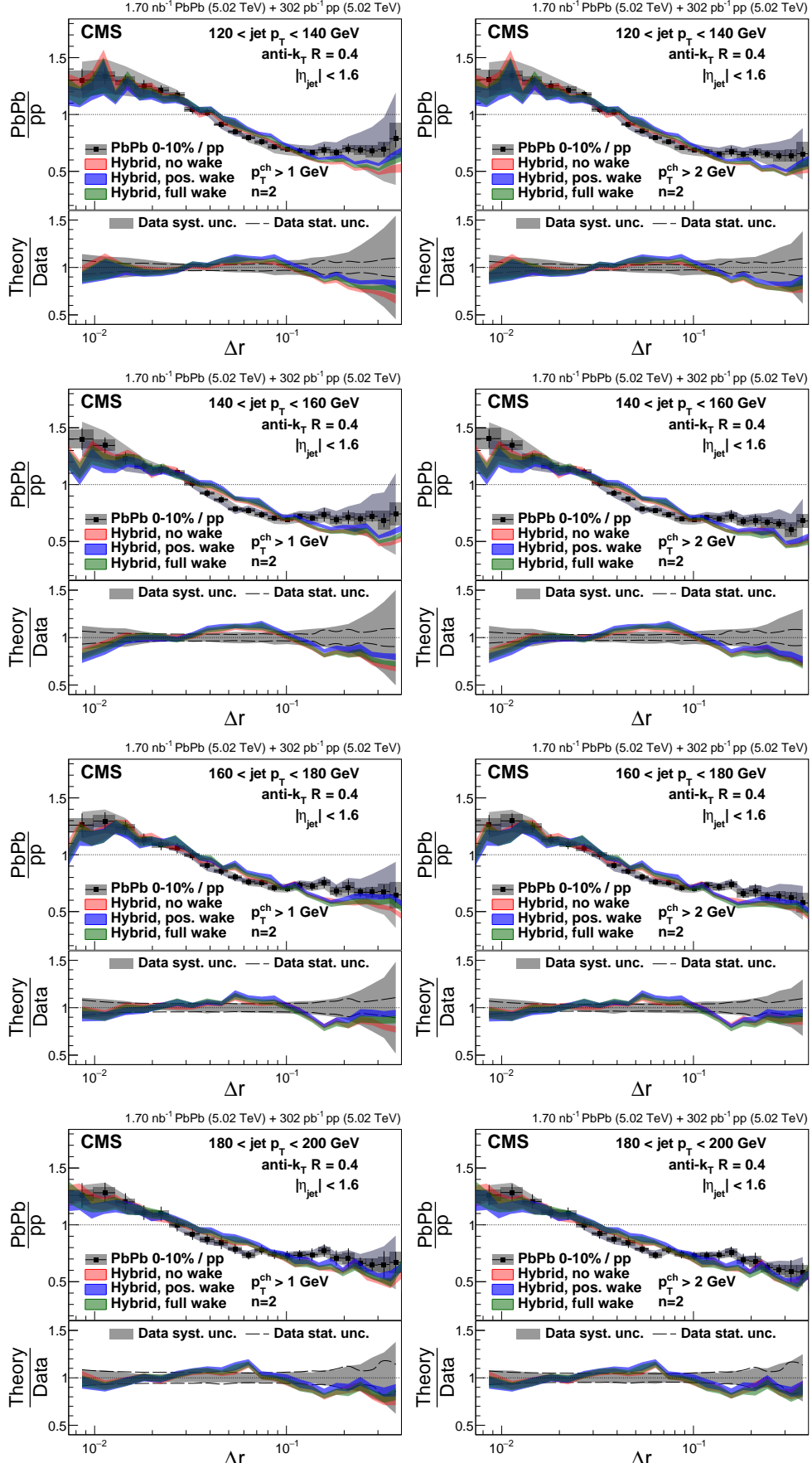


Figure A.23: Ratios of 0–10% central PbPb to pp energy-energy correlators with $n = 2$ in different p_T^{ch} and $p_{T,\text{jet}}$ bins compared to the hybrid model predictions with different jet wake settings.

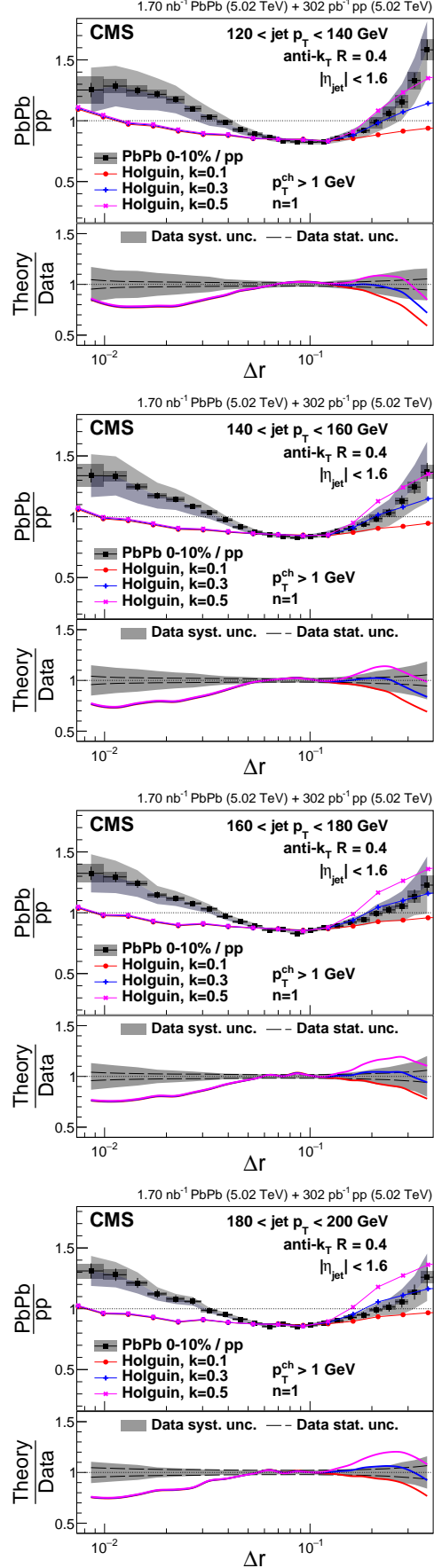


Figure A.24: Ratios of 0–10% central PbPb to pp energy-energy correlators with $n = 1$ and $p_T^{\text{ch}} > 1 \text{ GeV}$ in different $p_{T,\text{jet}}$ bins compared to predictions from perturbative calculation from Holguin and collaborators with different values of the k -parameter.

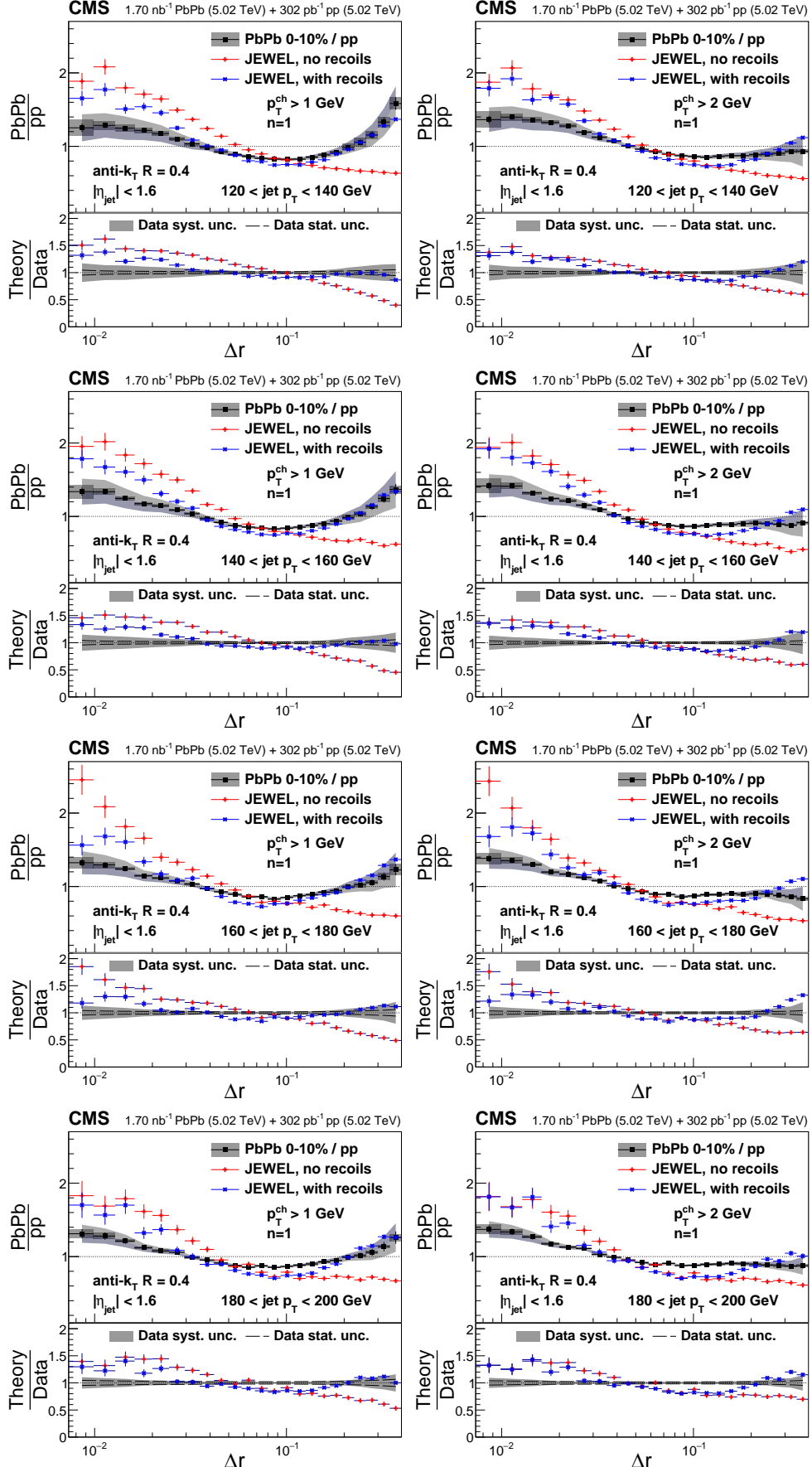


Figure A.25: Ratios of 0-10% central PbPb to pp energy-energy correlators with $n = 1$ in different p_T^{ch} and $p_{T,\text{jet}}$ bins compared to JEWEL predictions with and without recoils.

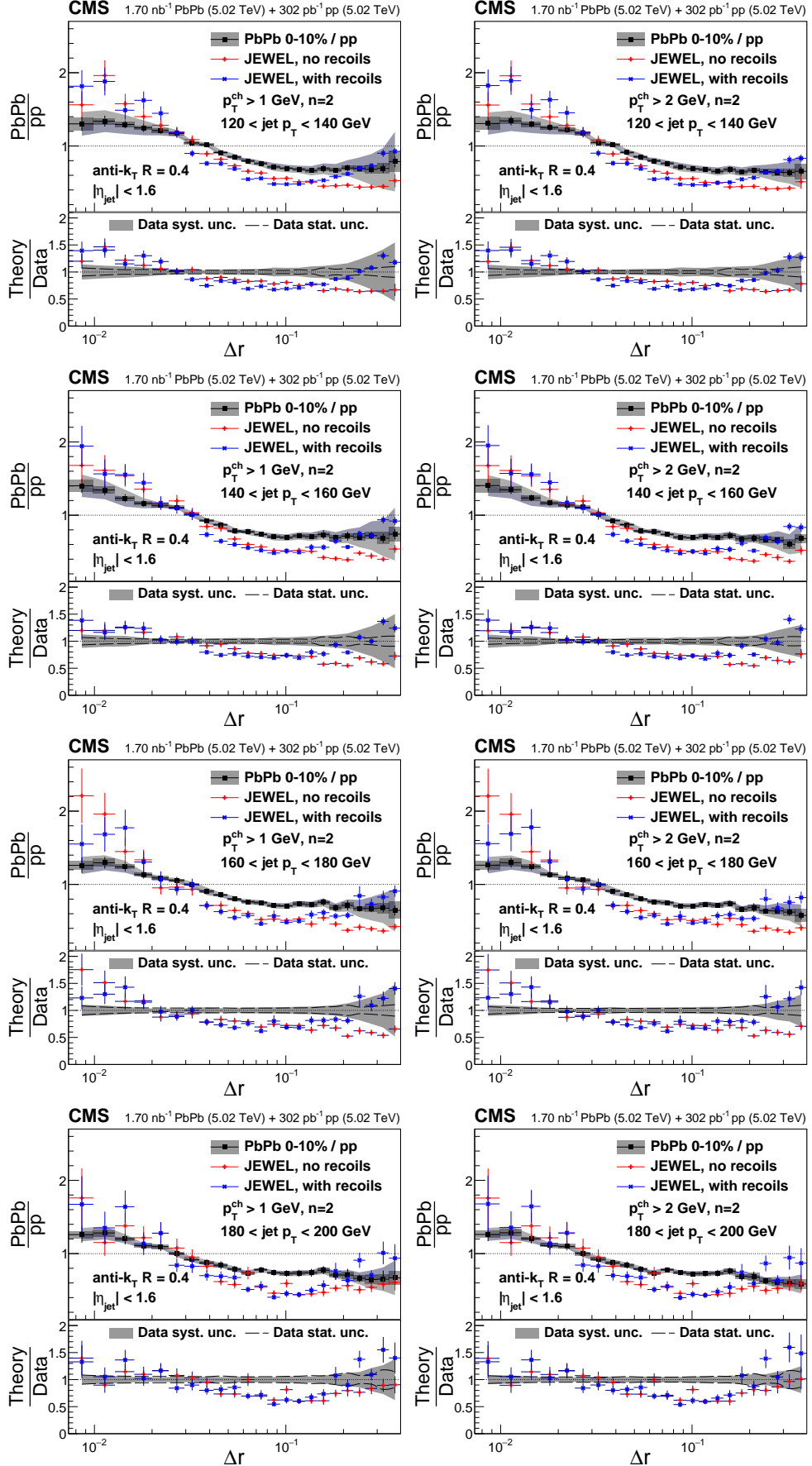


Figure A.26: Ratios of 0-10% central PbPb to pp energy-energy correlators with $n = 2$ in different p_T^{ch} and $p_{T,\text{jet}}$ bins compared to JEWEL predictions with and without recoils.

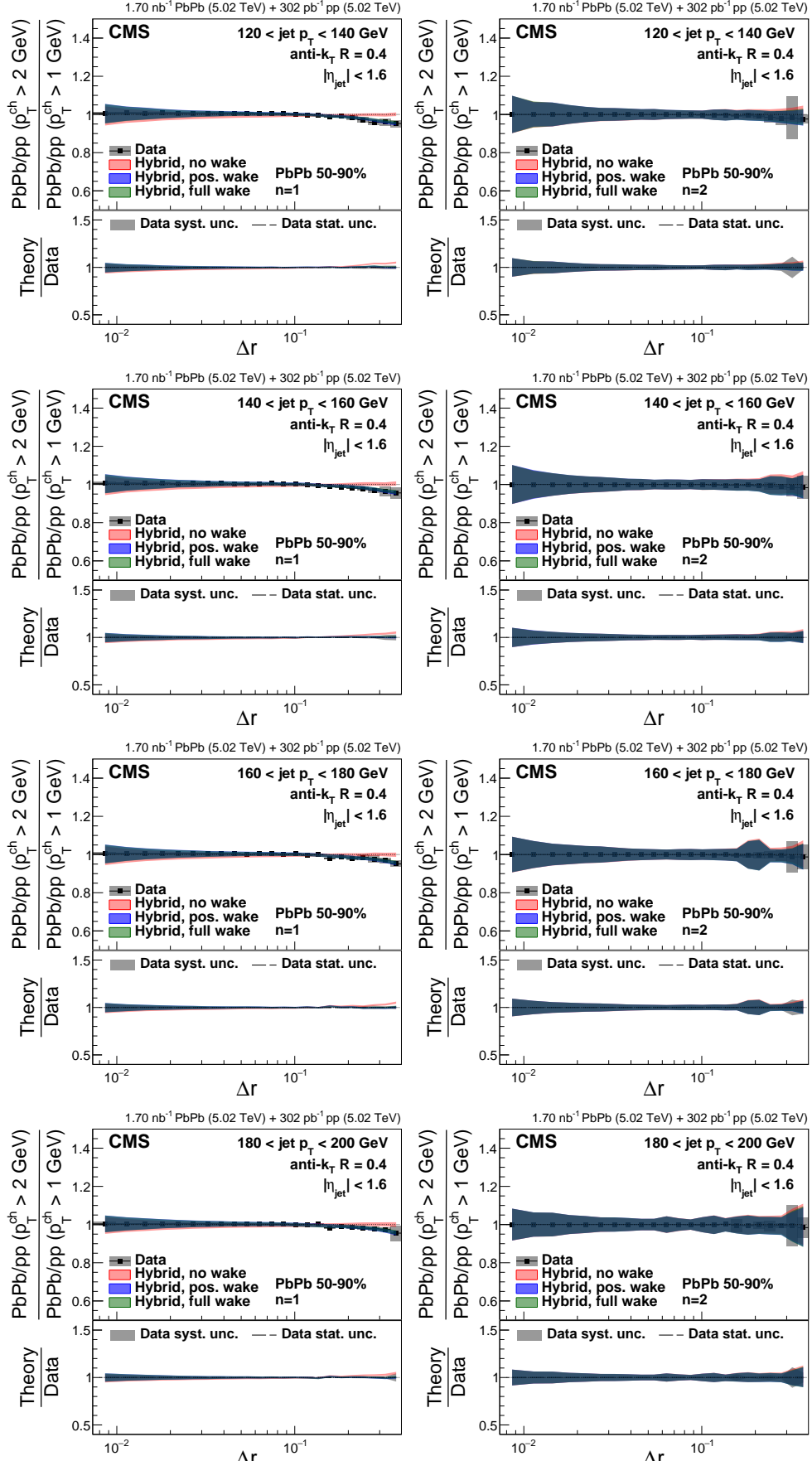


Figure A.27: The double ratios of 50–90% central PbPb to pp single ratios with $p_T^{\text{ch}} > 2 \text{ GeV}$ and $p_T^{\text{ch}} > 1 \text{ GeV}$ for $n = 1$ (left) and $n = 2$ (right) in different $p_{T,\text{jet}}$ bins compared to the hybrid model predictions with different jet wake settings.

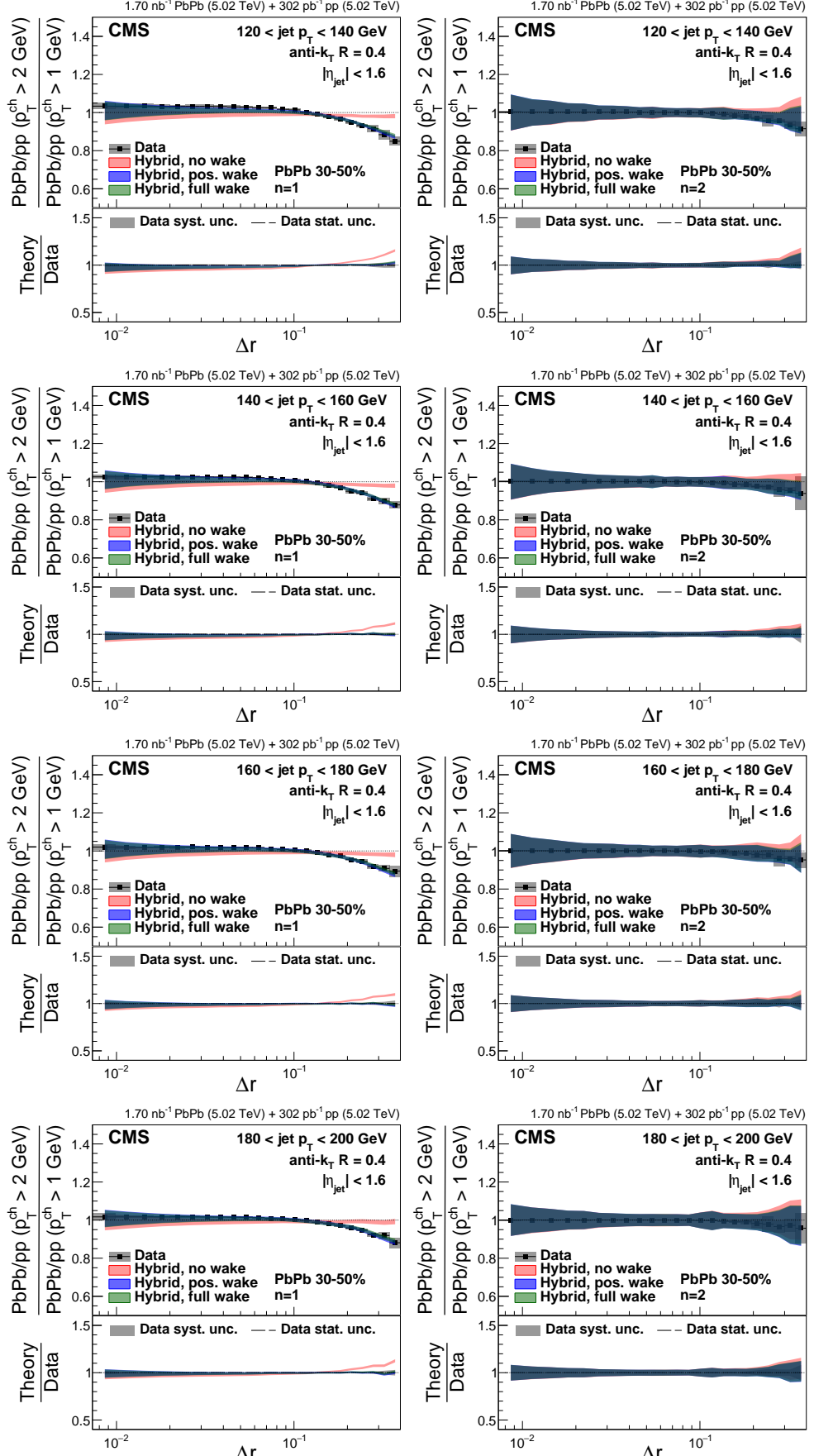


Figure A.28: The double ratios of 30–50% central PbPb to pp single ratios with $p_T^{\text{ch}} > 2 \text{ GeV}$ and $p_T^{\text{ch}} > 1 \text{ GeV}$ for $n = 1$ (left) and $n = 2$ (right) in different $p_{T,\text{jet}}$ bins compared to the hybrid model predictions with different jet wake settings.

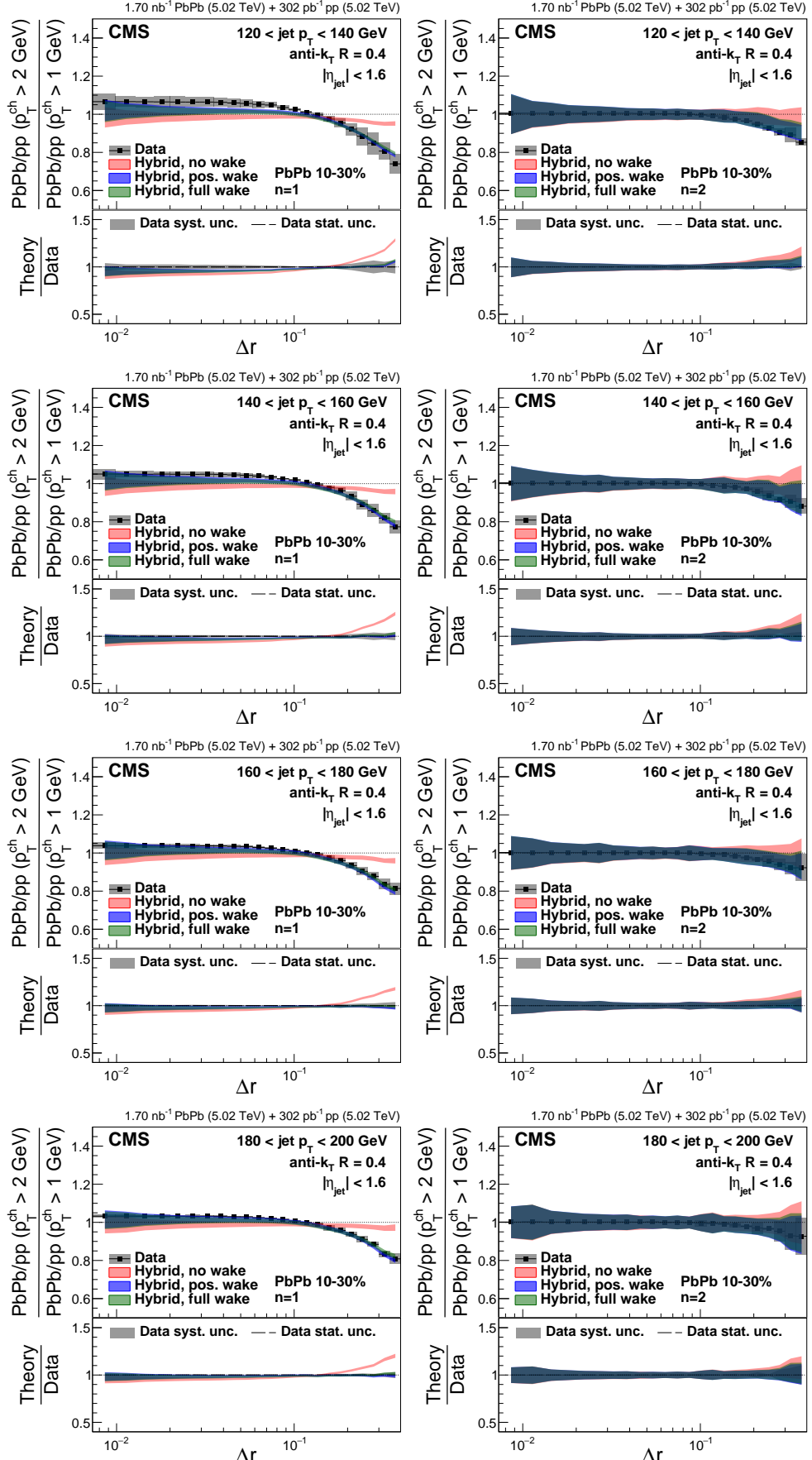


Figure A.29: The double ratios of 10–30% central PbPb to pp single ratios with $p_T^{\text{ch}} > 2 \text{ GeV}$ and $p_T^{\text{ch}} > 1 \text{ GeV}$ for $n = 1$ (left) and $n = 2$ (right) in different $p_{T,\text{jet}}$ bins compared to the hybrid model predictions with different jet wake settings.

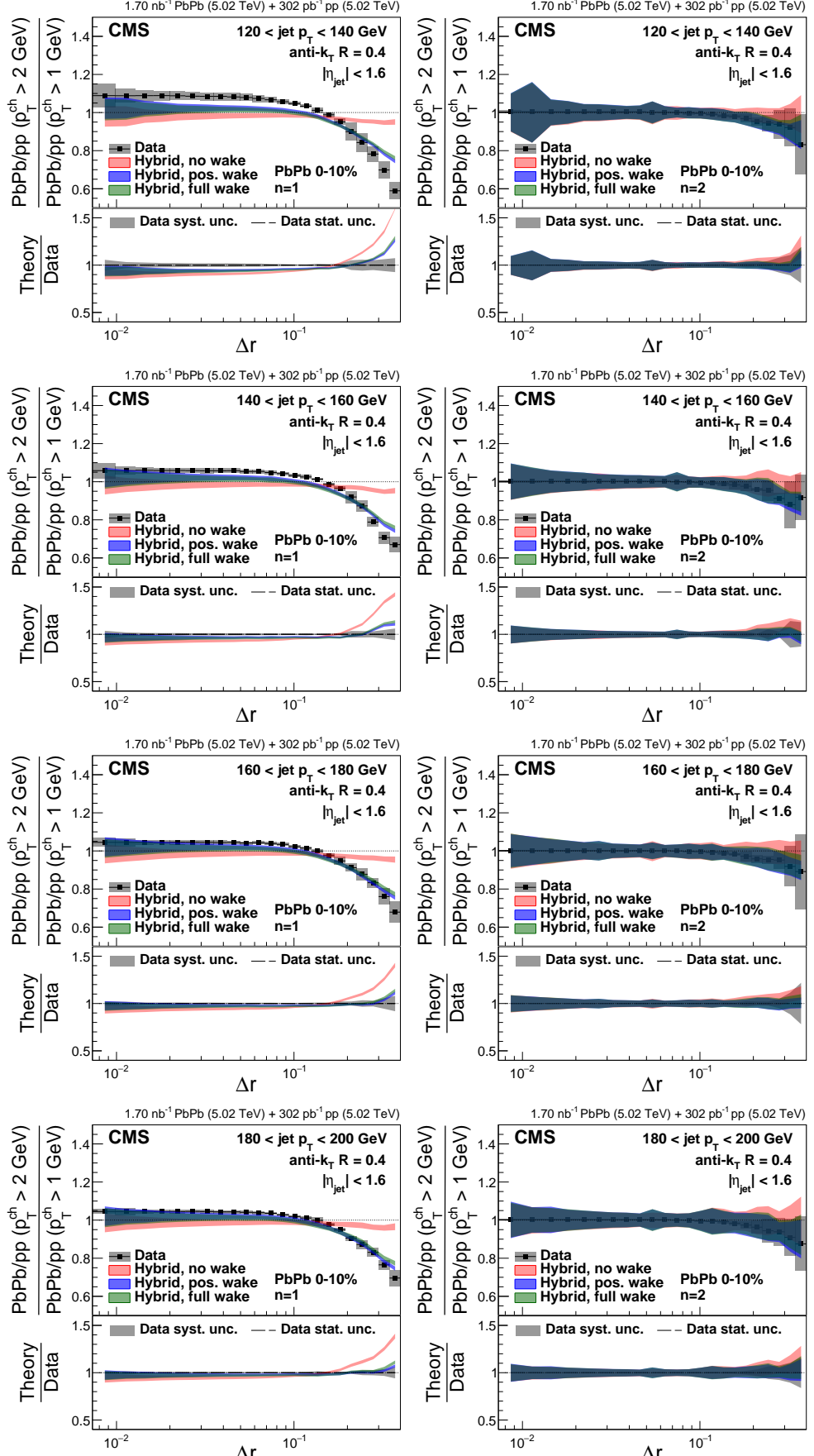


Figure A.30: The double ratios of 0–10% central PbPb to pp single ratios with $p_T^{\text{ch}} > 2 \text{ GeV}$ and $p_T^{\text{ch}} > 1 \text{ GeV}$ for $n = 1$ (left) and $n = 2$ (right) in different $p_{T,\text{jet}}$ bins compared to the hybrid model predictions with different jet wake settings.

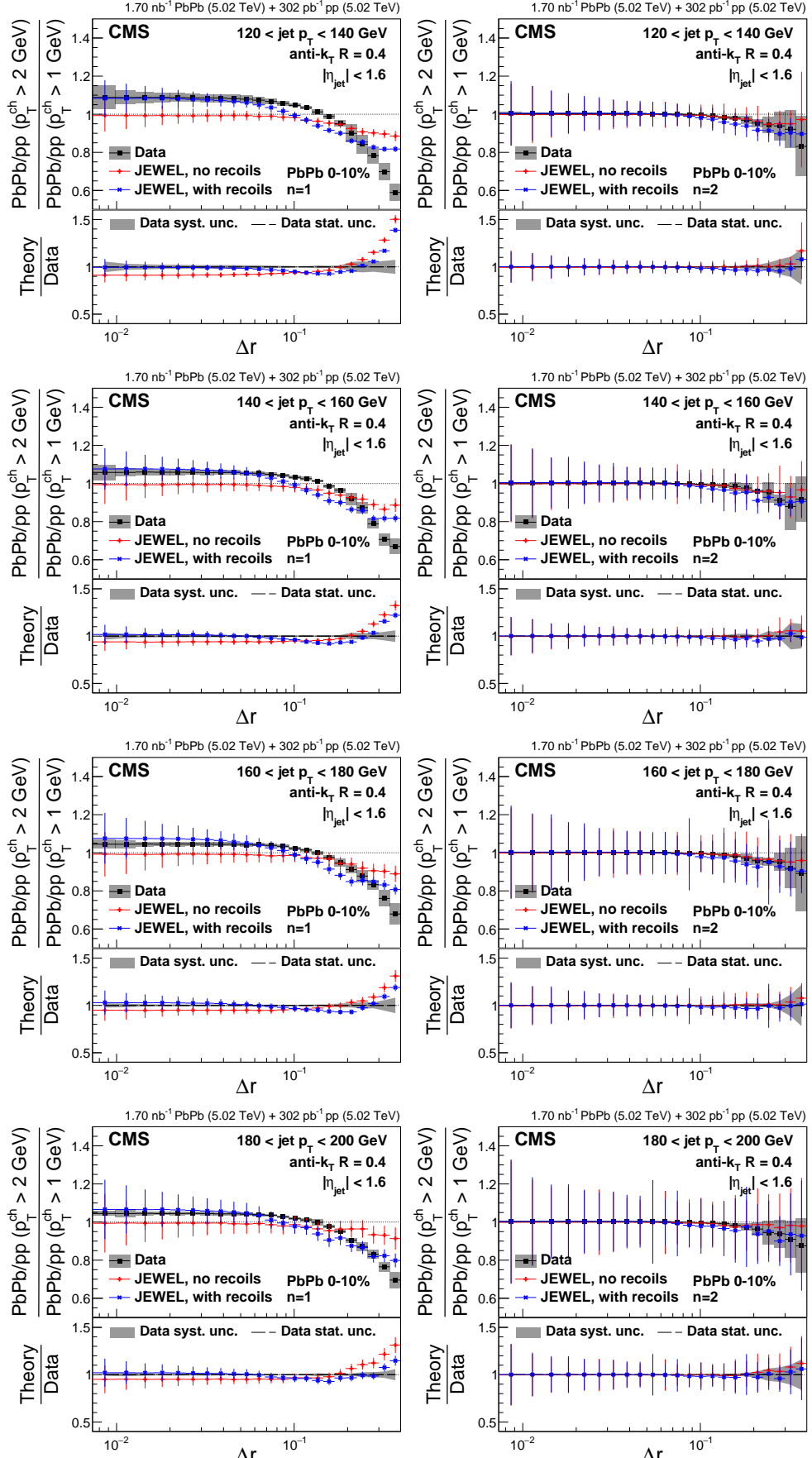


Figure A.31: The double ratios of 0–10% central PbPb to pp single ratios with $p_T^{\text{ch}} > 2 \text{ GeV}$ and $p_T^{\text{ch}} > 1 \text{ GeV}$ for $n = 1$ (left) and $n = 2$ (right) in different $p_{\text{T,jet}}$ bins compared to the JEWEL predictions with different recoil settings.

B The CMS Collaboration

Yerevan Physics Institute, Yerevan, Armenia

V. Chekhovsky, A. Hayrapetyan, V. Makarenko , A. Tumasyan¹ 

Institut für Hochenergiephysik, Vienna, Austria

W. Adam , J.W. Andrejkovic, L. Benato , T. Bergauer , S. Chatterjee , K. Damanakis , M. Dragicevic , P.S. Hussain , M. Jeitler² , N. Krammer , A. Li , D. Liko , I. Mikulec , J. Schieck² , R. Schöfbeck² , D. Schwarz , M. Sonawane , W. Waltenberger , C.-E. Wulz² 

Universiteit Antwerpen, Antwerpen, Belgium

T. Janssen , H. Kwon , T. Van Laer, P. Van Mechelen 

Vrije Universiteit Brussel, Brussel, Belgium

N. Breugelmans, J. D'Hondt , S. Dansana , A. De Moor , M. Delcourt , F. Heyen, Y. Hong , S. Lowette , I. Makarenko , D. Müller , S. Tavernier , M. Tytgat³ , G.P. Van Onsem , S. Van Putte , D. Vannerom 

Université Libre de Bruxelles, Bruxelles, Belgium

B. Bilin , B. Clerbaux , A.K. Das, I. De Bruyn , G. De Lentdecker , H. Evard , L. Favart , P. Gianneios , A. Khalilzadeh, F.A. Khan , K. Lee , A. Malara , M.A. Shahzad, L. Thomas , M. Vanden Bemden , C. Vander Velde , P. Vanlaer 

Ghent University, Ghent, Belgium

M. De Coen , D. Dobur , G. Gokbulut , J. Knolle , L. Lambrecht , D. Marckx , K. Skovpen , N. Van Den Bossche , J. van der Linden , L. Wezenbeek 

Université Catholique de Louvain, Louvain-la-Neuve, Belgium

S. Bein , A. Benecke , A. Bethani , G. Bruno , C. Caputo , J. De Favereau De Jeneret , C. Delaere , I.S. Donertas , A. Giannanco , A.O. Guzel , Sa. Jain , V. Lemaitre, J. Lidrych , P. Mastrapasqua , T.T. Tran , S. Turkcapar 

Centro Brasileiro de Pesquisas Fisicas, Rio de Janeiro, Brazil

G.A. Alves , E. Coelho , G. Correia Silva , C. Hensel , T. Menezes De Oliveira , C. Mora Herrera⁴ , P. Rebello Teles , M. Soeiro, E.J. Tonelli Manganote⁵ , A. Vilela Pereira⁴ 

Universidade do Estado do Rio de Janeiro, Rio de Janeiro, Brazil

W.L. Aldá Júnior , M. Barroso Ferreira Filho , H. Brandao Malbouisson , W. Carvalho , J. Chinellato⁶, E.M. Da Costa , G.G. Da Silveira⁷ , D. De Jesus Damiao , S. Fonseca De Souza , R. Gomes De Souza, T. Laux Kuhn⁷ , M. Macedo , J. Martins , K. Mota Amarilo , L. Mundim , H. Nogima , J.P. Pinheiro , A. Santoro , A. Sznajder , M. Thiel 

Universidade Estadual Paulista, Universidade Federal do ABC, São Paulo, Brazil

C.A. Bernardes⁷ , L. Calligaris , T.R. Fernandez Perez Tomei , E.M. Gregores , I. Maietto Silverio , P.G. Mercadante , S.F. Novaes , B. Orzari , Sandra S. Padula , V. Scheurer

Institute for Nuclear Research and Nuclear Energy, Bulgarian Academy of Sciences, Sofia, Bulgaria

A. Aleksandrov , G. Antchev , R. Hadjiiska , P. Iaydjiev , M. Misheva , M. Shopova , G. Sultanov 

University of Sofia, Sofia, Bulgaria

A. Dimitrov , L. Litov , B. Pavlov , P. Petkov , A. Petrov , E. Shumka 

Instituto De Alta Investigación, Universidad de Tarapacá, Casilla 7 D, Arica, Chile

S. Keshri , D. Laroze , S. Thakur 

Beihang University, Beijing, China

T. Cheng , T. Javaid , L. Yuan 

Department of Physics, Tsinghua University, Beijing, China

Z. Hu , Z. Liang, J. Liu

Institute of High Energy Physics, Beijing, China

G.M. Chen⁸ , H.S. Chen⁸ , M. Chen⁸ , F. Iemmi , C.H. Jiang, A. Kapoor⁹ , H. Liao , Z.-A. Liu¹⁰ , R. Sharma¹¹ , J.N. Song¹⁰, J. Tao , C. Wang⁸, J. Wang , Z. Wang⁸, H. Zhang , J. Zhao 

State Key Laboratory of Nuclear Physics and Technology, Peking University, Beijing, China

A. Agapitos , Y. Ban , A. Carvalho Antunes De Oliveira , S. Deng , B. Guo, C. Jiang , A. Levin , C. Li , Q. Li , Y. Mao, S. Qian, S.J. Qian , X. Qin, X. Sun , D. Wang , H. Yang, Y. Zhao, C. Zhou 

Guangdong Provincial Key Laboratory of Nuclear Science and Guangdong-Hong Kong Joint Laboratory of Quantum Matter, South China Normal University, Guangzhou, China

S. Yang 

Sun Yat-Sen University, Guangzhou, China

Z. You 

University of Science and Technology of China, Hefei, China

K. Jaffel , N. Lu 

Nanjing Normal University, Nanjing, China

G. Bauer¹², B. Li¹³, H. Wang , K. Yi¹⁴ , J. Zhang 

Institute of Modern Physics and Key Laboratory of Nuclear Physics and Ion-beam Application (MOE) - Fudan University, Shanghai, China

Y. Li

Zhejiang University, Hangzhou, Zhejiang, China

Z. Lin , C. Lu , M. Xiao 

Universidad de Los Andes, Bogota, Colombia

C. Avila , D.A. Barbosa Trujillo, A. Cabrera , C. Florez , J. Fraga , J.A. Reyes Vega

Universidad de Antioquia, Medellin, Colombia

J. Jaramillo , C. Rendón , M. Rodriguez , A.A. Ruales Barbosa , J.D. Ruiz Alvarez 

University of Split, Faculty of Electrical Engineering, Mechanical Engineering and Naval Architecture, Split, Croatia

D. Giljanovic , N. Godinovic , D. Lelas , A. Sculac 

University of Split, Faculty of Science, Split, Croatia

M. Kovac , A. Petkovic , T. Sculac 

Institute Rudjer Boskovic, Zagreb, Croatia

P. Bargassa , V. Brigljevic , B.K. Chitroda , D. Ferencek , K. Jakovcic, A. Starodumov¹⁵ ,

T. Susa 

University of Cyprus, Nicosia, Cyprus

A. Attikis , K. Christoforou , A. Hadjiagapiou, C. Leonidou , J. Mousa , C. Nicolaou, L. Paizanos, F. Ptochos , P.A. Razis , H. Rykaczewski, H. Saka , A. Stepennov 

Charles University, Prague, Czech Republic

M. Finger , M. Finger Jr. , A. Kveton 

Escuela Politecnica Nacional, Quito, Ecuador

E. Ayala 

Universidad San Francisco de Quito, Quito, Ecuador

E. Carrera Jarrin 

Academy of Scientific Research and Technology of the Arab Republic of Egypt, Egyptian Network of High Energy Physics, Cairo, Egypt

A.A. Abdelalim^{16,17} , S. Elgammal¹⁸, A. Ellithi Kamel¹⁹

Center for High Energy Physics (CHEP-FU), Fayoum University, El-Fayoum, Egypt

M. Abdullah Al-Mashad , M.A. Mahmoud 

National Institute of Chemical Physics and Biophysics, Tallinn, Estonia

K. Ehataht , M. Kadastik, T. Lange , C. Nielsen , J. Pata , M. Raidal , L. Tani , C. Veelken 

Department of Physics, University of Helsinki, Helsinki, Finland

K. Osterberg , M. Voutilainen 

Helsinki Institute of Physics, Helsinki, Finland

N. Bin Norjoharuddeen , E. Brücke , F. Garcia , P. Inkaew , K.T.S. Kallonen , T. Lampén , K. Lassila-Perini , S. Lehti , T. Lindén , M. Myllymäki , M.m. Rantanen , J. Tuominiemi 

Lappeenranta-Lahti University of Technology, Lappeenranta, Finland

H. Kirschenmann , P. Luukka , H. Petrow 

IRFU, CEA, Université Paris-Saclay, Gif-sur-Yvette, France

M. Besancon , F. Couderc , M. Dejardin , D. Denegri, J.L. Faure, F. Ferri , S. Ganjour , P. Gras , G. Hamel de Monchenault , M. Kumar , V. Lohezic , J. Malcles , F. Orlandi , L. Portales , A. Rosowsky , M.Ö. Sahin , A. Savoy-Navarro²⁰ , P. Simkina , M. Titov , M. Tornago 

Laboratoire Leprince-Ringuet, CNRS/IN2P3, Ecole Polytechnique, Institut Polytechnique de Paris, Palaiseau, France

F. Beaudette , G. Boldrini , P. Busson , A. Cappati , C. Charlot , M. Chiusi , T.D. Cuisset , F. Damas , O. Davignon , A. De Wit , I.T. Ehle , B.A. Fontana Santos Alves , S. Ghosh , A. Gilbert , R. Granier de Cassagnac , A. Hakimi , B. Harikrishnan , L. Kalipoliti , G. Liu , M. Nguyen , S. Obraztsov , C. Ochando , R. Salerno , J.B. Sauvan , Y. Sirois , G. Sokmen, L. Urda Gómez , E. Vernazza , A. Zabi , A. Zghiche 

Université de Strasbourg, CNRS, IPHC UMR 7178, Strasbourg, France

J.-L. Agram²¹ , J. Andrea , D. Apparu , D. Bloch , J.-M. Brom , E.C. Chabert , C. Collard , S. Falke , U. Goerlach , R. Haeberle , A.-C. Le Bihan , M. Meena , O. Poncet , G. Saha , M.A. Sessini , P. Van Hove , P. Vaucelle 

**Centre de Calcul de l’Institut National de Physique Nucléaire et de Physique des Particules,
CNRS/IN2P3, Villeurbanne, France**

A. Di Florio 

Institut de Physique des 2 Infinis de Lyon (IP2I), Villeurbanne, France

D. Amram, S. Beauceron , B. Blançon , G. Boudoul , N. Chanon , D. Contardo , P. Depasse , C. Dozen²² , H. El Mamouni, J. Fay , S. Gascon , M. Gouzevitch , C. Greenberg , G. Grenier , B. Ille , E. Jourd’huiy, I.B. Laktineh, M. Lethuillier , L. Mirabito, S. Perries, A. Purohit , M. Vander Donckt , P. Verdier , J. Xiao

Georgian Technical University, Tbilisi, Georgia

G. Adamov, I. Lomidze , Z. Tsamalaidze²³ 

RWTH Aachen University, I. Physikalisches Institut, Aachen, Germany

V. Botta , S. Consuegra Rodríguez , L. Feld , K. Klein , M. Lipinski , D. Meuser , A. Pauls , D. Pérez Adán , N. Röwert , M. Teroerde 

RWTH Aachen University, III. Physikalisches Institut A, Aachen, Germany

S. Diekmann , A. Dodonova , N. Eich , D. Eliseev , F. Engelke , J. Erdmann , M. Erdmann , B. Fischer , T. Hebbeker , K. Hoepfner , F. Ivone , A. Jung , M.y. Lee , F. Mausolf , M. Merschmeyer , A. Meyer , S. Mukherjee , D. Noll , F. Nowotny, A. Pozdnyakov , Y. Rath, W. Redjeb , F. Rehm, H. Reithler , V. Sarkisovi , A. Schmidt , C. Seth, A. Sharma , J.L. Spah , F. Torres Da Silva De Araujo²⁴ , S. Wiedenbeck , S. Zaleski

RWTH Aachen University, III. Physikalisches Institut B, Aachen, Germany

C. Dziwok , G. Flügge , T. Kress , A. Nowack , O. Pooth , A. Stahl , T. Ziemons , A. Zottz 

Deutsches Elektronen-Synchrotron, Hamburg, Germany

H. Aarup Petersen , M. Aldaya Martin , J. Alimena , S. Amoroso, Y. An , J. Bach , S. Baxter , M. Bayatmakou , H. Becerril Gonzalez , O. Behnke , A. Belvedere , F. Blekman²⁵ , K. Borras²⁶ , A. Campbell , A. Cardini , F. Colombina , M. De Silva , G. Eckerlin, D. Eckstein , L.I. Estevez Banos , E. Gallo²⁵ , A. Geiser , V. Guglielmi , M. Guthoff , A. Hinzmann , L. Jeppe , B. Kaech , M. Kasemann , C. Kleinwort , R. Kogler , M. Komm , D. Krücker , W. Lange, D. Leyva Pernia , K. Lipka²⁷ , W. Lohmann²⁸ , F. Lorkowski , R. Mankel , I.-A. Melzer-Pellmann , M. Mendizabal Morentin , A.B. Meyer , G. Milella , K. Moral Figueroa , A. Mussgiller , L.P. Nair , J. Niedziela , A. Nürnberg , J. Park , E. Ranken , A. Raspereza , D. Rastorguev , J. Rübenach, L. Rygaard, M. Scham^{29,26} , S. Schnake²⁶ , P. Schütze , C. Schwanenberger²⁵ , D. Selivanova , K. Sharko , M. Shchedrolosiev , D. Stafford , F. Vazzoler , A. Ventura Barroso , R. Walsh , D. Wang , Q. Wang , K. Wichmann, L. Wiens²⁶ , C. Wissing , Y. Yang , S. Zakharov, A. Zimermanne Castro Santos

University of Hamburg, Hamburg, Germany

A. Albrecht , S. Albrecht , M. Antonello , S. Bollweg, M. Bonanomi , P. Connor , K. El Morabit , Y. Fischer , E. Garutti , A. Grohsjean , J. Haller , D. Hundhausen, H.R. Jabusch , G. Kasieczka , P. Keicher , R. Klanner , W. Korcari , T. Kramer , C.c. Kuo, V. Kutzner , F. Labe , J. Lange , A. Lobanov , C. Matthies , L. Moureux , M. Mrowietz, A. Nigamova , Y. Nissan, A. Paasch , K.J. Pena Rodriguez , T. Quadfasel , B. Raciti , M. Rieger , D. Savoiu , J. Schindler , P. Schleper , M. Schröder , J. Schwandt , M. Sommerhalder , H. Stadie , G. Steinbrück , A. Tews, B. Wiederspan, M. Wolf

Karlsruher Institut fuer Technologie, Karlsruhe, Germany

S. Brommer [ID](#), E. Butz [ID](#), T. Chwalek [ID](#), A. Dierlamm [ID](#), G.G. Dincer [ID](#), U. Elicabuk, N. Faltermann [ID](#), M. Giffels [ID](#), A. Gottmann [ID](#), F. Hartmann³⁰ [ID](#), R. Hofsaess [ID](#), M. Horzela [ID](#), U. Husemann [ID](#), J. Kieseler [ID](#), M. Klute [ID](#), O. Lavoryk [ID](#), J.M. Lawhorn [ID](#), M. Link, A. Lintuluoto [ID](#), S. Maier [ID](#), S. Mitra [ID](#), M. Mormile [ID](#), Th. Müller [ID](#), M. Neukum, M. Oh [ID](#), E. Pfeffer [ID](#), M. Presilla [ID](#), G. Quast [ID](#), K. Rabbertz [ID](#), B. Regnery [ID](#), N. Shadskiy [ID](#), I. Shvetsov [ID](#), H.J. Simonis [ID](#), L. Sowa, L. Stockmeier, K. Tauqueer, M. Toms [ID](#), B. Topko [ID](#), N. Trevisani [ID](#), R.F. Von Cube [ID](#), M. Wassmer [ID](#), S. Wieland [ID](#), F. Wittig, R. Wolf [ID](#), X. Zuo [ID](#)

Institute of Nuclear and Particle Physics (INPP), NCSR Demokritos, Aghia Paraskevi, Greece

G. Anagnostou, G. Daskalakis [ID](#), A. Kyriakis [ID](#), A. Papadopoulos³⁰ [ID](#), A. Stakia [ID](#)

National and Kapodistrian University of Athens, Athens, Greece

G. Melachroinos, Z. Painesis [ID](#), I. Paraskevas [ID](#), N. Saoulidou [ID](#), K. Theofilatos [ID](#), E. Tziaferi [ID](#), K. Vellidis [ID](#), I. Zisopoulos [ID](#)

National Technical University of Athens, Athens, Greece

G. Bakas [ID](#), T. Chatzistavrou, G. Karapostoli [ID](#), K. Kousouris [ID](#), I. Papakrivopoulos [ID](#), E. Siamarkou, G. Tsipolitis [ID](#), A. Zacharopoulou

University of Ioánnina, Ioánnina, Greece

I. Bestintzanos, I. Evangelou [ID](#), C. Foudas, C. Kamtsikis, P. Katsoulis, P. Kokkas [ID](#), P.G. Kosmoglou Kiouseoglou [ID](#), N. Manthos [ID](#), I. Papadopoulos [ID](#), J. Strologas [ID](#)

HUN-REN Wigner Research Centre for Physics, Budapest, Hungary

C. Hajdu [ID](#), D. Horvath^{31,32} [ID](#), K. Márton, A.J. Rádl³³ [ID](#), F. Sikler [ID](#), V. Veszpremi [ID](#)

MTA-ELTE Lendület CMS Particle and Nuclear Physics Group, Eötvös Loránd University, Budapest, Hungary

M. Csand [ID](#), K. Farkas [ID](#), A. Fehrkuti³⁴ [ID](#), M.M.A. Gadallah³⁵ [ID](#), . Kadlecsik [ID](#), P. Major [ID](#), G. Pasztor [ID](#), G.I. Veres [ID](#)

Faculty of Informatics, University of Debrecen, Debrecen, Hungary

B. Ujvari [ID](#), G. Zilizi [ID](#)

HUN-REN ATOMKI - Institute of Nuclear Research, Debrecen, Hungary

G. Bencze, S. Czellar, J. Molnar, Z. Szillasi

Karoly Robert Campus, MATE Institute of Technology, Gyongyos, Hungary

T. Csorgo³⁴ [ID](#), F. Nemes³⁴ [ID](#), T. Novak [ID](#)

Panjab University, Chandigarh, India

S. Bansal [ID](#), S.B. Beri, V. Bhatnagar [ID](#), G. Chaudhary [ID](#), S. Chauhan [ID](#), N. Dhingra³⁶ [ID](#), A. Kaur [ID](#), A. Kaur [ID](#), H. Kaur [ID](#), M. Kaur [ID](#), S. Kumar [ID](#), T. Sheokand, J.B. Singh [ID](#), A. Singla [ID](#)

University of Delhi, Delhi, India

A. Bhardwaj [ID](#), A. Chhetri [ID](#), B.C. Choudhary [ID](#), A. Kumar [ID](#), A. Kumar [ID](#), M. Naimuddin [ID](#), K. Ranjan [ID](#), M.K. Saini, S. Saumya [ID](#)

Saha Institute of Nuclear Physics, HBNI, Kolkata, India

S. Baradia [ID](#), S. Barman³⁷ [ID](#), S. Bhattacharya [ID](#), S. Das Gupta, S. Dutta [ID](#), S. Dutta, S. Sarkar

Indian Institute of Technology Madras, Madras, India

M.M. Ameen [ID](#), P.K. Behera [ID](#), S.C. Behera [ID](#), S. Chatterjee [ID](#), G. Dash [ID](#), P. Jana [ID](#),

P. Kalbhor [ID](#), S. Kamble [ID](#), J.R. Komaragiri³⁸ [ID](#), D. Kumar³⁸ [ID](#), T. Mishra [ID](#), B. Parida³⁹ [ID](#), P.R. Pujahari [ID](#), N.R. Saha [ID](#), A. Sharma [ID](#), A.K. Sikdar [ID](#), R.K. Singh [ID](#), P. Verma [ID](#), S. Verma [ID](#), A. Vijay [ID](#)

Tata Institute of Fundamental Research-A, Mumbai, India

S. Dugad, G.B. Mohanty [ID](#), M. Shelake, P. Suryadevara

Tata Institute of Fundamental Research-B, Mumbai, India

A. Bala [ID](#), S. Banerjee [ID](#), S. Bhowmik [ID](#), R.M. Chatterjee, M. Guchait [ID](#), Sh. Jain [ID](#), A. Jaiswal, B.M. Joshi [ID](#), S. Kumar [ID](#), G. Majumder [ID](#), K. Mazumdar [ID](#), S. Parolia [ID](#), A. Thachayath [ID](#)

National Institute of Science Education and Research, An OCC of Homi Bhabha National Institute, Bhubaneswar, Odisha, India

S. Bahinipati⁴⁰ [ID](#), C. Kar [ID](#), D. Maity⁴¹ [ID](#), P. Mal [ID](#), K. Naskar⁴¹ [ID](#), A. Nayak⁴¹ [ID](#), S. Nayak, K. Pal [ID](#), P. Sadangi, S.K. Swain [ID](#), S. Varghese⁴¹ [ID](#), D. Vats⁴¹ [ID](#)

Indian Institute of Science Education and Research (IISER), Pune, India

S. Acharya⁴² [ID](#), A. Alpana [ID](#), S. Dube [ID](#), B. Gomber⁴² [ID](#), P. Hazarika [ID](#), B. Kansal [ID](#), A. Laha [ID](#), B. Sahu⁴² [ID](#), S. Sharma [ID](#), K.Y. Vaish [ID](#)

Isfahan University of Technology, Isfahan, Iran

H. Bakhshiansohi⁴³ [ID](#), A. Jafari⁴⁴ [ID](#), M. Zeinali⁴⁵ [ID](#)

Institute for Research in Fundamental Sciences (IPM), Tehran, Iran

S. Bashiri, S. Chenarani⁴⁶ [ID](#), S.M. Etesami [ID](#), Y. Hosseini [ID](#), M. Khakzad [ID](#), E. Khazaie [ID](#), M. Mohammadi Najafabadi [ID](#), S. Tizchang⁴⁷ [ID](#)

University College Dublin, Dublin, Ireland

M. Felcini [ID](#), M. Grunewald [ID](#)

INFN Sezione di Bari^a, Università di Bari^b, Politecnico di Bari^c, Bari, Italy

M. Abbrescia^{a,b} [ID](#), A. Colaleo^{a,b} [ID](#), D. Creanza^{a,c} [ID](#), B. D'Anzi^{a,b} [ID](#), N. De Filippis^{a,c} [ID](#), M. De Palma^{a,b} [ID](#), W. Elmtenawee^{a,b,16} [ID](#), N. Ferrara^{a,b} [ID](#), L. Fiore^a [ID](#), G. Iaselli^{a,c} [ID](#), L. Longo^a [ID](#), M. Louka^{a,b}, G. Maggi^{a,c} [ID](#), M. Maggi^a [ID](#), I. Margjeka^a [ID](#), V. Mastrapasqua^{a,b} [ID](#), S. My^{a,b} [ID](#), S. Nuzzo^{a,b} [ID](#), A. Pellecchia^{a,b} [ID](#), A. Pompili^{a,b} [ID](#), G. Pugliese^{a,c} [ID](#), R. Radogna^{a,b} [ID](#), D. Ramos^a [ID](#), A. Ranieri^a [ID](#), L. Silvestris^a [ID](#), F.M. Simone^{a,c} [ID](#), Ü. Sözbilir^a [ID](#), A. Stamerra^{a,b} [ID](#), D. Troiano^{a,b} [ID](#), R. Venditti^{a,b} [ID](#), P. Verwilligen^a [ID](#), A. Zaza^{a,b} [ID](#)

INFN Sezione di Bologna^a, Università di Bologna^b, Bologna, Italy

G. Abbiendi^a [ID](#), C. Battilana^{a,b} [ID](#), D. Bonacorsi^{a,b} [ID](#), P. Capiluppi^{a,b} [ID](#), A. Castro^{+a,b} [ID](#), F.R. Cavallo^a [ID](#), M. Cuffiani^{a,b} [ID](#), G.M. Dallavalle^a [ID](#), T. Diotalevi^{a,b} [ID](#), F. Fabbri^a [ID](#), A. Fanfani^{a,b} [ID](#), D. Fasanella^a [ID](#), P. Giacomelli^a [ID](#), L. Giommi^{a,b} [ID](#), C. Grandi^a [ID](#), L. Guiducci^{a,b} [ID](#), S. Lo Meo^{a,48} [ID](#), M. Lorusso^{a,b} [ID](#), L. Lunerti^a [ID](#), S. Marcellini^a [ID](#), G. Masetti^a [ID](#), F.L. Navarria^{a,b} [ID](#), G. Paggi^{a,b} [ID](#), A. Perrotta^a [ID](#), F. Primavera^{a,b} [ID](#), A.M. Rossi^{a,b} [ID](#), S. Rossi Tisbeni^{a,b} [ID](#), T. Rovelli^{a,b} [ID](#), G.P. Siroli^{a,b} [ID](#)

INFN Sezione di Catania^a, Università di Catania^b, Catania, Italy

S. Costa^{a,b,49} [ID](#), A. Di Mattia^a [ID](#), A. Lapertosa^a [ID](#), R. Potenza^{a,b}, A. Tricomi^{a,b,49} [ID](#)

INFN Sezione di Firenze^a, Università di Firenze^b, Firenze, Italy

P. Assiouras^a [ID](#), G. Barbagli^a [ID](#), G. Bardelli^{a,b} [ID](#), B. Camaiani^{a,b} [ID](#), A. Cassese^a [ID](#), R. Ceccarelli^a [ID](#), V. Ciulli^{a,b} [ID](#), C. Civinini^a [ID](#), R. D'Alessandro^{a,b} [ID](#), E. Focardi^{a,b} [ID](#), T. Kello^a [ID](#), G. Latino^{a,b} [ID](#), P. Lenzi^{a,b} [ID](#), M. Lizzo^a [ID](#), M. Meschini^a [ID](#), S. Paoletti^a [ID](#), A. Papanastassiou^{a,b}, G. Sguazzoni^a [ID](#), L. Viliani^a [ID](#)

INFN Laboratori Nazionali di Frascati, Frascati, ItalyL. Benussi , S. Bianco , S. Meola⁵⁰ , D. Piccolo **INFN Sezione di Genova^a, Università di Genova^b, Genova, Italy**M. Alves Gallo Pereira^a , F. Ferro^a , E. Robutti^a , S. Tosi^{a,b} **INFN Sezione di Milano-Bicocca^a, Università di Milano-Bicocca^b, Milano, Italy**A. Benaglia^a , F. Brivio^a , F. Cetorelli^{a,b} , F. De Guio^{a,b} , M.E. Dinardo^{a,b} , P. Dini^a , S. Gennai^a , R. Gerosa^{a,b} , A. Ghezzi^{a,b} , P. Govoni^{a,b} , L. Guzzi^a , G. Lavizzari^{a,b} , M.T. Lucchini^{a,b} , M. Malberti^a , S. Malvezzi^a , A. Massironi^a , D. Menasce^a , L. Moroni^a , M. Paganoni^{a,b} , S. Palluotto^{a,b} , D. Pedrini^a , A. Perego^{a,b} , B.S. Pinolini^a, G. Pizzati^{a,b} , S. Ragazzi^{a,b} , T. Tabarelli de Fatis^{a,b} **INFN Sezione di Napoli^a, Università di Napoli 'Federico II'^b, Napoli, Italy; Università della Basilicata^c, Potenza, Italy; Scuola Superiore Meridionale (SSM)^d, Napoli, Italy**S. Buontempo^a , A. Cagnotta^{a,b} , F. Carnevali^{a,b} , N. Cavallo^{a,c} , F. Fabozzi^{a,c} , A.O.M. Iorio^{a,b} , L. Lista^{a,b,51} , P. Paolucci^{a,30} , B. Rossi^a **INFN Sezione di Padova^a, Università di Padova^b, Padova, Italy; Università di Trento^c, Trento, Italy**R. Ardino^a , P. Azzi^a , N. Bacchetta^{a,52} , M. Biasotto^{a,53} , D. Bisello^{a,b} , P. Bortignon^a , G. Bortolato^{a,b} , A. Bragagnolo^{a,b} , A.C.M. Bulla^a , R. Carlin^{a,b} , P. Checchia^a , T. Dorigo^{a,54} , S. Fantinel^a , U. Gasparini^{a,b} , S. Giorgetti^a, E. Lusiani^a , M. Margoni^{a,b} , M. Migliorini^{a,b} , J. Pazzini^{a,b} , P. Ronchese^{a,b} , R. Rossin^{a,b} , F. Simonetto^{a,b} , M. Tosi^{a,b} , A. Triossi^{a,b} , S. Ventura^a , M. Zanetti^{a,b} , P. Zotto^{a,b} , A. Zucchetta^{a,b} , G. Zumerle^{a,b} **INFN Sezione di Pavia^a, Università di Pavia^b, Pavia, Italy**A. Braghieri^a , S. Calzaferri^a , D. Fiorina^a , P. Montagna^{a,b} , V. Re^a , C. Riccardi^{a,b} , P. Salvini^a , I. Vai^{a,b} , P. Vitulo^{a,b} **INFN Sezione di Perugia^a, Università di Perugia^b, Perugia, Italy**S. Ajmal^{a,b} , M.E. Ascotì^{a,b} , G.M. Bilei^a , C. Carrivale^{a,b} , D. Ciangottini^{a,b} , L. Fanò^{a,b} , V. Mariani^{a,b} , M. Menichelli^a , F. Moscatelli^{a,55} , A. Rossi^{a,b} , A. Santocchia^{a,b} , D. Spiga^a , T. Tedeschi^{a,b} **INFN Sezione di Pisa^a, Università di Pisa^b, Scuola Normale Superiore di Pisa^c, Pisa, Italy; Università di Siena^d, Siena, Italy**C. Aimè^a , C.A. Alexe^{a,c} , P. Asenov^{a,b} , P. Azzurri^a , G. Bagliesi^a , R. Bhattacharya^a , L. Bianchini^{a,b} , T. Boccali^a , E. Bossini^a , D. Bruschini^{a,c} , R. Castaldi^a , M.A. Ciocci^{a,b} , M. Cipriani^{a,b} , V. D'Amante^{a,d} , R. Dell'Orso^a , S. Donato^a , A. Giassi^a , F. Ligabue^{a,c} , A.C. Marini^a , D. Matos Figueiredo^a , A. Messineo^{a,b} , S. Mishra^a , V.K. Muraleedharan Nair Bindhu^{a,b,41} , M. Musich^{a,b} , S. Nandan^a , F. Palla^a , A. Rizzi^{a,b} , G. Rolandi^{a,c} , S. Roy Chowdhury^a , T. Sarkar^a , A. Scribano^a , P. Spagnolo^a , R. Tenchini^a , G. Tonelli^{a,b} , N. Turini^{a,d} , F. Vaselli^{a,c} , A. Venturi^a , P.G. Verdini^a **INFN Sezione di Roma^a, Sapienza Università di Roma^b, Roma, Italy**P. Barria^a , C. Basile^{a,b} , F. Cavallari^a , L. Cunqueiro Mendez^{a,b} , D. Del Re^{a,b} , E. Di Marco^{a,b} , M. Diemoz^a , F. Errico^{a,b} , R. Gargiulo^{a,b} , E. Longo^{a,b} , L. Martikainen^{a,b} , J. Mijuskovic^{a,b} , G. Organtini^{a,b} , F. Pandolfi^a , R. Paramatti^{a,b} , C. Quaranta^{a,b} , S. Rahatlou^{a,b} , C. Rovelli^a , F. Santanastasio^{a,b} , L. Soffi^a , V. Vladimirov^{a,b}

INFN Sezione di Torino^a, Università di Torino^b, Torino, Italy; Università del Piemonte Orientale^c, Novara, Italy

N. Amapane^{a,b} , R. Arcidiacono^{a,c} , S. Argiro^{a,b} , M. Arneodo^{a,c} , N. Bartosik^a , R. Bellan^{a,b} , C. Biino^a , C. Borca^{a,b} , N. Cartiglia^a , M. Costa^{a,b} , R. Covarelli^{a,b} , N. Demaria^a , L. Finco^a , M. Grippo^{a,b} , B. Kiani^{a,b} , F. Legger^a , F. Luongo^{a,b} , C. Mariotti^a , L. Markovic^{a,b} , S. Maselli^a , A. Mecca^{a,b} , L. Menzio^{a,b} , P. Meridiani^a , E. Migliore^{a,b} , M. Monteno^a , R. Mulargia^a , M.M. Obertino^{a,b} , G. Ortona^a , L. Pacher^{a,b} , N. Pastrone^a , M. Pelliccioni^a , M. Ruspa^{a,c} , F. Siviero^{a,b} , V. Sola^{a,b} , A. Solano^{a,b} , A. Staiano^a , C. Tarricone^{a,b} , D. Trocino^a , G. Umoret^{a,b} , R. White^{a,b}

INFN Sezione di Trieste^a, Università di Trieste^b, Trieste, Italy

J. Babbar^{a,b} , S. Belforte^a , V. Candelise^{a,b} , M. Casarsa^a , F. Cossutti^a , K. De Leo^a , G. Della Ricca^{a,b} 

Kyungpook National University, Daegu, Korea

S. Dogra , J. Hong , J. Kim, D. Lee, H. Lee, S.W. Lee , C.S. Moon , Y.D. Oh , M.S. Ryu , S. Sekmen , B. Tae, Y.C. Yang 

Department of Mathematics and Physics - GWNU, Gangneung, Korea

M.S. Kim 

Chonnam National University, Institute for Universe and Elementary Particles, Kwangju, Korea

G. Bak , P. Gwak , H. Kim , D.H. Moon 

Hanyang University, Seoul, Korea

E. Asilar , J. Choi⁵⁶ , D. Kim , T.J. Kim , J.A. Merlin, Y. Ryou

Korea University, Seoul, Korea

S. Choi , S. Han, B. Hong , K. Lee, K.S. Lee , S. Lee , J. Yoo 

Kyung Hee University, Department of Physics, Seoul, Korea

J. Goh , S. Yang 

Sejong University, Seoul, Korea

Y. Kang , H. S. Kim , Y. Kim, S. Lee

Seoul National University, Seoul, Korea

J. Almond, J.H. Bhyun, J. Choi , J. Choi, W. Jun , J. Kim , Y.W. Kim , S. Ko , H. Lee , J. Lee , J. Lee , B.H. Oh , S.B. Oh , H. Seo , U.K. Yang, I. Yoon 

University of Seoul, Seoul, Korea

W. Jang , D.Y. Kang, S. Kim , B. Ko, J.S.H. Lee , Y. Lee , I.C. Park , Y. Roh, I.J. Watson 

Yonsei University, Department of Physics, Seoul, Korea

S. Ha , K. Hwang , B. Kim , H.D. Yoo 

Sungkyunkwan University, Suwon, Korea

M. Choi , M.R. Kim , H. Lee, Y. Lee , I. Yu 

College of Engineering and Technology, American University of the Middle East (AUM), Dasman, Kuwait

T. Beyrouthy , Y. Gharbia 

Kuwait University - College of Science - Department of Physics, Safat, Kuwait

F. Alazemi 

Riga Technical University, Riga, Latvia

K. Dreimanis , A. Gaile , C. Munoz Diaz , D. Osite , G. Pikurs, A. Potrebko , M. Seidel , D. Sidiropoulos Kontos 

University of Latvia (LU), Riga, Latvia

N.R. Strautnieks 

Vilnius University, Vilnius, Lithuania

M. Ambrozas , A. Juodagalvis , A. Rinkevicius , G. Tamulaitis 

National Centre for Particle Physics, Universiti Malaya, Kuala Lumpur, Malaysia

I. Yusuff⁵⁷ , Z. Zolkapli

Universidad de Sonora (UNISON), Hermosillo, Mexico

J.F. Benitez , A. Castaneda Hernandez , H.A. Encinas Acosta, L.G. Gallegos Maríñez, M. León Coello , J.A. Murillo Quijada , A. Sehrawat , L. Valencia Palomo 

Centro de Investigacion y de Estudios Avanzados del IPN, Mexico City, Mexico

G. Ayala , H. Castilla-Valdez , H. Crotte Ledesma, E. De La Cruz-Burelo , I. Heredia-De La Cruz⁵⁸ , R. Lopez-Fernandez , J. Mejia Guisao , C.A. Mondragon Herrera, A. Sánchez Hernández 

Universidad Iberoamericana, Mexico City, Mexico

C. Oropeza Barrera , D.L. Ramirez Guadarrama, M. Ramírez García 

Benemerita Universidad Autonoma de Puebla, Puebla, Mexico

I. Bautista , F.E. Neri Huerta , I. Pedraza , H.A. Salazar Ibarguen , C. Uribe Estrada 

University of Montenegro, Podgorica, Montenegro

I. Bubanja , N. Raicevic 

University of Canterbury, Christchurch, New Zealand

P.H. Butler 

National Centre for Physics, Quaid-I-Azam University, Islamabad, Pakistan

A. Ahmad , M.I. Asghar, A. Awais , M.I.M. Awan, H.R. Hoorani , W.A. Khan 

AGH University of Krakow, Krakow, Poland

V. Avati, A. Bellora , L. Forthomme , L. Grzanka , M. Malawski , K. Piotrzkowski

National Centre for Nuclear Research, Swierk, Poland

H. Bialkowska , M. Bluj , M. Górski , M. Kazana , M. Szleper , P. Zalewski 

Institute of Experimental Physics, Faculty of Physics, University of Warsaw, Warsaw, Poland

K. Bunkowski , K. Doroba , A. Kalinowski , M. Konecki , J. Krolikowski , A. Muhammad 

Warsaw University of Technology, Warsaw, Poland

P. Fokow , K. Pozniak , W. Zabolotny 

Laboratório de Instrumentação e Física Experimental de Partículas, Lisboa, Portugal

M. Araujo , D. Bastos , C. Beirão Da Cruz E Silva , A. Boletti , M. Bozzo , T. Camporesi , G. Da Molin , P. Faccioli , M. Gallinaro , J. Hollar , N. Leonardo , G.B. Marozzo , A. Petrilli , M. Pisano , J. Seixas , J. Varela , J.W. Wulff 

Faculty of Physics, University of Belgrade, Belgrade, Serbia

P. Adzic , P. Milenovic 

VINCA Institute of Nuclear Sciences, University of Belgrade, Belgrade, SerbiaD. Devetak, M. Dordevic , J. Milosevic , L. Nadderd , V. Rekovic, M. Stojanovic **Centro de Investigaciones Energéticas Medioambientales y Tecnológicas (CIEMAT), Madrid, Spain**J. Alcaraz Maestre , Cristina F. Bedoya , J.A. Brochero Cifuentes , Oliver M. Carretero , M. Cepeda , M. Cerrada , N. Colino , B. De La Cruz , A. Delgado Peris , A. Escalante Del Valle , D. Fernández Del Val , J.P. Fernández Ramos , J. Flix , M.C. Fouz , O. Gonzalez Lopez , S. Goy Lopez , J.M. Hernandez , M.I. Josa , J. Llorente Merino , C. Martin Perez , E. Martin Viscasillas , D. Moran , C. M. Morcillo Perez , Á. Navarro Tobar , C. Perez Dengra , A. Pérez-Calero Yzquierdo , J. Puerta Pelayo , I. Redondo , J. Sastre , J. Vazquez Escobar **Universidad Autónoma de Madrid, Madrid, Spain**J.F. de Trocóniz **Universidad de Oviedo, Instituto Universitario de Ciencias y Tecnologías Espaciales de Asturias (ICTEA), Oviedo, Spain**B. Alvarez Gonzalez , J. Cuevas , J. Fernandez Menendez , S. Folgueras , I. Gonzalez Caballero , P. Leguina , E. Palencia Cortezon , J. Prado Pico , V. Rodríguez Bouza , A. Soto Rodríguez , A. Trapote , C. Vico Villalba , P. Vischia **Instituto de Física de Cantabria (IFCA), CSIC-Universidad de Cantabria, Santander, Spain**S. Blanco Fernández , I.J. Cabrillo , A. Calderon , J. Duarte Campderros , M. Fernandez , G. Gomez , C. Lasosa García , R. Lopez Ruiz , C. Martinez Rivero , P. Martinez Ruiz del Arbol , F. Matorras , P. Matorras Cuevas , E. Navarrete Ramos , J. Piedra Gomez , L. Scodellaro , I. Vila , J.M. Vizan Garcia **University of Colombo, Colombo, Sri Lanka**B. Kailasapathy⁵⁹ , D.D.C. Wickramarathna **University of Ruhuna, Department of Physics, Matara, Sri Lanka**W.G.D. Dharmaratna⁶⁰ , K. Liyanage , N. Perera **CERN, European Organization for Nuclear Research, Geneva, Switzerland**D. Abbaneo , C. Amendola , E. Auffray , G. Auzinger , J. Baechler, D. Barney , A. Bermúdez Martínez , M. Bianco , A.A. Bin Anuar , A. Bocci , L. Borgonovi , C. Botta , E. Brondolin , C.E. Brown , C. Caillol , G. Cerminara , N. Chernyavskaya , D. d'Enterria , A. Dabrowski , A. David , A. De Roeck , M.M. Defranchis , M. Deile , M. Dobson , G. Franzoni , W. Funk , S. Giani, D. Gigi, K. Gill , F. Glege , M. Glowacki, J. Hegeman , J.K. Heikkilä , B. Huber , V. Innocente , T. James , P. Janot , O. Kaluzinska , O. Karacheban²⁸ , G. Karathanasis , S. Laurila , P. Lecoq , E. Leutgeb , C. Lourenço , M. Magherini , L. Malgeri , M. Mannelli , M. Matthewman, A. Mehta , F. Meijers , S. Mersi , E. Meschi , V. Milosevic , F. Monti , F. Moortgat , M. Mulders , I. Neutelings , S. Orfanelli, F. Pantaleo , G. Petrucciani , A. Pfeiffer , M. Pierini , H. Qu , D. Rabady , B. Ribeiro Lopes , F. Riti , M. Rovere , H. Sakulin , R. Salvatico , S. Sanchez Cruz , S. Scarfi , C. Schwick, M. Selvaggi , A. Sharma , K. Shchelina , P. Silva , P. Sphicas⁶¹ , A.G. Stahl Leiton , A. Steen , S. Summers , D. Treille , P. Tropea , D. Walter , J. Wanczyk⁶² , J. Wang, S. Wuchterl , P. Zehetner , P. Zejdl , W.D. Zeuner**PSI Center for Neutron and Muon Sciences, Villigen, Switzerland**T. Bevilacqua⁶³ , L. Caminada⁶³ , A. Ebrahimi , W. Erdmann , R. Horisberger 

Q. Ingram [ID](#), H.C. Kaestli [ID](#), D. Kotlinski [ID](#), C. Lange [ID](#), M. Missiroli⁶³ [ID](#), L. Noehte⁶³ [ID](#), T. Rohe [ID](#), A. Samalan

ETH Zurich - Institute for Particle Physics and Astrophysics (IPA), Zurich, Switzerland

T.K. Arrestad [ID](#), M. Backhaus [ID](#), G. Bonomelli [ID](#), A. Calandri [ID](#), C. Cazzaniga [ID](#), K. Datta [ID](#), P. De Bryas Dexmiers D'archiac⁶² [ID](#), A. De Cosa [ID](#), G. Dissertori [ID](#), M. Dittmar, M. Donegà [ID](#), F. Eble [ID](#), M. Galli [ID](#), K. Gedia [ID](#), F. Glessgen [ID](#), C. Grab [ID](#), N. Härringer [ID](#), T.G. Harte, D. Hits [ID](#), W. Lustermann [ID](#), A.-M. Lyon [ID](#), R.A. Manzoni [ID](#), M. Marchegiani [ID](#), L. Marchese [ID](#), A. Mascellani⁶² [ID](#), F. Nesi-Tedaldi [ID](#), F. Pauss [ID](#), V. Perovic [ID](#), S. Pigazzini [ID](#), B. Ristic [ID](#), R. Seidita [ID](#), J. Steggemann⁶² [ID](#), A. Tarabini [ID](#), D. Valsecchi [ID](#), R. Wallny [ID](#)

Universität Zürich, Zurich, Switzerland

C. Amsler⁶⁴ [ID](#), P. Bärtschi [ID](#), M.F. Canelli [ID](#), K. Cormier [ID](#), M. Huwiler [ID](#), W. Jin [ID](#), A. Jofrehei [ID](#), B. Kilminster [ID](#), S. Leontsinis [ID](#), S.P. Liechti [ID](#), A. Macchiolo [ID](#), P. Meiring [ID](#), F. Meng [ID](#), J. Motta [ID](#), A. Reimers [ID](#), P. Robmann, M. Senger [ID](#), E. Shokr, F. Stäger [ID](#), R. Tramontano [ID](#)

National Central University, Chung-Li, Taiwan

C. Adloff⁶⁵ [ID](#), D. Bhowmik, C.M. Kuo, W. Lin, P.K. Rout [ID](#), P.C. Tiwari³⁸ [ID](#)

National Taiwan University (NTU), Taipei, Taiwan

L. Ceard, K.F. Chen [ID](#), Z.g. Chen, A. De Iorio [ID](#), W.-S. Hou [ID](#), T.h. Hsu, Y.w. Kao, S. Karmakar [ID](#), G. Kole [ID](#), Y.y. Li [ID](#), R.-S. Lu [ID](#), E. Paganis [ID](#), X.f. Su [ID](#), J. Thomas-Wilsker [ID](#), L.s. Tsai, D. Tsionou, H.y. Wu, E. Yazgan [ID](#)

High Energy Physics Research Unit, Department of Physics, Faculty of Science, Chulalongkorn University, Bangkok, Thailand

C. Asawatangtrakuldee [ID](#), N. Srimanobhas [ID](#), V. Wachirapusanand [ID](#)

Tunis El Manar University, Tunis, Tunisia

Y. Maghrbi [ID](#)

Çukurova University, Physics Department, Science and Art Faculty, Adana, Turkey

D. Agyel [ID](#), F. Boran [ID](#), F. Dolek [ID](#), I. Dumanoglu⁶⁶ [ID](#), E. Eskut [ID](#), Y. Guler⁶⁷ [ID](#), E. Gurpinar Guler⁶⁷ [ID](#), C. Isik [ID](#), O. Kara, A. Kayis Topaksu [ID](#), Y. Komurcu [ID](#), G. Onengut [ID](#), K. Ozdemir⁶⁸ [ID](#), A. Polatoz [ID](#), B. Tali⁶⁹ [ID](#), U.G. Tok [ID](#), E. Uslan [ID](#), I.S. Zorbakir [ID](#)

Middle East Technical University, Physics Department, Ankara, Turkey

M. Yalvac⁷⁰ [ID](#)

Bogazici University, Istanbul, Turkey

B. Akgun [ID](#), I.O. Atakisi [ID](#), E. Gülmez [ID](#), M. Kaya⁷¹ [ID](#), O. Kaya⁷² [ID](#), S. Tekten⁷³ [ID](#)

Istanbul Technical University, Istanbul, Turkey

A. Cakir [ID](#), K. Cankocak^{66,74} [ID](#), S. Sen⁷⁵ [ID](#)

Istanbul University, Istanbul, Turkey

O. Aydilek⁷⁶ [ID](#), B. Hacisahinoglu [ID](#), I. Hos⁷⁷ [ID](#), B. Kaynak [ID](#), S. Ozkorucuklu [ID](#), O. Potok [ID](#), H. Sert [ID](#), C. Simsek [ID](#), C. Zorbilmez [ID](#)

Yildiz Technical University, Istanbul, Turkey

S. Cerci [ID](#), B. Isildak⁷⁸ [ID](#), D. Sunar Cerci [ID](#), T. Yetkin [ID](#)

Institute for Scintillation Materials of National Academy of Science of Ukraine, Kharkiv, Ukraine

A. Boyaryntsev [ID](#), B. Grynyov [ID](#)

National Science Centre, Kharkiv Institute of Physics and Technology, Kharkiv, UkraineL. Levchuk **University of Bristol, Bristol, United Kingdom**D. Anthony , J.J. Brooke , A. Budson , F. Bury , E. Clement , D. Cussans , H. Flacher , J. Goldstein , H.F. Heath , M.-L. Holmberg , L. Kreczko , S. Paramesvaran , L. Robertshaw , V.J. Smith , K. Walkingshaw Pass **Rutherford Appleton Laboratory, Didcot, United Kingdom**A.H. Ball, K.W. Bell , A. Belyaev⁷⁹ , C. Brew , R.M. Brown , D.J.A. Cockerill , C. Cooke , A. Elliot , K.V. Ellis, K. Harder , S. Harper , J. Linacre , K. Manolopoulos, D.M. Newbold , E. Olaiya, D. Petyt , T. Reis , A.R. Sahasransu , G. Salvi , T. Schuh, C.H. Shepherd-Themistocleous , I.R. Tomalin , K.C. Whalen , T. Williams **Imperial College, London, United Kingdom**I. Andreou , R. Bainbridge , P. Bloch , O. Buchmuller, C.A. Carrillo Montoya , G.S. Chahal⁸⁰ , D. Colling , J.S. Dancu, I. Das , P. Dauncey , G. Davies , M. Della Negra , S. Fayer, G. Fedi , G. Hall , A. Howard, G. Iles , C.R. Knight , P. Krueper, J. Langford , K.H. Law , J. León Holgado , L. Lyons , A.-M. Magnan , B. Maier , S. Mallios, M. Mieskolainen , J. Nash⁸¹ , M. Pesaresi , P.B. Pradeep, B.C. Radburn-Smith , A. Richards, A. Rose , K. Savva , C. Seez , R. Shukla , A. Tapper , K. Uchida , G.P. Uttley , T. Virdee³⁰ , M. Vojinovic , N. Wardle , D. Winterbottom **Brunel University, Uxbridge, United Kingdom**J.E. Cole , A. Khan, P. Kyberd , I.D. Reid **Baylor University, Waco, Texas, USA**S. Abdullin , A. Brinkerhoff , E. Collins , M.R. Darwish , J. Dittmann , K. Hatakeyama , V. Hegde , J. Hiltbrand , B. McMaster , J. Samudio , S. Sawant , C. Sutantawibul , J. Wilson **Catholic University of America, Washington, DC, USA**R. Bartek , A. Dominguez , A.E. Simsek , S.S. Yu **The University of Alabama, Tuscaloosa, Alabama, USA**B. Bam , A. Buchot Perraguin , R. Chudasama , S.I. Cooper , C. Crovella , S.V. Gleyzer , E. Pearson, C.U. Perez , P. Rumerio⁸² , E. Usai , R. Yi **Boston University, Boston, Massachusetts, USA**A. Akpinar , C. Cosby , G. De Castro, Z. Demiragli , C. Erice , C. Fangmeier , C. Fernandez Madrazo , E. Fontanesi , D. Gastler , F. Golf , S. Jeon , J. O'cain, I. Reed , J. Rohlf , K. Salyer , D. Sperka , D. Spitzbart , I. Suarez , A. Tsatsos , A.G. Zecchinelli **Brown University, Providence, Rhode Island, USA**G. Barone , G. Benelli , D. Cutts , L. Gouskos , M. Hadley , U. Heintz , K.W. Ho , J.M. Hogan⁸³ , T. Kwon , G. Landsberg , K.T. Lau , J. Luo , S. Mondal , T. Russell, S. Sagir⁸⁴ , X. Shen , M. Stamenkovic , N. Venkatasubramanian **University of California, Davis, Davis, California, USA**S. Abbott , B. Barton , C. Brainerd , R. Breedon , H. Cai , M. Calderon De La Barca Sanchez , M. Chertok , M. Citron , J. Conway , P.T. Cox , R. Erbacher , F. Jensen , O. Kukral , G. Mocellin , M. Mulhearn , S. Ostrom 

W. Wei , S. Yoo , F. Zhang 

University of California, Los Angeles, California, USA

K. Adamidis, M. Bachtis , D. Campos, R. Cousins , A. Datta , G. Flores Avila , J. Hauser , M. Ignatenko , M.A. Iqbal , T. Lam , Y.f. Lo, E. Manca , A. Nunez Del Prado, D. Saltzberg , V. Valuev

University of California, Riverside, Riverside, California, USA

R. Clare , J.W. Gary , G. Hanson 

University of California, San Diego, La Jolla, California, USA

A. Aportela, A. Arora , J.G. Branson , S. Cittolin , S. Cooperstein , D. Diaz , J. Duarte , L. Giannini , Y. Gu, J. Guiang , R. Kansal , V. Krutelyov , R. Lee , J. Letts , M. Masciovecchio , F. Mokhtar , S. Mukherjee , M. Pieri , D. Primosch, M. Quinnan , V. Sharma , M. Tadel , E. Vourliotis , F. Würthwein , Y. Xiang , A. Yagil

University of California, Santa Barbara - Department of Physics, Santa Barbara, California, USA

A. Barzdukas , L. Brennan , C. Campagnari , K. Downham , C. Grieco , M.M. Hussain, J. Incandela , J. Kim , A.J. Li , P. Masterson , H. Mei , J. Richman , S.N. Santpur , U. Sarica , R. Schmitz , F. Setti , J. Sheplock , D. Stuart , T.Á. Vámi , X. Yan , D. Zhang

California Institute of Technology, Pasadena, California, USA

S. Bhattacharya , A. Bornheim , O. Cerri, J. Mao , H.B. Newman , G. Reales Gutiérrez, M. Spiropulu , J.R. Vlimant , C. Wang , S. Xie , R.Y. Zhu 

Carnegie Mellon University, Pittsburgh, Pennsylvania, USA

J. Alison , S. An , P. Bryant , M. Cremonesi, V. Dutta , T. Ferguson , T.A. Gómez Espinosa , A. Harilal , A. Kallil Tharayil, M. Kanemura, C. Liu , T. Mudholkar , S. Murthy , P. Palit , K. Park, M. Paulini , A. Roberts , A. Sanchez , W. Terrill

University of Colorado Boulder, Boulder, Colorado, USA

J.P. Cumalat , W.T. Ford , A. Hart , A. Hassani , N. Manganelli , J. Pearkes , C. Savard , N. Schonbeck , K. Stenson , K.A. Ulmer , S.R. Wagner , N. Zipper , D. Zuolo 

Cornell University, Ithaca, New York, USA

J. Alexander , X. Chen , D.J. Cranshaw , J. Dickinson , J. Fan , X. Fan , S. Hogan , P. Kotamnives, J. Monroy , M. Oshiro , J.R. Patterson , M. Reid , A. Ryd , J. Thom , P. Wittich , R. Zou 

Fermi National Accelerator Laboratory, Batavia, Illinois, USA

M. Albrow , M. Alyari , O. Amram , G. Apollinari , A. Apresyan , L.A.T. Bauerick , D. Berry , J. Berryhill , P.C. Bhat , K. Burkett , J.N. Butler , A. Canepa , G.B. Cerati , H.W.K. Cheung , F. Chlebana , G. Cummings , I. Dutta , V.D. Elvira , J. Freeman , A. Gandrakota , Z. Gecse , L. Gray , D. Green, A. Grummer , S. Grünendahl , D. Guerrero , O. Gutsche , R.M. Harris , T.C. Herwig , J. Hirschauer , B. Jayatilaka , S. Jindariani , M. Johnson , U. Joshi , T. Klijnsma , B. Klima , K.H.M. Kwok , S. Lammel , C. Lee , D. Lincoln , R. Lipton , T. Liu , K. Maeshima , D. Mason , P. McBride , P. Merkel , S. Mrenna , S. Nahm , J. Ngadiuba , D. Noonan , S. Norberg, V. Papadimitriou , N. Pastika , K. Pedro , C. Pena⁸⁵ , F. Ravera , A. Reinsvold Hall⁸⁶ , L. Ristori , M. Safdari , E. Sexton-Kennedy , N. Smith

A. Soha [id](#), L. Spiegel [id](#), S. Stoynev [id](#), J. Strait [id](#), L. Taylor [id](#), S. Tkaczyk [id](#), N.V. Tran [id](#), L. Uplegger [id](#), E.W. Vaandering [id](#), I. Zoi [id](#)

University of Florida, Gainesville, Florida, USA

C. Aruta [id](#), P. Avery [id](#), D. Bourilkov [id](#), P. Chang [id](#), V. Cherepanov [id](#), R.D. Field, C. Huh [id](#), E. Koenig [id](#), M. Kolosova [id](#), J. Konigsberg [id](#), A. Korytov [id](#), K. Matchev [id](#), N. Menendez [id](#), G. Mitselmakher [id](#), K. Mohrman [id](#), A. Muthirakalayil Madhu [id](#), N. Rawal [id](#), S. Rosenzweig [id](#), Y. Takahashi [id](#), J. Wang [id](#)

Florida State University, Tallahassee, Florida, USA

T. Adams [id](#), A. Al Kadhim [id](#), A. Askew [id](#), S. Bower [id](#), R. Hashmi [id](#), R.S. Kim [id](#), S. Kim [id](#), T. Kolberg [id](#), G. Martinez, H. Prosper [id](#), P.R. Prova, M. Wulansatiti [id](#), R. Yohay [id](#), J. Zhang

Florida Institute of Technology, Melbourne, Florida, USA

B. Alsufyani [id](#), S. Butalla [id](#), S. Das [id](#), T. Elkafrawy⁸⁷ [id](#), M. Hohlmann [id](#), E. Yanes

University of Illinois Chicago, Chicago, Illinois, USA

M.R. Adams [id](#), A. Baty [id](#), C. Bennett, R. Cavanaugh [id](#), R. Escobar Franco [id](#), O. Evdokimov [id](#), C.E. Gerber [id](#), M. Hawksworth, A. Hingrajiya, D.J. Hofman [id](#), J.h. Lee [id](#), D. S. Lemos [id](#), C. Mills [id](#), S. Nanda [id](#), G. Oh [id](#), B. Ozek [id](#), D. Pilipovic [id](#), R. Pradhan [id](#), E. Prifti, T. Roy [id](#), S. Rudrabhatla [id](#), N. Singh, M.B. Tonjes [id](#), N. Varelas [id](#), M.A. Wadud [id](#), Z. Ye [id](#), J. Yoo [id](#)

The University of Iowa, Iowa City, Iowa, USA

M. Alhusseini [id](#), D. Blend, K. Dilsiz⁸⁸ [id](#), L. Emediato [id](#), G. Karaman [id](#), O.K. Köseyan [id](#), J.-P. Merlo, A. Mestvirishvili⁸⁹ [id](#), O. Neogi, H. Ogul⁹⁰ [id](#), Y. Onel [id](#), A. Penzo [id](#), C. Snyder, E. Tiras⁹¹ [id](#)

Johns Hopkins University, Baltimore, Maryland, USA

B. Blumenfeld [id](#), L. Corcodilos [id](#), J. Davis [id](#), A.V. Gritsan [id](#), L. Kang [id](#), S. Kyriacou [id](#), P. Maksimovic [id](#), M. Roguljic [id](#), J. Roskes [id](#), S. Sekhar [id](#), M. Swartz [id](#)

The University of Kansas, Lawrence, Kansas, USA

A. Abreu [id](#), L.F. Alcerro Alcerro [id](#), J. Anguiano [id](#), S. Arteaga Escatel [id](#), P. Baringer [id](#), A. Bean [id](#), Z. Flowers [id](#), D. Grove [id](#), J. King [id](#), G. Krintiras [id](#), M. Lazarovits [id](#), C. Le Mahieu [id](#), J. Marquez [id](#), M. Murray [id](#), M. Nickel [id](#), M. Pitt [id](#), S. Popescu⁹² [id](#), C. Rogan [id](#), C. Royon [id](#), S. Sanders [id](#), C. Smith [id](#), G. Wilson [id](#)

Kansas State University, Manhattan, Kansas, USA

B. Allmond [id](#), R. Guju Gurunadha [id](#), A. Ivanov [id](#), K. Kaadze [id](#), Y. Maravin [id](#), J. Natoli [id](#), D. Roy [id](#), G. Sorrentino [id](#)

University of Maryland, College Park, Maryland, USA

A. Baden [id](#), A. Belloni [id](#), J. Bistany-riebman, Y.M. Chen [id](#), S.C. Eno [id](#), N.J. Hadley [id](#), S. Jabeen [id](#), R.G. Kellogg [id](#), T. Koeth [id](#), B. Kronheim, Y. Lai [id](#), S. Lascio [id](#), A.C. Mignerey [id](#), S. Nabili [id](#), C. Palmer [id](#), C. Papageorgakis [id](#), M.M. Paranjpe, E. Popova⁹³ [id](#), A. Shevelev [id](#), L. Wang [id](#), L. Zhang [id](#)

Massachusetts Institute of Technology, Cambridge, Massachusetts, USA

C. Baldenegro Barrera [id](#), J. Bendavid [id](#), S. Bright-Thonney [id](#), I.A. Cali [id](#), P.c. Chou [id](#), M. D'Alfonso [id](#), J. Eysermans [id](#), C. Freer [id](#), G. Gomez-Ceballos [id](#), M. Goncharov, G. Grossi, P. Harris, D. Hoang, D. Kovalskyi [id](#), J. Krupa [id](#), L. Lavezzi [id](#), Y.-J. Lee [id](#), K. Long [id](#), C. Mcginn [id](#), A. Novak [id](#), M.I. Park [id](#), C. Paus [id](#), C. Reissel [id](#), C. Roland [id](#), G. Roland [id](#), S. Rothman [id](#), G.S.F. Stephans [id](#), Z. Wang [id](#), B. Wyslouch [id](#), T. J. Yang [id](#)

University of Minnesota, Minneapolis, Minnesota, USA

B. Crossman , C. Kapsiak , M. Krohn , D. Mahon , J. Mans , B. Marzocchi , M. Revering , R. Rusack , R. Saradhy , N. Strobbe

University of Nebraska-Lincoln, Lincoln, Nebraska, USA

K. Bloom , D.R. Claes , G. Haza , J. Hossain , C. Joo , I. Kravchenko , A. Rohilla , J.E. Siado , W. Tabb , A. Vagnerini , A. Wightman , F. Yan , D. Yu

State University of New York at Buffalo, Buffalo, New York, USA

H. Bandyopadhyay , L. Hay , H.w. Hsia , I. Iashvili , A. Kalogeropoulos , A. Kharchilava , M. Morris , D. Nguyen , S. Rappoccio , H. Rejeb Sfar, A. Williams , P. Young

Northeastern University, Boston, Massachusetts, USA

G. Alverson , E. Barberis , J. Bonilla , B. Bylsma, M. Campana , J. Dervan , Y. Haddad , Y. Han , I. Israr , A. Krishna , P. Levchenko , J. Li , M. Lu , R. McCarthy , D.M. Morse , V. Nguyen , T. Orimoto , A. Parker , L. Skinnari , E. Tsai , D. Wood

Northwestern University, Evanston, Illinois, USA

S. Dittmer , K.A. Hahn , D. Li , Y. Liu , M. Mcginnis , Y. Miao , D.G. Monk , M.H. Schmitt , A. Taliercio , M. Velasco

University of Notre Dame, Notre Dame, Indiana, USA

G. Agarwal , R. Band , R. Bucci, S. Castells , A. Das , R. Goldouzian , M. Hildreth , K. Hurtado Anampa , T. Ivanov , C. Jessop , K. Lannon , J. Lawrence , N. Loukas , L. Lutton , J. Mariano, N. Marinelli, I. Mcalister, T. McCauley , C. McGrady , C. Moore , Y. Musienko²³ , H. Nelson , M. Osherson , A. Piccinelli , R. Ruchti , A. Townsend , Y. Wan, M. Wayne , H. Yockey, M. Zarucki , L. Zygala

The Ohio State University, Columbus, Ohio, USA

A. Basnet , M. Carrigan , L.S. Durkin , C. Hill , M. Joyce , M. Nunez Ornelas , K. Wei, D.A. Wenzl, B.L. Winer , B. R. Yates 

Princeton University, Princeton, New Jersey, USA

H. Bouchamaoui , K. Coldham, P. Das , G. Dezoort , P. Elmer , P. Fackeldey , A. Frankenthal , B. Greenberg , N. Haubrich , K. Kennedy, G. Kopp , S. Kwan , D. Lange , A. Loeliger , D. Marlow , I. Ojalvo , J. Olsen , F. Simpson , D. Stickland , C. Tully , L.H. Vage

University of Puerto Rico, Mayaguez, Puerto Rico, USA

S. Malik , R. Sharma

Purdue University, West Lafayette, Indiana, USA

A.S. Bakshi , S. Chandra , R. Chawla , A. Gu , L. Gutay, M. Jones , A.W. Jung , A.M. Koshy, M. Liu , G. Negro , N. Neumeister , G. Paspalaki , S. Piperov , J.F. Schulte , A. K. Virdi , F. Wang , A. Wildridge , W. Xie , Y. Yao

Purdue University Northwest, Hammond, Indiana, USA

J. Dolen , N. Parashar , A. Pathak 

Rice University, Houston, Texas, USA

D. Acosta , A. Agrawal , T. Carnahan , K.M. Ecklund , P.J. Fernández Manteca , S. Freed, P. Gardner, F.J.M. Geurts , I. Krommydas , W. Li , J. Lin , O. Miguel Colin , B.P. Padley , R. Redjimi, J. Rotter , E. Yigitbasi , Y. Zhang

University of Rochester, Rochester, New York, USA

A. Bodek , P. de Barbaro , R. Demina , J.L. Dulemba , A. Garcia-Bellido , O. Hindrichs , A. Khukhunaishvili , N. Parmar , P. Parygin⁹³ , R. Taus 

Rutgers, The State University of New Jersey, Piscataway, New Jersey, USA

B. Chiarito, J.P. Chou , S.V. Clark , D. Gadkari , Y. Gershtein , E. Halkiadakis , M. Heindl , C. Houghton , D. Jaroslawski , S. Konstantinou , I. Laflotte , A. Lath , R. Montalvo, K. Nash, J. Reichert , P. Saha , S. Salur , S. Schnetzer, S. Somalwar , R. Stone , S.A. Thayil , S. Thomas, J. Vora 

University of Tennessee, Knoxville, Tennessee, USA

D. Ally , A.G. Delannoy , S. Fiorendi , S. Higginbotham , T. Holmes , A.R. Kanuganti , N. Karunaratnha , L. Lee , E. Nibigira , S. Spanier 

Texas A&M University, College Station, Texas, USA

D. Aebi , M. Ahmad , T. Akhter , K. Androsov⁶² , O. Bouhali⁹⁴ , R. Eusebi , J. Gilmore , T. Huang , T. Kamon⁹⁵ , H. Kim , S. Luo , R. Mueller , D. Overton , A. Safonov 

Texas Tech University, Lubbock, Texas, USA

N. Akchurin , J. Damgov , Y. Feng , N. Gogate , Y. Kazhykarim, K. Lamichhane , S.W. Lee , C. Madrid , A. Mankel , T. Peltola , I. Volobouev 

Vanderbilt University, Nashville, Tennessee, USA

E. Appelt , Y. Chen , S. Greene, A. Gurrola , W. Johns , R. Kunnawalkam Elayavalli , A. Melo , D. Rathjens , F. Romeo , P. Sheldon , S. Tuo , J. Velkovska , J. Viinikainen 

University of Virginia, Charlottesville, Virginia, USA

B. Cardwell , H. Chung, B. Cox , J. Hakala , R. Hirosky , A. Ledovskoy , C. Mantilla , C. Neu , C. Ramón Álvarez 

Wayne State University, Detroit, Michigan, USA

S. Bhattacharya , P.E. Karchin 

University of Wisconsin - Madison, Madison, Wisconsin, USA

A. Aravind , S. Banerjee , K. Black , T. Bose , E. Chavez , S. Dasu , P. Everaerts , C. Galloni, H. He , M. Herndon , A. Herve , C.K. Koraka , A. Lanaro, R. Loveless , J. Madhusudanan Sreekala , A. Mallampalli , A. Mohammadi , S. Mondal, G. Parida , L. Pétré , D. Pinna, A. Savin, V. Shang , V. Sharma , W.H. Smith , D. Teague, H.F. Tsoi , W. Vetens , A. Warden 

Authors affiliated with an international laboratory covered by a cooperation agreement with CERN

S. Afanasiev , V. Alexakhin , D. Budkouski , I. Golutvin[†] , I. Gorbunov , V. Karjavine , O. Kodolova^{96,93} , V. Korenkov , A. Lanev , A. Malakhov , V. Matveev⁹⁷ , A. Nikitenko^{98,96} , V. Palichik , V. Perelygin , M. Savina , V. Shalaev , S. Shmatov , S. Shulha , V. Smirnov , O. Teryaev , N. Voytishin , B.S. Yuldashev⁹⁹, A. Zarubin , I. Zhizhin , Yu. Andreev , A. Dermenev , S. Gninenko , N. Golubev , A. Karneyeu , D. Kirpichnikov , M. Kirsanov , N. Krasnikov , I. Tlisova , A. Toropin 

Authors affiliated with an institute formerly covered by a cooperation agreement with CERN

G. Gavrilov , V. Golovtcov , Y. Ivanov , V. Kim¹⁰⁰ , V. Murzin , V. Oreshkin , D. Sosnov , V. Sulimov , L. Uvarov , A. Vorobyev[†], T. Aushev , K. Ivanov , V. Gavrilov , N. Lychkovskaya , V. Popov , A. Zhokin , R. Chistov¹⁰⁰ , M. Danilov¹⁰⁰ 

S. Polikarpov¹⁰⁰ , V. Andreev , M. Azarkin , M. Kirakosyan, A. Terkulov , E. Boos , A. Demiyanov , A. Ershov , A. Gribushin , L. Khein , V. Korotkikh, S. Petrushanko , V. Savrin , A. Snigirev , I. Vardanyan , V. Blinov¹⁰⁰, T. Dimova¹⁰⁰ , A. Kozyrev¹⁰⁰ , O. Radchenko¹⁰⁰ , Y. Skovpen¹⁰⁰ , V. Kachanov , S. Slabospitskii , A. Uzunian , A. Babaev , V. Borshch , D. Druzhkin 

†: Deceased

¹Also at Yerevan State University, Yerevan, Armenia

²Also at TU Wien, Vienna, Austria

³Also at Ghent University, Ghent, Belgium

⁴Also at Universidade do Estado do Rio de Janeiro, Rio de Janeiro, Brazil

⁵Also at FACAMP - Faculdades de Campinas, Sao Paulo, Brazil

⁶Also at Universidade Estadual de Campinas, Campinas, Brazil

⁷Also at Federal University of Rio Grande do Sul, Porto Alegre, Brazil

⁸Also at University of Chinese Academy of Sciences, Beijing, China

⁹Also at China Center of Advanced Science and Technology, Beijing, China

¹⁰Also at University of Chinese Academy of Sciences, Beijing, China

¹¹Also at China Spallation Neutron Source, Guangdong, China

¹²Now at Henan Normal University, Xinxiang, China

¹³Also at University of Shanghai for Science and Technology, Shanghai, China

¹⁴Now at The University of Iowa, Iowa City, Iowa, USA

¹⁵Also at an institute formerly covered by a cooperation agreement with CERN

¹⁶Also at Helwan University, Cairo, Egypt

¹⁷Now at Zewail City of Science and Technology, Zewail, Egypt

¹⁸Now at British University in Egypt, Cairo, Egypt

¹⁹Now at Cairo University, Cairo, Egypt

²⁰Also at Purdue University, West Lafayette, Indiana, USA

²¹Also at Université de Haute Alsace, Mulhouse, France

²²Also at Istinye University, Istanbul, Turkey

²³Also at an international laboratory covered by a cooperation agreement with CERN

²⁴Also at The University of the State of Amazonas, Manaus, Brazil

²⁵Also at University of Hamburg, Hamburg, Germany

²⁶Also at RWTH Aachen University, III. Physikalisches Institut A, Aachen, Germany

²⁷Also at Bergische University Wuppertal (BUW), Wuppertal, Germany

²⁸Also at Brandenburg University of Technology, Cottbus, Germany

²⁹Also at Forschungszentrum Jülich, Juelich, Germany

³⁰Also at CERN, European Organization for Nuclear Research, Geneva, Switzerland

³¹Also at HUN-REN ATOMKI - Institute of Nuclear Research, Debrecen, Hungary

³²Now at Universitatea Babes-Bolyai - Facultatea de Fizica, Cluj-Napoca, Romania

³³Also at MTA-ELTE Lendület CMS Particle and Nuclear Physics Group, Eötvös Loránd University, Budapest, Hungary

³⁴Also at HUN-REN Wigner Research Centre for Physics, Budapest, Hungary

³⁵Also at Physics Department, Faculty of Science, Assiut University, Assiut, Egypt

³⁶Also at Punjab Agricultural University, Ludhiana, India

³⁷Also at University of Visva-Bharati, Santiniketan, India

³⁸Also at Indian Institute of Science (IISc), Bangalore, India

³⁹Also at Amity University Uttar Pradesh, Noida, India

⁴⁰Also at IIT Bhubaneswar, Bhubaneswar, India

⁴¹Also at Institute of Physics, Bhubaneswar, India

⁴²Also at University of Hyderabad, Hyderabad, India

- ⁴³Also at Deutsches Elektronen-Synchrotron, Hamburg, Germany
⁴⁴Also at Isfahan University of Technology, Isfahan, Iran
⁴⁵Also at Sharif University of Technology, Tehran, Iran
⁴⁶Also at Department of Physics, University of Science and Technology of Mazandaran, Behshahr, Iran
⁴⁷Also at Department of Physics, Faculty of Science, Arak University, ARAK, Iran
⁴⁸Also at Italian National Agency for New Technologies, Energy and Sustainable Economic Development, Bologna, Italy
⁴⁹Also at Centro Siciliano di Fisica Nucleare e di Struttura Della Materia, Catania, Italy
⁵⁰Also at Università degli Studi Guglielmo Marconi, Roma, Italy
⁵¹Also at Scuola Superiore Meridionale, Università di Napoli 'Federico II', Napoli, Italy
⁵²Also at Fermi National Accelerator Laboratory, Batavia, Illinois, USA
⁵³Also at Laboratori Nazionali di Legnaro dell'INFN, Legnaro, Italy
⁵⁴Also at Lulea University of Technology, Lulea, Sweden
⁵⁵Also at Consiglio Nazionale delle Ricerche - Istituto Officina dei Materiali, Perugia, Italy
⁵⁶Also at Institut de Physique des 2 Infinis de Lyon (IP2I), Villeurbanne, France
⁵⁷Also at Department of Applied Physics, Faculty of Science and Technology, Universiti Kebangsaan Malaysia, Bangi, Malaysia
⁵⁸Also at Consejo Nacional de Ciencia y Tecnología, Mexico City, Mexico
⁵⁹Also at Trincomalee Campus, Eastern University, Sri Lanka, Nilaveli, Sri Lanka
⁶⁰Also at Saegis Campus, Nugegoda, Sri Lanka
⁶¹Also at National and Kapodistrian University of Athens, Athens, Greece
⁶²Also at Ecole Polytechnique Fédérale Lausanne, Lausanne, Switzerland
⁶³Also at Universität Zürich, Zurich, Switzerland
⁶⁴Also at Stefan Meyer Institute for Subatomic Physics, Vienna, Austria
⁶⁵Also at Laboratoire d'Annecy-le-Vieux de Physique des Particules, IN2P3-CNRS, Annecy-le-Vieux, France
⁶⁶Also at Near East University, Research Center of Experimental Health Science, Mersin, Turkey
⁶⁷Also at Konya Technical University, Konya, Turkey
⁶⁸Also at Izmir Bakircay University, Izmir, Turkey
⁶⁹Also at Adiyaman University, Adiyaman, Turkey
⁷⁰Also at Bozok Universitetesi Rektörlüğü, Yozgat, Turkey
⁷¹Also at Marmara University, Istanbul, Turkey
⁷²Also at Milli Savunma University, Istanbul, Turkey
⁷³Also at Kafkas University, Kars, Turkey
⁷⁴Now at Istanbul Okan University, Istanbul, Turkey
⁷⁵Also at Hacettepe University, Ankara, Turkey
⁷⁶Also at Erzincan Binali Yıldırım University, Erzincan, Turkey
⁷⁷Also at Istanbul University - Cerrahpasa, Faculty of Engineering, Istanbul, Turkey
⁷⁸Also at Yildiz Technical University, Istanbul, Turkey
⁷⁹Also at School of Physics and Astronomy, University of Southampton, Southampton, United Kingdom
⁸⁰Also at IPPP Durham University, Durham, United Kingdom
⁸¹Also at Monash University, Faculty of Science, Clayton, Australia
⁸²Also at Università di Torino, Torino, Italy
⁸³Also at Bethel University, St. Paul, Minnesota, USA
⁸⁴Also at Karamanoğlu Mehmetbey University, Karaman, Turkey
⁸⁵Also at California Institute of Technology, Pasadena, California, USA

⁸⁶Also at United States Naval Academy, Annapolis, Maryland, USA

⁸⁷Also at Ain Shams University, Cairo, Egypt

⁸⁸Also at Bingol University, Bingol, Turkey

⁸⁹Also at Georgian Technical University, Tbilisi, Georgia

⁹⁰Also at Sinop University, Sinop, Turkey

⁹¹Also at Erciyes University, Kayseri, Turkey

⁹²Also at Horia Hulubei National Institute of Physics and Nuclear Engineering (IFIN-HH), Bucharest, Romania

⁹³Now at another institute formerly covered by a cooperation agreement with CERN

⁹⁴Also at Texas A&M University at Qatar, Doha, Qatar

⁹⁵Also at Kyungpook National University, Daegu, Korea

⁹⁶Also at Yerevan Physics Institute, Yerevan, Armenia

⁹⁷Also at another international laboratory covered by a cooperation agreement with CERN

⁹⁸Also at Imperial College, London, United Kingdom

⁹⁹Also at Institute of Nuclear Physics of the Uzbekistan Academy of Sciences, Tashkent, Uzbekistan

¹⁰⁰Also at another institute formerly covered by a cooperation agreement with CERN